THEORETICAL STUDIES OF IO'S ATMOSPHERE

Thesis by

Michael Earl Summers

In Partial Fulfillment of the Requirements

for the Degree of

Doctor of Philosophy

California Institute of Technology

Pasadena, California

1985

(Submitted September 28, 1984)

Acknowledgements

I am grateful to my thesis advisor, Yuk Yung, for suggesting the topic of this thesis and for providing advice, encouragement, and friendship during the course of this work.

I would like to thank the entire faculty of the Planetary Science Department at Caltech for the opportunities they have given me to do science. I am especially grateful for the patience and understanding they have shown me during the past five years.

I wish to thank Mark Allen for our many discussions concerning photochemistry and programming. I want to thank John Trauger for helping me understand the phenomenology of the Io plasma torus.

I offer my thanks to Donna Lathrop for typing part of this thesis, and to Kay Campbell for helping me understand the ways of Caltech. I thank them both for their valuable help and advice.

My fellow graduate students have helped make my stay at Caltech rewarding in many ways. I offer my thanks to them all for the good (and bad) times we've shared.

A very special thanks goes to Diane Michelangeli: for her good humour and friendship, encouragement and support, and for helping me to survive my last year of graduate school. I sincerely appreciate the many interesting conversations we have shared over the past year.

And most of all I want to thank my family. None of this would have been possible without their love.

Abstract

A range of theoretical models of the compositional structure of Io's dayside atmosphere and ionosphere are developed. The dominant neutral gas, SO_2, is provided by sublimation of surface frost. Photochemical processes lead to the build up of O, S, SO, and O_2 as minor gasses near Io's surface while O becomes the dominant gas near the exobase. The vertical column density of O_2 in all models considered is less than 10^{14} cm^{-2}. The dayside ionosphere is formed as a result of ionization of neutral species by solar UV radiation. Charge exchange and rearrangement reactions are important for determining the ionic composition of the ionosphere. The dominant ion in the models considered is SO^+. A number of charge exchange reactions are identified whose rates need to be better determined in order to refine the present model of the ionosphere. The best matches of the model ionospheres to that observed by the Pioneer 10 radio occultation experiment require atmospheric surface concentrations of SO_2 in the range of 2.5×10^9 to 1×10^{11} cm^{-3}, and an exospheric temperature in the range of 960 K to 1230 K. The ratio of the escape fluxes of O to S from the exobase is ≥ 2 in the models considered, while the models which allow surface deposition of minor constituents always have a total sulfur depositional rate greater than 1/2 of the total oxygen depositional rate, thus a surface enrichment of S relative to that predicted by a pure SO_2 surface. The depositional rate of this "excess" sulfur is in the range 100 m to 1 km thickness per billion years.

Atmospheric Na is provided by surface sputtering of SO_2 surface frost with Na impurities by MeV type magnetospheric ions. An upward

flux of Na_2O of 5×10^7 cm^{-2} s^{-1} leads to an escape flux of Na from the exobase of 1×10^7 cm^{-2} s^{-1}. The chemistry (ion and neutral) of Na species in the atmosphere has only minor effects on the major characteristics of the atmosphere and ionosphere.

It is generally accepted that Io is the source of S, O, Na, and K which, subsequent to ionization, form the constituents of the Io plasma torus. It is shown in chapter II that the escape of S and O from Io can be understood in terms of the photochemistry of a predominantly SO_2 atmosphere created by the high vapor pressure of SO_2. However, the vapor pressures of Na_2S, K_2S and other common compounds containing Na and K are negligible at the surface temperature of Io. In chapter III we propose that Na and K escape from Io in two stages. Atoms of Na and K (or molecules containing these atoms) are first sputtered into the atmosphere from the surface by high energy magnetospheric ions. Atmospheric sputtering by low energy corotating ions then removes these constituents (along with others present) out of Io's gravitational control. The estimated injection rates are sufficiently large to maintain the observed Na, K, and O clouds observed around Io.

Table of Contents

I. Introduction

The purpose of this introductory chapter is to set the context and provide the motivation for a theoretical study of the atmosphere of Io. The phenomena that may have an influence on the physical properties of Io's atmosphere are, indeed, many and complex. This introduction is not meant to be a comprehensive review of these phenomena. Neither will it contain a complete historical account of the ideas developed to explain the many observations of Io and its immediate spatial environment. Rather, it is intended as an overview of the many problems facing the development of a complete theoretical description of the physical processes occurring in Io's atmosphere. For a more comprehensive discussion of Io observations and their interpretation the reader is referred to the excellent reviews by Brown and Yung(1975), Fanale et al.(1982), and Kumar and Hunten(1982). Brown et at.(1983) contains a lucid summary of observations of the Io Torus.

The first section of this chapter is a summary and discussion of those observations which probably have the most intimate bearing on the physical properties of Io's atmosphere. The second section is a description of the "locally buffered" model of Io's SO_2 atmosphere. The reasons that this model may and may not be a reasonable starting point for modeling atmospheric processes are stated. The final section lists the major attributes of a complete theoretical model of Io's atmosphere. In this last section we discuss the strategy for our theoretical study of Io's atmosphere.

1. Observational Constraints on Atmospheric Properties

(a) Post-eclipse brightening.

The earliest evidence for an atmosphere on Io came from the discovery of post-eclipse brightenings(PEB) (Binder and Cruikshank, 1964). For about 2.3 hours of each Io day (τ_p = 42.46 hours) the satellite is in Jupiter's shadow. Binder and Cruikshank(1964) found that upon emergence from Jupiter's shadow, Io's visual brightness was 10-15% higher than it's pre-eclipse value. This excess brightness was found to dissapear on a time scale of τ_b ~ 0.25 hrs. ~ 9×10^2 s.

Binder and Cruikshank(1964) and later Sinton(1973) suggested that the PEB are caused by an atmospheric constituent that condenses onto Io's surface during eclipse, forming an optically thick surface frost, which then sublimates upon Io's emergence. The surface of Io near the subsolar point cools from ~ 130 K to ~ 90 K during eclipse (Morrison and Cruikshank, 1974; Veverka et al., 1981). Upon emergence the surface heats up to it's pre-eclipse temperature on a timescale of τ_e ~ 1×10^3 s. For this surface temperature change Lewis(1971) found that a frost condensate, possibly CH_4 or NH_3, could produce the PEB if the initial partial pressure above the surface was of order 10^{-7} bar.

Since the discovery of PEB many investigators have searched for them (see references in Fanale et al., 1981, and Veverka et al., 1981) with about 60% of the observers reporting positive results. This sporadic nature of the PEB has generated considerable controversy. Furthermore, three eclipse reappearances of Io were observed during the two Voyager encounters and no whole-disc brightening at the 10% level

was detected (Veverka et al, 1981). This places severe limits on the abundance of a condensable gas in Io's atmosphere. In section 2 the PEB will be discussed in the context of a "locally buffered" model of Io's SO_2 atmosphere.

(b) Stellar occultation by Io.

In 1971 the occultation of the fifth magnitude star β Scorpii C was observed by Smith and Smith(1972). Within their limits of determination, the disappearance and reappearance of the star were found to be instantaneous. This was used to set an upper limit on the surface pressure on Io. For assumed mean molecular weights 16 and 28 Smith and Smith(1972) calculated upper limits on surface pressure of 1.3×10^{-7} bar and 9×10^{-8} bar respectively. The calculated upper limit decreases with increasing molecular weight. Strictly speaking, this upper limit is applicable only in that region that is within 12^{o} of Io's terminator. Thus it is fair to say that if the mean molecular weight of Io's atmosphere is 28 or larger, then a globally uniform atmosphere should have been detected if the surface pressure was larger than 10^{-7} bar.

(c) Ionosphere.

The first direct measurements of physical properties of Io's gravitationally bound atmosphere were provided by the Pioneer 10 radio occultation experiment (Kliore et al.,1975). The trajectory of Pioneer 10 was fixed so that the spacecraft would be occulted by Io (as seen from earth). The geometry of the occultation is shown in figures 1 and

Figure 1. Geometry of the Io occultation of Pioneer 10. At the time of the occultation Io had been out of Jupiter eclipse for approximately 22 hours (after Kliore et al., 1975).

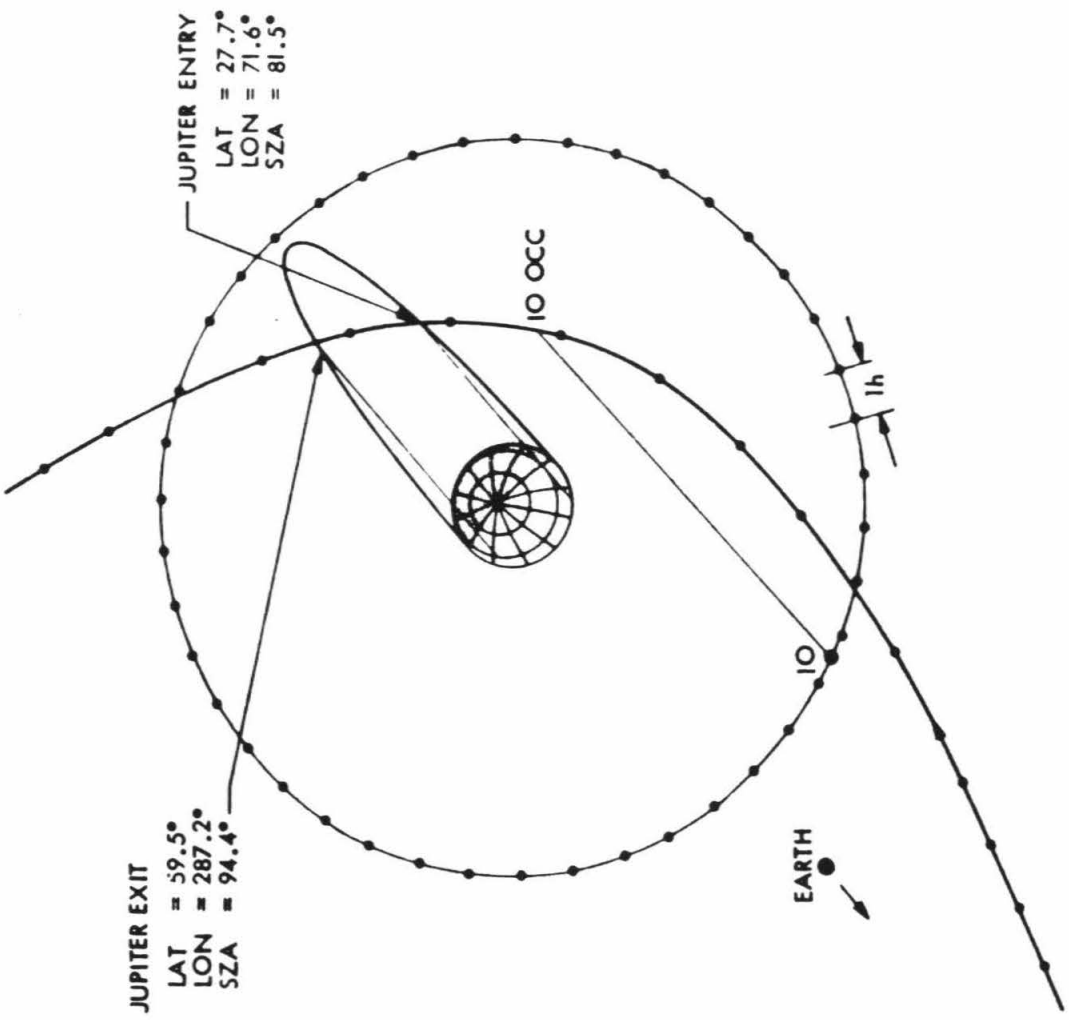
JUPITER ENTRY
LAT = 27.7°
LON = 71.6°
SZA = 81.5°
JUPITER EXIT
LAT = 59.5°
LON = 287.2°
SZA = 94.4°
IO OCC
1h
IO
EARTH

Figure 2. Geometry of the occultation of Pioneer 10 by Io. The entry (dayside) ionosphere is mostly shielded from the undeviated corotating plasma. The exit (nightside) ionosphere is subject to direct corotating ion and electron impact (after Cloutier et al., 1978).

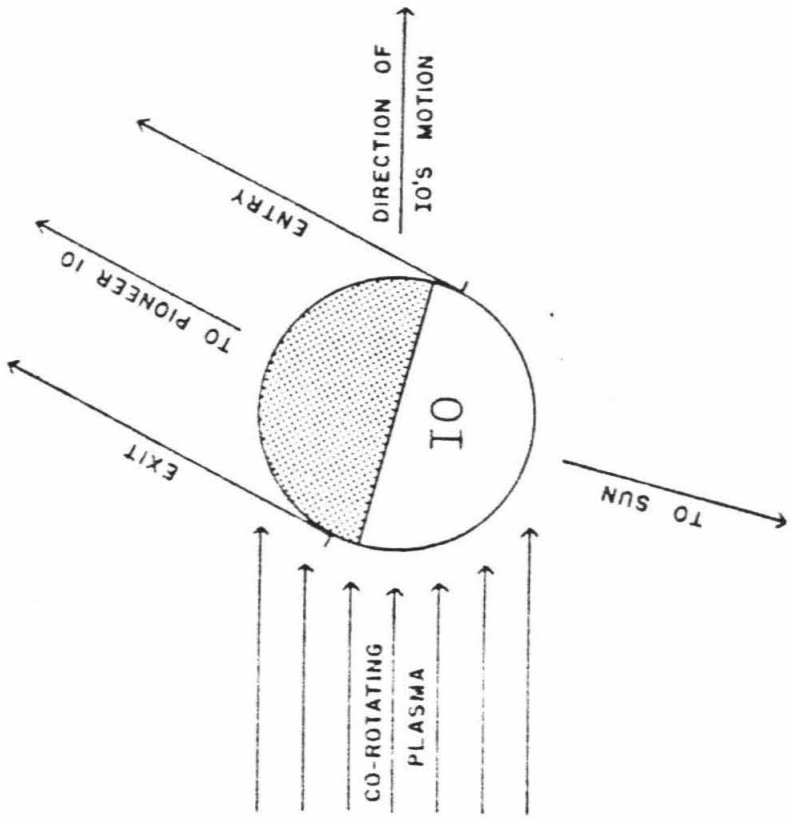
DIRECTION OF
IO'S MOTION
ENTRY
TO PIONEER 10
EXIT
IO
TO SUN
CO-ROTATING
PLASMA

2. The phase deviations in the radio signal from the spacecraft before (Entry) and after (Exit) the occultation by the solid body of the satellite were analyzed to deduce the electron density profiles in Io's ionosphere.

Two well developed (in the classical sense, see Chamberlain, 1978) ionospheric electron density profiles were obtained (see figure 3). However, the profiles showed marked differences from each other. The entry electron density profile shows a peak of 6×10^4 cm^{-3} at approximately 100 km altitude. The plasma scale height above the peak (at say 200 km) is 190 km. The peak electron density for the exit ionosphere is 9×10^3 cm^{-3} and occurs at 40 km altitude. The plasma scale height above this peak is about 60 km at 200 km altitude and decreases with increasing altitude.

Two possible causes of the differences between the entry and exit ionospheres are illustrated in figure 2. First, the entry ionosphere was above the dayside of Io at a zenith angle of 81^o. The exit profile was above the nightside, but the shadow height was at only 30 km altitude. If solar UV was producing the ionization then one would expect a highter electron density on the dayside. However, there are problems with sustaining an ionosphere in a predominantly molecular atmosphere into the nightime. Also if the atmosphere is predominantly atomic, then one does not expect such a fast decrease in electron density at night. These issues are discussed more fully in Chapter 2.

A second effect to consider for possible causes of the entry/exit ionospheric asymmetry is that due to interaction with the ambient magnetospheric plasma. Low energy plasma ($E < 1$ keV) in the

Figure 3. The entry (dayside) and exit (nightside) electron density profiles as obtained from an analysis of radio occultation measurements by Pioneer 10 (after Kliore et al., 1975).

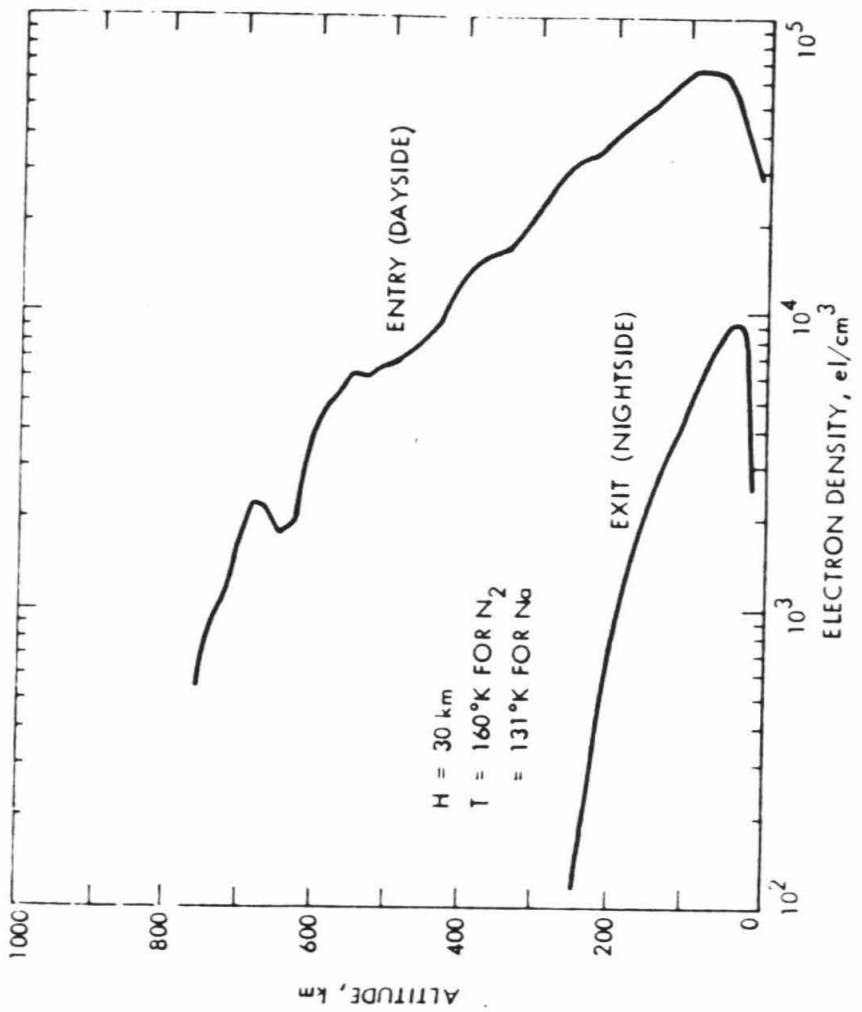
ENTRY (DAYSIDE)
EXIT (NIGHTSIDE)
H = 30 km
T = 160°K FOR N_2
= 131°K FOR Na
ALTITUDE, km
ELECTRON DENSITY, el/cm^3
1000
800
600
400
200
0
10^2
10^3
10^4
10^5

neighborhood of Io rotates about Jupiter with Jupiter's angular velocity = 1.77×10^{-4} s^{-1}. At Io's orbital radius of 5.9 R_J (1 R_J = 7.13×10^9 cm) the corotation velocity of the plasma is 74.5 km s^{-1}. Io's Keplerian velocity is 17.4 km s^{-1}, so the relative velocity between Io and the low energy plasma is 57.1 km s^{-1}. If there is no substantial deviation of the plasma velocity very near Io then the atmosphere on the side of the satellite corresponding to the exit(nightime) ionosphere will be subject to low energy ion and electron impact. The atmosphere on the downstream side will then be shielded by the body of the satellite.

(d) Voyager IRIS detection of SO_2.

The Voyager IR experiment(IRIS) detected absorption due to gaseous SO_2 in spectra taken over a 'hot spot' near the volcanic plume Loki. The hot spot was near the subsolar point on Io. The estimated abundance of 0.2 cm atm is almost exactly that expected if the gas was in local vapor pressure equilibrium with surface frost at the local ambient surface temperature T = 130 K. The corresponding surface pressure for an isothermal atmosphere is $P = 1.4 \times 10^{-7}$ bar, about a factor of 10^4 too high for the atmosphere to be an exosphere. Because of the strong vapor pressure dependence on T, one would expect the atmospheric SO_2 content to vary greatly between the subsolar and antisolar points on Io. In section 2 we will discuss the characteristics of a "locally buffered" SO_2 atmosphere on Io.

(e) Io's visible and IR reflectance spectrum.

Early studies of Io's visible and IR reflectance spectrum (Fanale et al.,1974) identified elemental S as a possible dominant component of Io's surface. Subsequent to the Voyager I IRIS detection of SO_2 in Io's atmosphere, Fanale et al.(1979) suggested that SO_2 surface frost was the cause of an observed 4.1 absorption feature in Io's IR reflectance spectrum. Laboratory studies of SO_2 frost supported this hypothesis (Fanale et al.,1979; Smythe et al.,1979). At the time of this writing there is still a considerable controversy brewing over the phase of the material on Io's surface (Nash, 1983; Howell et al.,1983). Whether SO_2 free frost or an SO_2 adsorbate is producing the characteristics of the IR spectrum may not be decided until more laboratory studies at low temperature are undertaken, or until the Galileo multiple flybys of Io occur.

Nash and Nelson (1979) studied the spectral properties of alkali sulphides and sulfur containing compounds in the laboratory in an attempt to interpret Io's visible and IR reflectance spectrum. They found that Na_2S, K_2S, and NaHS all have absorption features in the IR at the locations of strong absorption features in Io's spectrum. Also, Na_2S which was subject to bombardment by high energy protons (5 keV) showed an absorption band at 0.56 microns, where Io has a feature.

As will be discussed in (h) Na and K are minor constituents in the neutral clouds around Io. Presumably Na and K are also minor constituents in Io's gravitationally bound atmosphere. However, because of the ease of their detectability (see(h)) they probably act as ideal 'tracers' of the processes which control the removal of mass from Io.

Knowledge of the quantity and phase of Na and K compounds on the surface of Io is therefore quite important. Hopefully through laboratory and theoretical studies this knowledge will be available in the near future.

(f) Volcanoes.

One of the most exciting discoveries during the Voyager I encounter with the Jupiter system was that Io is volcanically active. The fact that Io is outgassing has important implications for atmospheric structure and evolution. Smith et al. (1979) concluded that SO_2 is the volatile which drives the volcanism. Johnson et al. (1979) used observations of the then-known plumes to estimate volatile ejection rates. They found that if only 1 % of plume ejecta is volatile, then the volatile ejection rate would be of order 10^{10} to 10^{12} atoms cm^{-2} s^{-1} averaged over Io's surface. Assuming that the volatile is pure SO_2, then it would take less than 10^8 seconds for the volcanoes to supply enough SO_2 to produce a globally uniform atmosphere at the level detected by IRIS(if no condensation occured). In fact, the volatile ejection rate may be as much as 100 times greater than this (Cook et al., 1979), and the global average atmospheric SO_2 content is probably 10 to 100 times less than the amount detected by IRIS (see section 2). Estimates of the torus mass supply rate lie in the range of 10^{10} to 10^{11} atoms cm^{-2} s^{-1} ejected from Io (see (h)). Thus it seems reasonable to assume that the volcanoes supply volatiles at a rate greater than the mass loss rate from Io.

Strom et al. (1979) analyzed eight plumes revealed in Voyager 1 images. From their estimates of plume widths, we find the area covered

by these plumes to be roughly 3 % of Io's surface area. McEwen and Soderblom (1983) suggest that another class of volcano, only one of which was active during the Voyager flybys, may produce plumes with diameters about 5 times the diameters of most of those studied by Strom et al. (1979). McEwen and Soderblom (1983) find evidence for 3 of these large Pele-class volcanoes and estimate that their typical duration of activity is at least a factor of 100 less than that of the smaller Prometheus-class volcano. Thus, a time weighted average of the area covered by these larger plumes leads one to conclude that their direct effect on atmospheric structure is smaller than that produced by the smaller plumes. In any case, the plumes occupy only a small fraction of the volume of Io's atmosphere, and to first order may be ignored in modeling the atmospheric structure on Io.

(g) Airglow.

During the Voyager 1 encounter with the Jovian system, wide angle('clear') pictures were taken of Io when both Io and the spacecraft were in Jupiter's shadow. These images showed "faint diffuse luminous glows" (Cook et al., 1981) on the disk of Io (Figure 4). These "glows" came from areas close to several known plumes and also from extended regions near the poles . The mechanism producing these "glows" is not known. Cook et al. (1981) referred to the luminous polar "glows" as aurora, from an analogy with terrestrial aurora.

Figure 4. Diagram of the positions of Io and the glows (aurora) observed with the Voyager I camera (taken from Cook et al., 1981).

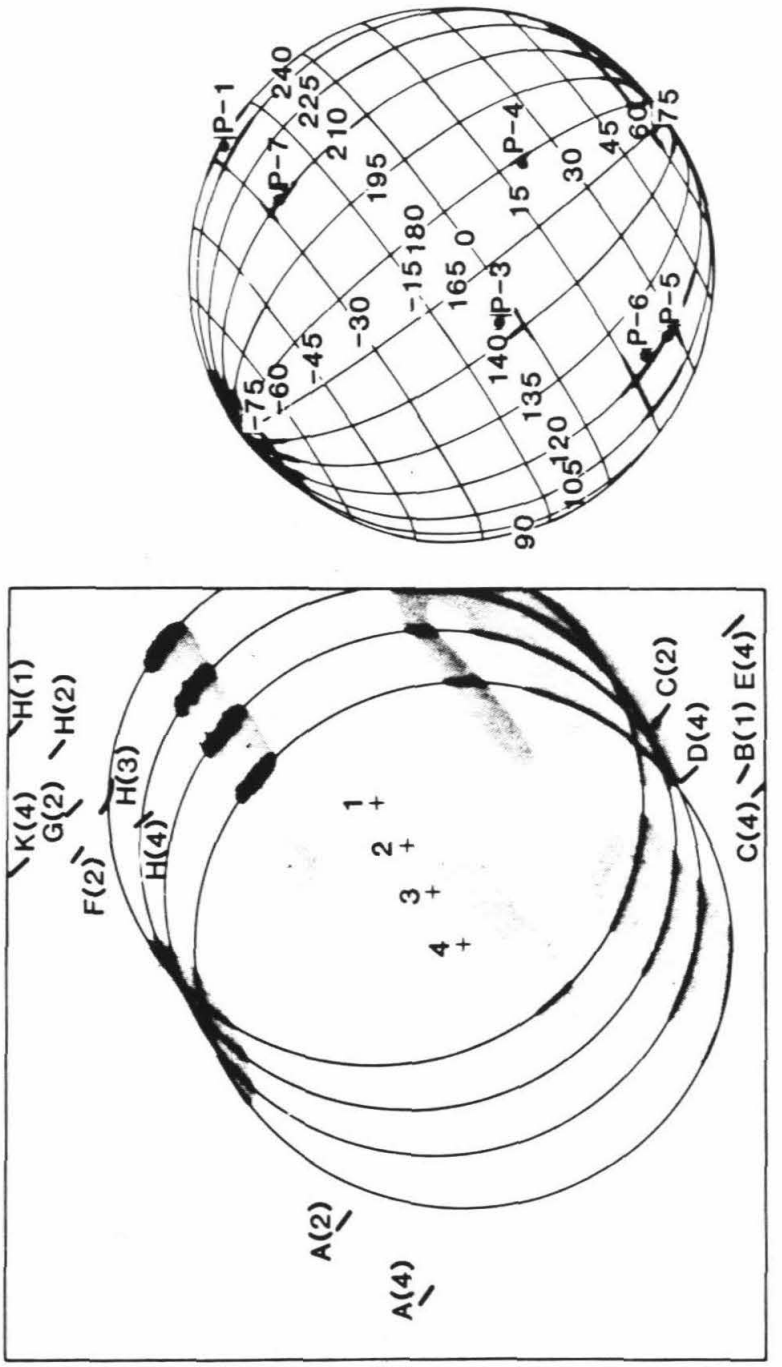
P-1
P-7
P-4
P-3
P-6
P-5
240
225
210
195
180
165
150
135
120
105
90
75
60
45
30
15
0
-15
-30
-45
-60
-75
K(4)
G(2)
H(1)
H(2)
F(2)
H(3)
H(4)
A(2)
A(4)
C(2)
D(4)
C(4)
B(1)
E(4)
1
2
3
4

(h) Dark polar regions.

The lack of visible polar caps has been a puzzling characteristic of Io, expecially in view of the presumably huge amounts of SO_2 produced by the volcanoes in the equatorial region (Fanale et al., 1982). In fact, the principal argument against a global SO_2 atmosphere on Io rests on the obersvation that Io's polar regions are relatively dark (Fanale et al.,1982; Kumar and Hunten, 1982). Even though it is a matter of interpretation just how 'dark' the poles are (Fanale et al.,1983), it is unlikely that they are covered by an optically thick layer of relatively pure SO_2 frost. The volcanos in the equatorial region apparently produce copious amounts of SO_2 (Johnson et al., 1979). Transport to the polar regions should lead to a build-up of thick SO_2 frost caps. Several authors have listed mechanisms that might prevent the creation of polar caps (Fanale et al.,1982; Kumar and Hunten, 1982). However, the efficacy of any such mechanism cannot be ascertained until the magnitude of the frost transport to the polar regions is known. The frost transport rate depends of many of the characteristics of Io's atmosphere. One of the most important of these is the composition. For example, if the dominant constituent in Io's atmosphere is SO_2, then the transport may be hydrodynamic and very rapid. This is due to the large difference in vapor pressure of SO_2 between the equator and poles (see section 2). However, if the major constituent is a photodissociation product of SO_2, say O_2, then the transport of SO_2 to the poles might occur in a slower diffusive manner. Chapter 2 of this thesis is a theoretical study of the chemical composition of Io's atmosphere. One

of the prime motivations of this study was the desire to understand the mode of SO_2 frost transport.

(i) The Io Torus.

Observations of the Io-associated neutral and ionized gas clouds can provide constraints on atmospheric processes. The reason for this is simple. Io is the dominant source of mass for the Torus and probably the entire Jovian magnetosphere. Given that an atmosphere exists on Io, then this atmosphere must in some sense modulate the transport of mass from Io's surface to the torus.

The first constituent detected in the near-Io cloud was sodium (Brown, 1974). Optical emission in the Na D-lines (5890 Å, 5896 Å) was observed in a cloud mostly inside Io's orbit extending ahead of the satellite about 70^{o} in orbital longitude(see figures 5 and 6). The excitation mechanism for the lines is the resonant scattering of sunlight (Brown and Yung, 1975). Early modeling of the observed near-Io cloud led to the consensus that atoms were escaping Io with a residual velocity slightly greater than the surface escape velocity (V_{esc} = 2.56 km s^{-1}) (Smyth and McElroy, 1978; Brown et al., 1983). The best model fits to cloud morphology and spectral line shapes requires that the sodium atoms originate from the hemisphere of Io facing Jupiter (Matson et al., 1977; Smyth and McElroy, 1978; Porco et al., 1980).

The Na cloud supply rate is somewhat uncertain. The reason for this is that the lifetime of the Na in the Io plasma torus is not accurately known. Na in the near-Io cloud is lost through electron impact ionization. Smyth and McElroy(1978) assumed a Na lifetime

Figure 5. Image of Io's sodium cloud. A picture of Jupiter and a drawing of Io's orbit have been added. The white dot indicates the position and size of Io. The dark area within the cloud is due to the occultating disk (taken from Matson et al., 1977).

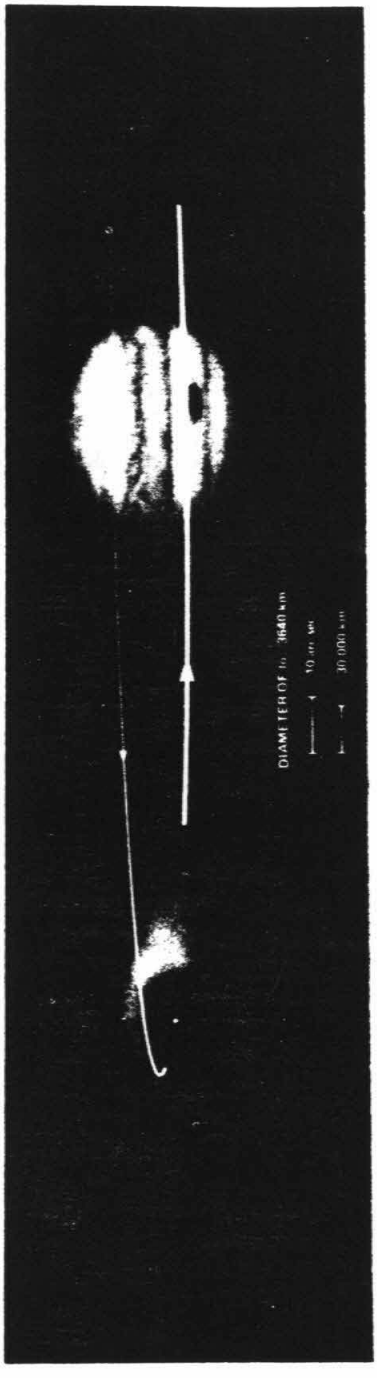
DIAMETER OF
3640 km

Figure 6. Orbital cloud model as calculated by Smyth and McElroy (1978). The shape of the sodium cloud in the satellite plane as predicted by trajectories of atoms emitted radially and uniformly from the 130° to 310° hemispherical portion of Io's exobase is shown for a phase angle of 55° and compared with the simple triangular cloud model. An emission velocity of 2.6 km s^{-1} and a lifetime of 20 hours were assumed. Atomic concentration is proportional to the density of points shown (taken from Smyth and McElroy, 1978).

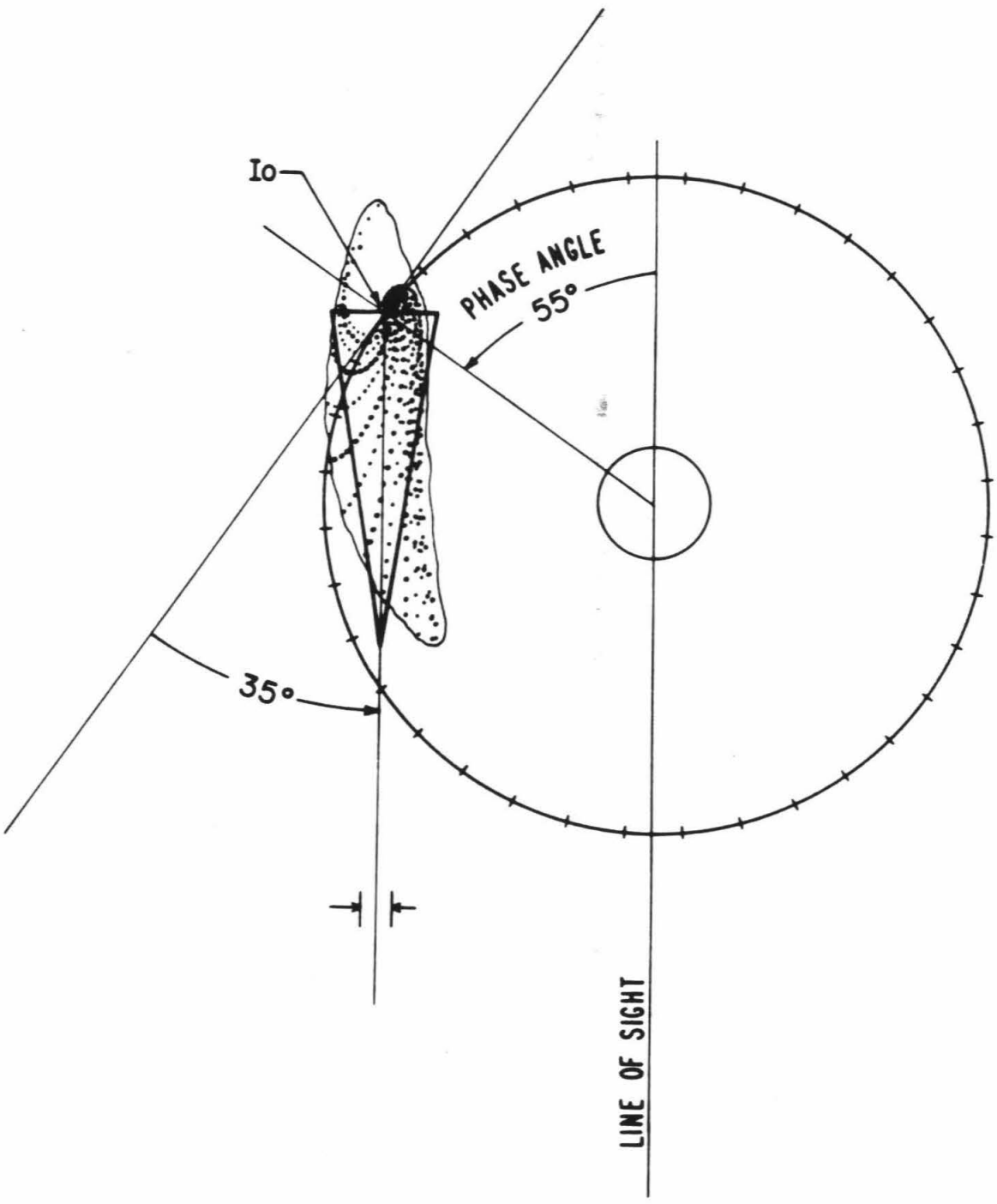
Io
PHASE ANGLE
55°
35°
LINE OF SIGHT

against ionization of 20 hours to deduce a supply rate from Io of 2 x 10^{25} atoms s^{-1}, which corresponds to a surface flux from Io of 5 x 10^{7} cm^{-2} s^{-1}. Brown et al. (1983) argue that a lifetime of 2 to 3 hours is more realistic, which may imply that the Na escape rate from Io is as much as a factor of 50 larger than the value deduced by Smyth and McElroy(1978). Much more refined models of Io's sodium cloud, incorporating the spatial and time dependence of the Na lifetime against electron impact ionization, are needed in order to more accurately calculate the supply rate.

Resonant emission lines from K (7665 Å, 7699 Å) have also been observed near Io (Trafton, 1975). An observational study of the K cloud by Trafton (1981) suggests that both Na and K are ejected from Io from the same general locality on Io and by the same mechanism. Porco et al. (1980) obtained high resolution emission line profiles of NaI (5889 Å) and KI (7699 Å) near Io and found similar velocity structures (in the FWHM sense). They found a KI/NaI abundance ratio in their field of view of 1/17. If the KI cloud coincides with the NaI cloud, then the loss of K from Io should be approximately a factor of 17 less than that for Na. However, it is likely that the lifetime of KI against electron impact ionization is different from that of NaI. This has an important bearing on the relative escape rates.

The identification of neutral oxygen in the Io torus was made on the basis of an observation of the OI 6300 Å forbidden line in a localized region near Io (Brown, 1981). The apparent emission rate was 8 $\pm$ 4 Rayleighs, and the integration time was $\simeq$ 3 hours during which Io moved $\simeq$ 25° in orbital longitude. The velocity distribution of OI atoms

in the torus was not determined.

Smyth and Shemansky(1982) have modeled the escape of atomic oxygen from Io and its subsequent loss by ionization in the plasma torus. Assuming that neutral oxygen escapes from Io in the same manner that Na does, they find the escape rate for atomic oxygen to be ~ 5×10^9 cm^{-2} s^{-1} normalized to the surface of Io. This escape flux should be considered as a lower limit since Smyth and Shemansky (1982) only considered loss of OI by electron impact ionization in the plasma torus. It is likely that charge exchange processes and elastic scattering may be more important as loss mechanisms than ionization by electron impact.

Durrance et al. (1982) reported the UV detection of SI (1425 Å) from a region of Jupiter's magnetosphere which intersected the torus near its eastern ansa, at which time Io was near western elongation. This would indicate that the SI cloud is very pervasive. However, due to the nature of the marginal detection of SI (a signal to noise of ~ 2, and the nearness of this emission line to another very strong unidentified one at 1429 Å) this interpretation is suspect. No modeling of the SI cloud has yet been performed with this observation serving as a constraint.

Further clues to the escape process and mass ejection rates for the various species can be obtained by studying the phenomenology of the Io plasma torus. Many emitting species have been observed in the plasma torus, among them SII, SIII, SIV, OII, and OIII (Brown et al., 1983). Also, Voyager I provided information on the relative abundance of OII, SII, and NaII at various locations in the Jovian magnetosphere (Vogt et al.,1979; Bagenal and Sullivan, 1981). In particular, Voyager I found a

mixing ratio for sodium ions of ~ 0.05 in the inner torus and ~ 0.10 in the middle magnetosphere. As noted by Brown et al. (1983), if this mixing ratio is the same as that of the escaping atoms from Io then the total ejection rate would be $\sim 1 - 2 \times 10^{28}$ cm^{-2} s^{-1}.

The Io torus electron density has been determined by ground based observations of SII forbidden lines (Trauger et al., 1980) and from Voyager I experiments (Bagenal and Sullivan, 1981). The electron temperature has been determined from several Voyager 1 and Voyager 2 experiments (Brown et al., 1983). As average values for the torus Brown et al. (1983) characterizes the electron number density by $N_e \simeq 2000$ cm^{-3} and the electron temperature by $T_e \simeq 4$-6 eV. Brown (1981) used the determination of the OI density along with the properties of the torus electron populations to deduce the electron impact ionization rate for OI. He found an OI ionization rate of 5×10^{27} s^{-1} for the entire torus. From the Voyager results we know that OII is overall the dominant ion. Thus this derived value can be considered as a rough estimate of the plasma torus supply rate. The closeness of this rate to the estimated ejection rate from Io is striking.

Once an ion is created it is accelerated to the corotational velocity of Jupiter's magnetic field. For oxygen and sulfur leaving Io this results in ion cyclotron energies of 280 eV and 550 eV respectively. This energy is transferred to the electron gas by Coulomb collisions or possibly by collective charged particle processes. The electrons collisionally excite electronic states in the ions which then decay spontaneously and emit photons. The total observed UV emission rate from the torus is of order 2×10^{12} Watts (Broadfoot et al., 1979).

This implies a total ionization rate of order 3 x 10^{28} atoms s^{-1}.

The three estimates for the torus total atomic supply rate are in order of magnitude agreement. However, many simplifying assumptions have been made. Also, better observational studies are needed in order to determine more accurately the physical properties of the torus (e.g. the OI and SI number density). Even in the absence of a detailed model of the Io torus it is clear that many observational and theoretical constraints already exist on the possible excape processes operative in the atmosphere of Io.

2. A "locally buffered" SO_2 atmosphere on Io

It is known that SO_2 frost exists on the surface of Io (Fanale et al., 1979). Gaseous SO_2 was also detected in the subsolar region in the amount which would be expected if the gas was in approximate vapor pressure equilibrium with SO_2 surface frost at a local surface temperature of T = 130 K (Pearl et al., 1979). These observations gave rise to the suggestion that the SO_2 atmosphere on Io is "locally buffered" by SO_2 surface frost, i.e., the SO_2 atmosphere is everywhere in local vapor pressure equilibrium (Pearl et al.,1979; Fanale et al.,1980). Here we describe the characteristics of a simplified version of a "locally buffered" model of Io's SO_2 atmosphere.

First we make several simplifying approximations and assumptions, as follows.

(a) We will work in spherical coordinates and assume azimuthal symmetry about a line joining the center of the satellite and the sun. We assume that any atmospheric quantity $\xi = \xi(\theta,z)$, where θ is the subsolar longitude (equivalent to the zenith angle of the sun), $z = r - R_{Io}$ is the altitude above the surface, r is the radius from the center of Io, and R_{Io} = 1820 km is Io's radius. It is assumed that surface variables depend only on θ .

(b) Perfect local buffering is assumed, i.e., the SO_2 gas pressure just above the surface is exactly equal to the saturation vapor pressure of SO_2 (P_s)at the local surface temperature. By making

this assumption we ignore what is possibly a very important process in Io's atmosphere, i.e., the horizontal transport of SO_2.

(c) The atmospheric pressure P is assumed to be related to the gas mass density ρ and temperature T by the ideal gas equation of state

$$P = \rho kT/m = nkT \ , \qquad (1)$$

where $n = \rho/m$ is the number density of SO_2 molecules, $m = 1.06 \times 10^{-22}$ gm is the mass of a single SO_2 molecule, and $k = 1.38 \times 10^{-16}$ erg K^{-1} is the Boltzmann constant.

(d) Each unit column of atmosphere is assumed to be isothermal at the local surface temperature $T_s(\theta)$. The spatial variation of surface brightness temperature on Io was measured by the Voyager IRIS experiment (Pearl et al., 1979). We have taken the spatial variation of Io's surface temperature to be of the form

$$T_s = T_{av} + \Delta T \cos \theta \ . \qquad (2)$$

As an approximation to the IRIS data, we take $T_{av} = 110K$ and $\Delta T = 20$ K.

(e) It is assumed that the atmosphere is in hydrostatic equilibrium. The scale height is defined by

$$H = kT/mg = C^2/g \ , \qquad (3)$$

where g(z) is the local gravitational acceleration, and $C = (kT/m)^{1/2}$ is the isothermal sound speed. At Io's surface g(z=0) = 180 cm s^{-2}. Since $H(z=0)/R_{Io} << 1$, we neglect the variation of g with altitude within the first few scale heights from the surface. The hydrostatic pressure variation can with these assumptions be shown to be

$$P(\theta,z) = P(\theta,0)\ e^{-z/H} \qquad (4)$$

$$= P_s(\theta)\ e^{-z/H},$$

where $P_s(\theta)$ is the saturation vapor pressure of SO_2 at location θ where the surface temperature is $T_s(\theta)$.

The vapor pressure of SO_2 as a function of temperature has been measured in the range 170 K < T < 197.6 K by Burrell and Robertson (1915) and theoretically extended to T = 90 K by Wagman (1979). The SO_2 vapor pressure dependence on temperature is adequately represented by the function

$$P_s(T) = A \exp(-B/T)\ , \qquad (5)$$

where the constants $A = 1.52 \times 10^{14}$ dynes cm^{-2} and B = 4510 K were obtained by a least squares fit to the calculated values given by Wagman (1979). In figure 7 we show a plot of $P_s(\theta)$. It can be seen that if the SO_2 atmosphere is indeed "buffered" by SO_2 frost, then the surface

Figure 7. Surface pressure for a local vapor pressure equilibrium model of Io's SO_2 atmosphere. P_o is the pressure at which the molecular mean free path is equal to the local scale height.

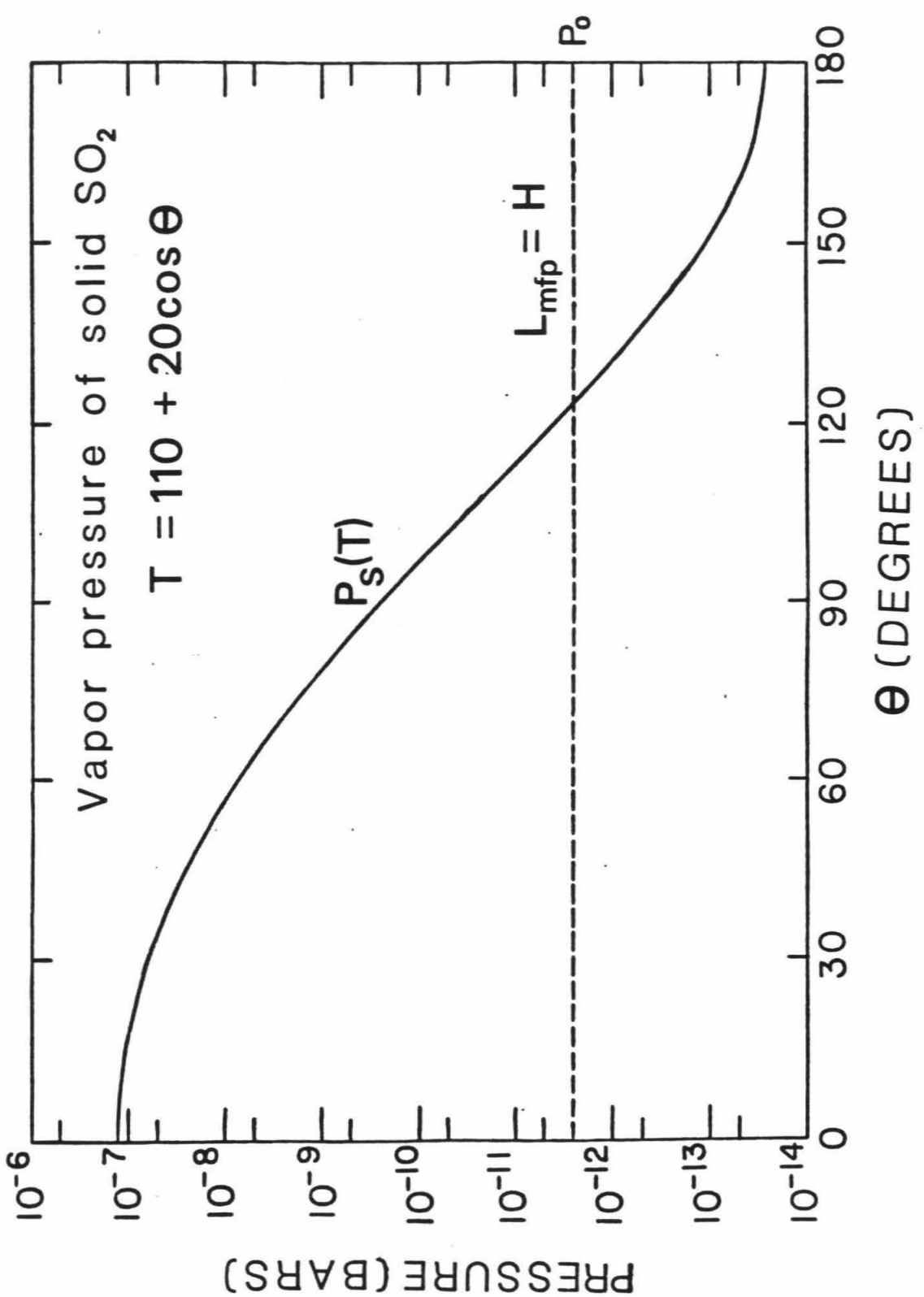
Vapor pressure of solid SO_2
$T = 110 + 20\cos\Theta$
$P_s(T)$
$L_{mfp} = H$
P_o
PRESSURE (BARS)
10^{-6}
10^{-7}
10^{-8}
10^{-9}
10^{-10}
10^{-11}
10^{-12}
10^{-13}
10^{-14}
0
30
60
90
120
150
180
Θ (DEGREES)

pressure would vary between a maximum in the subsolar region of 1.4 x 10^{-7} bar to a minimum on the nightside of 2.4 x 10^{-14} bar. Table 1 lists several parameter values for such an atmosphere at three selected subsolar longitudes on Io.

From the values in Table 1 it can be seen that the surface density n_o, the column density N, and SO_2 self-collision mean free path L_{mfp} each vary by more than 6 orders of magnitude between the subsolar point ($\theta = 0$) and the antisolar point ($\theta = 180^o$). The scale height, on the other hand, changes by only 30%. In fact, $L_{mfp} \sim 10^2$ H at $\theta = 180^o$, thus the atmosphere here can more accurately be called an exosphere (the transition to an exopshere occurs at approximately the pressure at which $L_{mfp} = H$, i.e., at $P_s(\theta) = P_o = mg/\sqrt{2}\ Q = 2.4 \times 10^{-6}$ dynes cm^{-2}, which occurs at $\theta = 125^o$. In the context of this locally buffered model of Io's atmosphere, approximately 21 % of the surface area, centered on the antisolar point, is covered by an atmosphere which is exospheric in character. If an SO_2 atmosphere with a surface pressure P_o were to condense, then roughly 1 monolayer of SO_2 molecules would be deposited on Io's surface.

The locally buffered (LB) model of Io's atmosphere is completely consistent with the upper limit on surface pressure as determined by the stellar occultation observation (see (b)). The upper limit on surface pressure of order 10^{-7} bar (Smith and Smith,1972) is applicable only near Io's terminator ($\theta = 90^o$). At the terminator the LB atmosphere has a surface pressure of 2.4 x 10^{-10} bar.

A much more severe test of the applicability of the LB model is found in its implications for post-eclipse brightenings. First we

TABLE I

Parameter Values for a Pure SO_2 Equilibrium Atmosphere on Io

	$\theta = 0$	$\theta = 90^\bullet$	$\theta = 180^\bullet$
T (K)	130	110	90
p_s (10^6 dynes cm^{-2})	1.4×10^{-7}	2.5×10^{-10}	2.4×10^{-14}
$H = \frac{kT}{mg}$ (10^5 cm)	9.3	7.9	6.4
$n_o = \frac{p_v}{kT}$ (cm^{-3})	7.8×10^{12}	1.6×10^{10}	1.9×10^{6}
$N = n_o H$ (cm^{-2})	7.2×10^{18}	1.3×10^{16}	1.2×10^{12}
$L_{mfp} = \frac{1}{\sqrt{2}\, n_o Q}$ (cm)	1.6×10^{1}	7.6×10^{3}	6.4×10^{7}

consider the local atmospheric SO_2 content as predicted by the LB model. Local condensation of the atmosphere would produce a surface mass density $\sigma(\Theta) = P_s(\Theta)/g$ of SO_2 frost. Thus $\sigma(0) = 7.8 \times 10^{-4}$ gm cm^{-2}. Assuming a volume mass density $\rho_s = 0.2$ gm cm^{-3} for SO_2 frost them implies a condensate thickness of ~ 40 microns at $\Theta = 0^o$. If we assume that it requires at least 10 microns of frost to appreciably change the reflectance of the surface, then for $\Theta < 40^o$ local atmospheric condensation can conceivably cause a brighteneing of Io's surface.

Upon emergence from eclipse the dayside surface temperature returns to its pre-eclipse value on a time scale of $\tau_e \sim 10^3$ s (Morrison and Cruikshank, 1974). The SO_2 frost that has condensed during eclipse will now begin to sublimate.

The surface of Io acts as a source or sink for atmospheric SO_2 depending on whether $P_s(\Theta)$ or the surface atmospheric pressure $P(\Theta,0)$ is larger, respectively. For a constant temperature surface, the vertical flux of SO_2 molecules at z = 0 is given approximately by

$$S(\Theta) = \frac{\alpha}{\sqrt{2\pi}\ mC} [P_s(\Theta) - P(\Theta,0)] , \qquad (6)$$

where α is the evaporation coefficient. For single component systems α is close to unity, and we will set $\alpha = 1.0$ in what follows.

We consider the sublimation of SO_2 molecules into a vacuum ($P(\Theta,0) = 0.0$). If there is no horizontal transport, the characteristic time it takes for the sublimating frost to produce at atmosphere which is both in hydrostatic equilibrium and vapor pressure equilibrium with the surface frost is

$$\tau_h \sim \frac{n_o H}{S(\Theta)} \sim \frac{C}{g} \quad . \qquad (7)$$

This characteristic time varies little over the surface of Io; for an average temperature T_{av} = 110 K, $\tau_h \sim 100$ s. Since $\tau_h << \tau_e$, we expect the surface pressure to follow closely the equilibrium vapor pressure of SO_2 at the instantaneous surface temperature. The quantity of SO_2 surface frost necessary to supply a LB atmosphere will then disappear with a time scale τ_e upon emergence from eclipse. Incorporation of energy constraints changes this conclusion by less than a factor of 2 (Fanale et al., 1981). The above considerations and the fact that $\tau_e \sim \tau_b$ lends credibility to the LB model. However, the LB model alone provides no insight on the reason for the possible sporadic nature of the PEB.

The LB model of Io's atmosphere is inadequate in many respects. For instance it completely ignores photochemical and thermal processes in the atmosphere. The photodissociation rate at zero optical depth for SO_2 is $J \sim 10^{-5}$ s^{-1} (Kumar, 1981). The characteristic time for photodissociation of a unit column of SO_2 (for dissociating wavelengths, unit optical depth occurs at a column density of $\sim 10^{17}$ cm^{-2}) is $\tau_c \sim J^{-1} \sim 10^5$ s $\sim \tau_p$. Thus photochemical processes may be extremely important in determining Io's atmospheric structure.

In a similar vein the temperature structure may be other than isothermal. Number densities of order 10^{11} cm^{-3} are comparable to those at the base of the thermospheres of the earth and mars (Chamberlain,

1978). The most characteristic feature of a thermosphere is a gas kinetic temperature which increases with altitude. A scale height for the atmosphere much larger than that given in Table 16 could have important implications for atmospheric escape mechanisms (see chapter II).

The LB model does not incorporate any possible effects due to the presence of Na and K or compounds which incorporate them. The model also does not in itself give any indication of the ionic composition of the ionosphere. Neither does it suggest a reason for the drastic differences between the upstream and downstream ionospheric structures. And finally, the LB model does not give any clues for determining the mechanism(s) which is(are) responsible for the escape of mass from Io.

Many other processes may be listed which are not incorporated in the LB model, but which are probably important for determining the physical characteristics of Io's atmosphere. Suffice it to say that the LB model is incomplete in many important aspects for understanding the many observations which exist of Io and its near-spatial environment.

4. A Theoretical Study of Io's Atmosphere

This thesis consists of several theoretical models of Io's atmosphere and physical processes occurring within it. The primary goals of this thesis are as follows.

(A) We wish to ascertain the chemical composition of Io's atmosphere. For reasons mentioned earlier in this chapter it is important to know which chemical component is the dominant constituent both near Io's surface and also at the exobase.

(B) We wish to determine the total surface pressure on Io, and also if the surface pressure depends on location as it does in the LB model.

(C) In the course of studying atmospheric processes we would like to learn the source of ionization which produces Io's ionosphere. This source (or sources) should be consistent with the upstream/downstream asymmetries as deduced by Pioneer 10(Kliore et al., 1975).

(D) Given a picture of atmospheric structure as provided by obtaining goals A, B, and C, we hope to determine the mechanism(s) which is (are) responsible for the ejection of mass from Io's atmosphere into the Io plasma torus. Of particular importance are the escape rates of the different constituents. It is of interest to learn the manner of interaction between Io's atmosphere and the Io plasma torus.

The plan of this thesis is as follows. In Chapter II we will theoretically investigate the chemical composition of Io's atmosphere. A range of models will be presented which can reproduce the major characteristics of the downstream(dayside) ionosphere. As a by-product we will find the minimum atmospheric density of SO_2 near the terminator (at the surface) required for formation of the ionosphere. A range of plausible exospheric temperatures will be deduced. The effects of having atmospheric Na will also be discussed. In Chapter III we discuss a possible mechanism whereby Na and K might be removed from Io's surface and ejected into the atmosphere. We will also suggest a means by which atmospheric constituents may escape from Io.

REFERENCES

Bagenal, F. and J.D. Sullivan (1981). Direct plasma measurements in the Io torus and inner magnetosphere of Jupiter. J. Geophys. Res. **86**, 8447-8466.

Belton,M.J.S. (1982). An interpretation of the near-ultraviolet absorption spectrum of SO_2: Implications for Venus, Io, and laboratory measurements. Icarus **52**, 149-165.

Binder, A.B. and D.P. Cruikshank (1964). Evidence for an Atmosphere on Io. Icarus **3**, 299-305.

Broadfoot, A.L., and the Voyager Ultraviolet spectrometer Team (1979). Extreme ultraviolet observations from Voyager I encounter with Jupiter. Science **204**, 979-982.

Brown, R.A. (1974). Optical line emission from Io. In Exploration of the planetary system.(A. Woszczyk and C. Iwaniszewska, eds.), D.Reidel Publ. Co., Dordrecht,Holland, pp. 527-531.

Brown, R.A. (1981). The Jupiter hot plasma torus: Observed electron temperature and energy flows. Astrophys. J. **244**, 1072-1080.

Brown, R.A., C.B. Pilcher, and D.F. Strobel (1983). Spectrophotometric studies of the Io torus. In Physics of the Jovian Magnetosphere(A. Dessler, ed.), Cambridge University Press, Cambridge, pp. 197-225.

Brown, R.A. and Y.L. Yung (1975). Io, its atmosphere and optical emissions. In Jupiter(T. Gehrels, ed.), University of Arizona Press, Tucson, pp.1102-1145.

Burrell, G.A. and I.W. Robertson (1915). The vapor pressure of sulfur

dioxide and nitrous oxide at temperatures below their normal boiling points. J. Am. Chem. Soc. **37**, 2691-2694.

Carlson, R.A. (1978). Astrophys. J. **223**,1082-1086.

Chamberlain, J.W.(1978). Theory of Planetary Atmospheres, Academic Press, New York.

Cloutier, P.A., R.E. Daniell,Jr., A.J. Dessler, and T.W. Hill (1978). A cometary ionosphere model for Io. Astrophys. Sp. Sci. **55**, 93-112.

Cook, A.F., E.M. Shoemaker, B.A. Smith, G.E. Danielson, T.V. Johnson and S.P. Synnot (1981). Volcanic Origin of the Eruptive Plumes on Io. Science **211**, 1419-1422.

Cook, A.F., E.M. Shoemaker, and B.A. Smith (1979). Dynamics of volcanic plumes on Io. Nature **280**, 743-746.

Durrance, S.T., P.D. Feldman, and H.A. Weaver (1982). Rocket detection of ultraviolet emissions from neutral oxygen and sulfur in the Io torus. B.A.A.S. **14**, 763.

Fanale, F.P., W.B. Banerdt, L.S. Elson, T.V. Johnson, and R.W. Zurek (1982). Io's surface: Its phase composition and influence on Io's atmosphere and Jupiter's magnetosphere. In Satellites of Jupiter (D. Morrison, ed.), Univ. of Arizona press, Tucson, pp. 756-781.

Fanale, F.P., W.B. Banerdt, and D.P. Cruikshank (1981). Io: Could SO_2 condensation/sublimation cause the sometimes reported post-eclipse brightening? Geophys. Res. Lett. **8**, 625-628.

Fanale, F.P., R.H. Brown, D.P. Cruikshank, and R.N. Clarke(1979). Significance of absorption features in Io's IR reflectance spectrum. Nature **280**, 761-763.

Fanale, F.P., T.V. Johnson, and D.L. Matson (1974). Io: A surface evaporite deposit? Nature **186**, 922-925.

Hirschfelder, J.D., C.F. Curtiss, and R.B. Bird (1954). Molecular Theory of Gases and Liquids, John Wiley and Sons, Inc., New York.

Howell, R.R., D.P. Cruikshank, and F.P. Fanale (1983). Sulfur dioxide abundance and location on Io. Paper given at IAU Colloquium No 77. Natural Satellites, at Cornell Univ., N.Y.

Johnson, T.V.,A.F. Cook, III, C.Sagan, and L.A.Soderblom(1979). Volcanic resurfacing rates and implications for volatiles on Io. Nature **280**, 746-750.

Kliore, A.J., G. Fjeldbo, B.L. Seidel, D.N. Sweetnam, T.T.Sesplaukis, and P.M. Woiceshyn (1975). The atmosphere of Io from Pioneer 10 radio occultation measurements. Icarus **24**, 407-410.

Kumar, S. (1979). The stability of the SO_2 atmosphere on Io. Nature **280**, 758-760.

Kumar, S. (1980). A model of the SO_2 atmosphere and ionosphere of Io. Geophys Res. Lett. **7**, 9-12.

Kumar, S. (1982). Photochemistry of SO_2 in the atmosphere of Io and implications on atmospheric escape. J. Geophys. Res. **87**, 1677-1684.

Kumar, S. and D.M. Hunten (1982). The atmosphere of Io and other satellites. In Satellites of Jupiter (D. Morrison, ed.) Univ. of Arizona Press, Tucson, pp. 782-806.

Lewis, J.S. (1971). Satellites of the outer planets: their physical and chemical nature. Icarus **15**, 174-185.

Matson, D.L., B.A. Goldberg, T.V. Johnson, and R.W. Carlson (1977). Images of Io's sodium cloud. Science **199**, 531-533.

McEwen, A.S. and L.A. Soderblom (1983). Two Classes of Volcanic Plumes on Io. Icarus **55**, 191-217.

Morrison, D. and D.P. Cruikshank (1974). Physical properties of the natural satellites. Space Science Reviews **15**, 641-739.

Nash, D.B. (1983). Laboratory IR spectra of SO_2 frost, adsorbate, and gas over various substrates, and applications to Io's surface composition. Paper given at IAU Colloquium 77, Natural Satellites, Cornell University, N.Y.

Nash, D.B. and R.M. Nelson (1979). Spectral evidence for sublimates and adsorbates on Io. Nature **280**, 763-766.

Pearl, J., R. Hanel, V. Kunde, W. Maguire, K. Fox, S. Gupta, C. Ponnamperuma, and F. Raulin (1979). Identification of gaseous SO_2 and new upper limits for other gases on Io. Nature **280**, 755-758.

Porco, C.C., J.T. Trauger, and R.W. Carlson (1980). A comparison of sodium and potassium velocity structures near Io. Paper given at IAU Colloquium 57, Satellites of Jupiter, Kailua-Kona, Hawaii, May 13-16, 1980.

Sinton, W.M. (1973). Does Io have an Ammonia Atmosphere? Icarus **20**, 284-296.

Smith, B.A., E.M. Shoemaker, S.W. Keiffer, and A.F. Cook (1979). The role of SO_2 in volcanism on Io. Nature **280**, 738-743.

Smith, B.A. and S.A. Smith (1972). Upper limits for an atmosphere on Io. Icarus **17**, 218-222.

Smyth, W.H. and M.B. McElroy (1978). Io's sodium cloud: Comparison of models and two-dimensional images. Astrophys. J. **226**, 336-346.

Smyth, W.H. and D.E. Shemansky (1982). Escape and ionization of atomic oxygen from Io.

Smythe, W.D., R.M. Nelson, and D.B. Nash (1979). Spectral evidence for SO_2 frost or adsorbate on Io's surface. Nature **280**, 766.

Strom, R.G., R.J. Terrile, H. Masursky and C. Hansen (1979). Volcanic eruption plumes on Io. Nature **280**, 733-736.

Trafton, L. (1975). Detection of a potassium cloud near Io. Nature **258**, 690-692.

Trafton, L. (1981). A survey of Io's potassium cloud. Astrophys. J. **247**, 1125-1140.

Veverka, J., D. Simonelli, P. Thomas, D. Morrison, and T.V. Johnson (1981). Voyager search for posteclipse brightening on Io. Icarus **47**, 60-74.

Wagman, D.D. (1979). Sublimation pressure and enthalpy of sublimation of SO_2 from 90 K to 197.6 K (triple point). Chemical Thermodynamics Data Center Report, National Bureau of Standards, Washington, D.C.

The Atmosphere and Ionosphere of Io

M.E. Summers and Y.L. Yung

Division of Geological and Planetary Sciences

California Institute of Technology

Pasadena, California 91125

Contribution number 4085 from the Division of Geological and Planetary Sciences, California Institute of Technology, Pasadena, California 91125.

Abstract

A range of theoretical models of the compositional structure of Io's dayside atmosphere and ionosphere are developed. The dominant neutral gas, SO_2, is provided by sublimation of surface frost. Photochemical processes lead to the build up of O, S, SO, and O_2 as minor gasses near Io's surface while O becomes the dominant gas near the exobase. The vertical column density of O_2 in all models considered is less than 10^{14} cm^{-2}. The dayside ionosphere is formed as a result of ionization of neutral species by solar UV radiation. Charge exchange and rearrangement reactions are important for determining the ionic composition of the ionosphere. The dominant ion in the models considered is SO^+. A number of charge exchange reactions are identified whose rates need to be better determined in order to refine the present model of the ionosphere. The best matches of the model ionospheres to that observed by the Pioneer 10 radio occultation experiment require atmospheric surface concentrations of SO_2 in the range of 2.5×10^9 to 1×10^{11} cm^{-3}, and an exospheric temperature in the range of 960 K to 1230 K. The ratio of the escape fluxes of O to S from the exobase is ≥ 2 in the models considered, while the models which allow surface deposition of minor constituents always have a total sulfur depositional rate greater than 1/2 of the total oxygen depositional rate. Thus a surface enrichment of S relative to that predicted by a pure SO_2 surface. The depositional rate of this "excess" sulfur is in the range 100 m to 1 km thickness per billion years.

Atmospheric Na is provided by surface sputtering of SO_2 surface frost with Na impurities by MeV type magnetospheric ions. An upward flux of Na_2O of 5×10^7 cm^{-2} s^{-1} leads to an escape flux of Na from the exobase of 1×10^7 cm^{-2} s^{-1}. The chemistry (ion and neutral) of Na species in the atmosphere has only minor effects on the major characteristics of the atmosphere and ionosphere.

1. Introduction

In this paper we discuss the chemical and ionic composition of Io's dayside atmosphere. The observational basis for our theoretical study of the sunlit atmosphere consists principally of three parts. The IRIS detection of gaseous SO_2 on Io's dayside (Pearl et al., 1979) provides the first part. We assume that atmospheric photochemistry is primarily based on the SO_2 molecule and its photodissociation products. The second part of our observational basis is the dayside (downstream) ionospheric electron density profile as determined by Pioneer 10 (Kliore et al., 1975). The third part consists of the fact that Na is observed to be streaming away from Io (Matson et al., 1977).

The dayside (downstream) ionosphere electron density profile was determined by the Pioneer 10 radio occultation experiment (Kliore et al., 1975). The point of closest approach of the grazing radio ray to the satellite was at a zenith angle of $\theta = 81°$, which corresponds to about 5:24 pm local time. Fanale et al. (1982) discuss a locally buffered SO_2 atmosphere on Io in the context of the IRIS discovery of gaseous SO_2 above the dayside surface. In Fanale's model near the terminator ($\theta = 90°$) the surface number density of SO_2 is of order of 10^{10} cm^{-3}. Atmospheric total number densities of this order of magnitude are characteristically found in the thermospheres of the planets. For example, in the earth's atmosphere eddy mixing processes become less important than molecular diffusion above 100 km (Banks, 1969). Above 120 km each major neutral gas constituent of the atmosphere assumes a density distribution with altitude that is

determined by the temperature profile and the individual species' scale height, i.e., the species are in diffusive equilibrium. The atmospheric total number density at 120 km above the earth's surface is of order 10^{12} cm^{-3} (primarily N_2; Banks, 1969). This region at ~120 km is generally known as the turbopause or equivalently the homopause (Houghton, 1977). On Venus the turbopause occurs at an altitude of roughly 150 km on the dayside at which point the principal constituent CO_2 has a number density of order 10^{11} cm^{-3} (Kumar and Hunten, 1974). Mars also has a CO_2 atmosphere and in this case the turbopause probably lies near 120 km where the density is of order 10^{11} cm^{-3} (McElroy et al., 1977). The density and temperature profiles for Jupiter's H_2 atmosphere are not known accurately for the upper atmosphere. However, it is likely that the turbopause (if one does exist) lies more than 200 km above the tropopause and at a density $< 10^{14}$ cm^{-3} (Chamberlain, 1978).

For the earth, it is known that above 120 km the temperature profile of the mid-latitude neutral atmosphere is determined by local energy deposition due to absorption of solar ultraviolet radiation and the downward transport of thermal energy by molecular conduction (Banks, 1969). This implies a neutral gas kinetic temperature that increases with altitude above the turbopause, which has been verified by numerous rocket and satellite measurements (Banks, 1969). In general, a gas in diffusive equilibrium has a number density which decreases exponentially with increasing altitude. The scale height which controls the rate of decrease is proportional to the temperature. The rate of heating of the neutral gas by absorption of solar ultraviolet photons is proportional

to the local density of the absorbing gas (Bauer, 1973). The neutral gas thermal conductivity is to first order independent of gas density. Thus at sufficiently low densities (high altitudes) an almost isothermal state of the neutral atmosphere should exist. This, too, has been verified by observations (Banks, 1969). The case for the other planets' thermospheres, and probably Io's as well, is slightly more complicated due to the presence of gases which can radiate in the infrared and effectively cool the gas. However, the gas must first reach a sufficiently high kinetic temperature so as to be able to excite the infrared molecular states which can then decay, radiating to space, and cool the gas. In general, this means a temperature higher than that at the turbopause.

In summary then, a thermosphere has two main physical characterizations. First, the individual constituents present approach diffusive equilibrium above the turbopause. Second, the gas kinetic temperature increases with altitude above the turbopause and approaches an asymptotic value at high altitudes (usually a few scale heights above the turbopause). By comparing gas number densities at the base of the thermospheres of the other planets to that predicted by the "locally buffered" model of Io's SO_2 atmosphere we infer that over much if not all of Io's surface the atmosphere may be thermospheric in character.

A quantitative description of the formation of the terrestrial ionosphere was first developed by S. Chapman (1931). The actual atmosphere is much more complicated than implied by Chapman's original analysis and many elaborations on his original theory have been made (see Chamberlain, 1978); however, the basic principles remain unchanged. The

ion production rate in the upper atmosphere (thermosphere) due to ionization by solar EUV radiation is proportional to the number density of the neutral gas, the ionization cross-section of the molecule, and the flux of ionizing photons. Thus, the shape of the ion production profile is partly determined by the neutral gas profile. If diffusion of plasma is unimportant, then the electron density profile will also be determined by the neutral density distribution (Bauer, 1973). On the other hand, if plasma transport (ambipolar diffusion) dominates, then the electron density profile will depend on the plasma temperature. For thermal equilibrium where the electron, ion, and neutral temperatures are equal, the plasma scale height is equal to twice the neutral gas scale height. In general, it is found that for steady state and thermal equilibrium conditions, the electron density profile is directly related to the neutral density and temperature profiles (Banks, 1969; Bauer, 1973; Chamberlain, 1978). For cases where sources of ionization other than solar ultraviolet produce the ionosphere, the characteristics of the ionosphere may depend on other parameters.

We proceed by assuming that the form of variation with altitude of the gas kinetic temperature in Io's atmosphere is similar to that of the thermosphere of the other planets. Then we will use the diffusion equation along with the calculated production and loss rates for each neutral constituent to determine the degree to which the neutral species are in diffusive equilibrium. Once the properties of the neutral atmosphere are determined, we will calculate the production and loss rates for ions due to solar ultraviolet ionization. In the following analysis the surface number density of SO_2 and the exospheric temperature will be

varied in order to produce an ionosphere that is a best match to the observed ionosphere. A wide variety of imposed boundary conditions on atmospheric constituents will be investigated.

The goal of this paper is to answer a set of five key questions regarding the structure of Io's atmosphere. The questions are as follows.

(A) What is the dominant neutral constituent of Io's atmosphere, and does the dominant constituent change as one moves from Io's surface to the exobase?

(B) What is the source of ionization for Io's ionosphere?

(C) What surface concentration of SO_2 is required for formation of the observed ionosphere?

(D) What is the radial extent of the atmosphere, i.e., where is the location of the exobase?

(E) What is the atmospheric temperature at the exobase?

Answers to these questions will set the stage for a theoretical study of the interaction between Io's atmosphere and Jupiter's magnetosphere.

The plan of this paper is as follows. In section 2 we discuss the assumptions made in the development of our theoretical model of Io's atmosphere. Photochemical processes involving SO_2 and the effects caused by diffusion of atmospheric constituents are described. Section 3 is an examination of the boundary conditions at Io's surface and at the exobase that are expected to be most suitable for modeling Io's atmospheric composition. The processes that may be responsible for

formation of the downstream ionosphere are discussed in section 4. Section 5 is a presentation of the numerical results for the different cases considered. In section 6 we discuss atmospheric sodium. And finally, in section 7 we discuss the implications of our results and present a summary of our findings.

2. Atmospheric Temperature and Compositional Structure

(a) Model atmosphere

The atmosphere and gravity field surrounding Io are taken to be spherically symmetric. The radial variation of the local acceleration of gravity is given by

$$g(r) = g(r_o)\left(\frac{r_o}{r}\right)^2 \qquad (1)$$

where $g(r_o) = 180$ cm s^{-2} is the value at the surface of Io ($r_o = 1820$ km, the radius of Io). Equation (1) breaks down near the L1 and L2 points located at a distance $r_L = 5.77\ r_o$ from Io's center. However, (1) is inaccurate by less than 15% for $r < r_o$. The geopotential distance is defined in terms of the local gravity by

$$\eta(r) = \int_{r_o}^{r} \frac{g(r')}{g(r_o)}\,dr' = r_o\left(1.0 - \frac{r_o}{r}\right). \qquad (2)$$

The radial dependence of gas kinetic temperature T(r) is not known. We note the analogy drawn between Io's atmosphere and the thermospheres of the other planets to parameterize T(r) in a form that has shown to provide reasonable agreement with gas kinetic temperatures in the upper atmospheres of the Earth and Mars (Chamberlain, 1978). The analytic form for T(r) that we use was developed by David Bates (1959) for the

terrestrial thermosphere. The temperature variation may be expressed as

$$T(r) = T_\infty \, (1.0 - ae^{-\tau\eta}) \tag{3}$$

where a and τ are constants

$$a = 1.0 - \frac{T_o}{T_\infty} \tag{4}$$

$$\tau = \frac{1.0}{T_\infty - T_o} \left(\frac{dT}{dr} \right)_o \quad . \tag{5}$$

The three parameters that must be specified to uniquely define T(r) are: T_o, the temperature at the base of the atmosphere; T_∞, the asymptotic temperature in the upper atmosphere (the exospheric temperature); and $(dT/dr)_o$, the vertical temperature gradient at the base of the atmosphere ($r = r_o$). We have taken $T_o = 110$ K which is identical to the area weighted average surface temperature T_{av} defined in Fanale et al., (1981). Bates (1959) showed that in the case of the earth's thermosphere, good agreement with observations was obtained by taking $(dT/dr)_o = (T/H)_o$, where $H = kT/mg$ is the scale height of the major atmospheric constituent. In any case, Bates (1959) found that the agreement was not very sensitive to the exact value of $(dT/dr)_o$. For Io's atmosphere we take

$$\left(\frac{dT}{dr}\right)_o = \left(\frac{T}{H}\right)_o = \frac{mg(r_o)}{k} = 14 \text{ K/km} \quad . \tag{6}$$

We are thus left with one as yet undefined parameter, T_∞, for complete specification of T(r).

The characteristic hydrostatic adjustment time for an SO_2 atmosphere, $\tau_h \sim C/g \sim 10^2$ s (where $C^2 = kT/m$ is the isothermal sound speed), is much smaller than Io's rotational period, $\tau_p \sim 10^5$ s. Here we assume that the atmosphere is in hydrostatic equilibrium. The barometric equation

$$\frac{dP(r)}{dr} = -\rho(r)\, g(r) \quad , \tag{7}$$

where $P = NkT$ is the pressure, $\rho = mN$ is the mass density, and N(r) is the number density of SO_2 molecules, may be then used with T(r) defined by equation (3) to determine N(r). Integration of (7) for a single constitutent atmosphere leads to an analytic expression for N(r) (Chamberlain, 1978).

With the above assumptions the model atmosphere for Io is seen to be dependent upon two as yet unspecified parameters, $N(r_o)$ and T_∞. These parameters will be adjusted in order to obtain the best agreement between the modeled ionosphere and the observed ionosphere.

(b) Photochemistry and chemical kinetics

Table 1 lists the most important chemical reactions along with their preferred rate coefficients that are used in our photochemical study of Io's SO_2 atmosphere. This set of reactions includes some of the sulfur chemistry considered in previous works related to the stratosphere of Venus (Yung and DeMore, 1982; Winick and Stewart, 1980) and the stratosphere of the Earth (DeMore et al., 1983), but which has been reassessed and updated. Our set also greatly improves upon the set of reactions used by Kumar (1982) in an earlier study of Io's SO_2 atmosphere. Some of the measured reaction rates involving sulfur in Table 1 have been reviewed and evaluated by Baulch and Drysdale (1976), and more recently by DeMore et al. (1983). The references from which we have taken the preferred rate coefficients are listed on the right hand side of Table 1.

The solar ultraviolet photon flux that produces dissociation of molecules in Io's atmosphere lies principally between 1200 Å and 2400 Å. The solar photon flux used in our calculations of photodissociation rates was taken from Mount et al. (1980) and adjusted to solar minimum conditions (solar minimum occurred in 1976 and the Pioneer 10 occultation in 1974), although Mount et al. (1980) found no evidence for solar cycle variability of the photon flux exceeding 15% for wavelengths above 2000 Å. More than 70% of SO_2 and SO dissociation occurs at wavelengths longward of 2000 Å. The solar photon flux of Mount et al. (1980) was averaged over 50 Å intervals from 12 Å to 1850 Å, and over 10 Å intervals from 1850 Å to 2500 Å. The photon fluxes of Mount et al.

TABLE 1

List of Essential Reactions for the Neutral Atmosphere of Io
with Their Preferred Rate Coefficients

	Reaction	Rate	Reference
(R1)	$O_2 + h\nu \rightarrow 2O$	$J_1 = 9.1(-8)$	Hudson (1971)
(R2)	$SO + h\nu \rightarrow S + O$	$J_2 = 1.1(-5)$	Phillips (1981)
(R3)	$SO_2 + h\nu \rightarrow SO + O$	$J_3 = 2.8(-6)$	Golomb et al. (1962), Thompson et al. (1963),
(R4)	$SO_2 + h\nu \rightarrow S + O_2$	$J_4 = 1.0(-6)$, $y_4 = 0.5$	Warneck et al. (1964), Okabe (1971), Welge (1984), Driscoll and Warneck (1968)
(R5)	$S_2 + h\nu \rightarrow 2S$	$J_5 = 5.2(-5)$	Brewer and Brabson(1966) Meyer et al. (1971)
(R6)	$S + O_2 \rightarrow SO + O$	$k_6 = 2.3(-12)$	DeMore et al. (1983)
(R7)	$SO + O_2 \rightarrow SO_2 + O$	$k_7 = 2.4(-13)\ e^{-2370/T}$	DeMore et al. (1983)
(R8)	$SO + SO \rightarrow SO_2 + S$	$k_8 = 5.8(-12)\ e^{-1760/T}$	Herron and Huie (1980)
(R9)	$O + O_3 \rightarrow 2O_2$	$k_9 = 1.5(-11)\ e^{-2218/T}$	Yung and DeMore (1982)
(R10)	$S + O_3 \rightarrow SO + O_2$	$k_{10} = 1.2(-11)$	Yung and DeMore (1982)
(R11)	$SO + O_3 \rightarrow SO_2 + O_2$	$k_{11} = 2.5(-12)\ e^{-1100/T}$	Yung and DeMore (1982)
(R12)	$SO_3 + SO \rightarrow 2SO_2$	$k_{12} = 2.0(-15)$	Yung and DeMore (1982)
(R13)	$2O + M \rightarrow O_2 + M$	$k_{13} = 8.6(-28)\ T^{-2}$	Yung and DeMore (1982)
(R14)	$2S + M \rightarrow S_2 + M$	$k_{14} = 2.0(-33)$	Baulch and Drysdale (1973)
(R15)	$O_2 + O + M \rightarrow O_3 + M$	$k_{15} = 1.35(-33)$	Yung and DeMore (1982)
(R16)	$SO + O + M \rightarrow SO_2 + M$	$k_{16} = 6.0(-31)$	Yung and DeMore (1982)
(R17)	$SO_2 + O + M \rightarrow SO_3 + M$	$k_{17} = 8.0(-32)\ e^{-1000/T}$	Yung and DeMore (1982)
(R18)	$NaO + O \rightarrow Na + O_2$	$k_{18} = 1.6(-10)$	Liu and Reed (1979)
(R19)	$NaO_2 + O \rightarrow NaO + O_2$	$k_{19} = 2.5(-11)$	Kirchhoff and Clemesh (1983)

TABLE 1 - Continued

	Reaction	Rate	Reference
(R20)	$Na_2O + O \rightarrow 2NaO$	$k_{20} = 2.0(-11)$	estimated
(R21)	$Na + O + M \rightarrow NaO + M$	$k_{21} = 1.0(-33)$	estimated
(R22)	$Na + O_2 \rightarrow NaO_2 + M$	$k_{22} = 8.4(-34)\ e^{-290/T}$	Liu and Reed (1979)

Note. The units for photolysis rates (J), and two-body and three-body reactions (k) are sec^{-1}, $cm^3\ sec^{-1}$, and $cm^6\ sec^{-1}$, respectively.

(1980) were reduced by a factor of $(5.2)^2 = 27.04$ to account for the reduction of flux (photons cm^{-2} s^{-1}) between the earth and Io. The photolysis rates at zero optical depth for several molecules are presented in Table 1 along with references from which the appropriate cross sections were taken.

A schematic diagram summarizing the major pathways for production and loss of chemical species in the atmosphere of Io is shown in Figure 1. The surface supplies SO_2 to the atmosphere via sublimation of SO_2 surface frost. Once in the atmosphere, SO_2 may photodissociate along two possible branches as discussed below.

In its ground state, SO_2 is a nonlinear molecule with an O-S-O angle of 119.5° (Okabe, 1978). The bond energy $D(OS-O) = 5.65 \pm 0.01$ eV (Huie and Rice, 1972; Okabe, 1972). The photochemistry of SO_2 is initiated by absorption of ultraviolet photons which have enough energy to break this bond,

$$SO_2 + h\nu \rightarrow SO + O \qquad \lambda \leq 2190 \text{ Å} \quad . \qquad (R3)$$

The absorption cross sections for SO_2 have been measured by Golomb et al. (1962), Thompson et al. (1963), and Warneck et al. (1964) finding substantial agreement in the spectral region 1850 Å to 2170 Å where the data overlapped. The data of Golomb et al. (1962) extended to 1050 Å, close to SO_2's ionization threshold at 1010 Å. The region longward of 1900 Å shows a highly structured absorption spectrum with as many as 18 bands seen between 2000 Å and 2300 Å (see also Okabe, 1971). The fluorescence spectrum of SO_2 between 2000 Å and 2300 Å has been measured

Figure 1. Schematic diagram showing the major sources and sinks for atmospheric constituents.

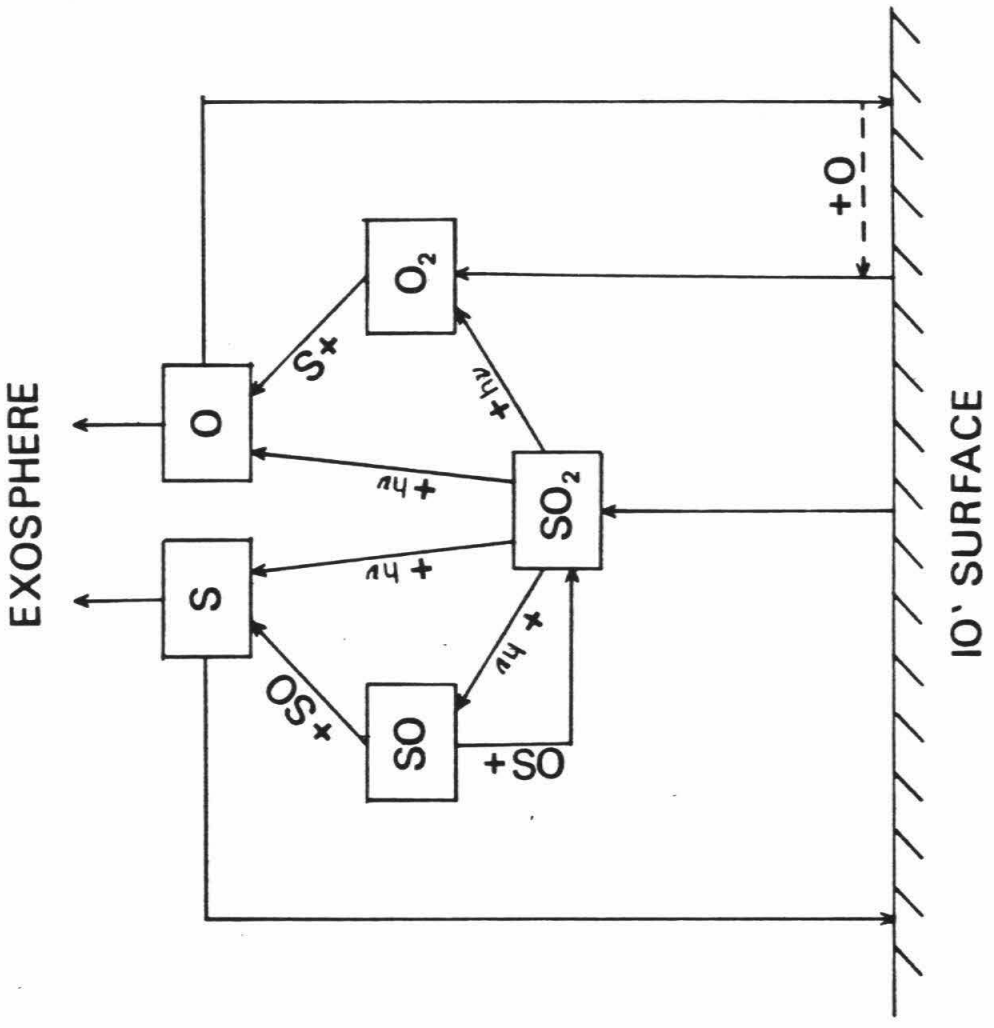
EXOSPHERE
O
S
O_2
SO
SO_2
+O
+S
+SO
+hν
IO' SURFACE

by Okabe (1971). We have used this spectrum to estimate quantum yields for reaction (R3). The yield is approximately 0.65 at the dissociation threshold at 2190 Å and increase to nearly 1.0 at 2000 Å.

At a photon energy of $h\nu \geq 5.99$ eV the photodissociation branch

$$SO_2 + h\nu \rightarrow S + O_2 \qquad \lambda \leq 2070 \text{ Å} \qquad (R4)$$

becomes energetically feasible (Welge, 1974). Since an energy of 5.99 eV is insufficient to break SO_2 into 3 atoms, the primary process (R4) requires that SO_2 is first produced in an atomic rearranged state in which the O-S-O bond angle is decreased sufficiently at the moment of the S ejection so that an O-O bond can be formed. Process (R4) is analogous to NO_2 photodecomposition (Doering and Mahan, 1961) in which the branch forming N and O_2 is about 10 times more likely than that forming NO and O (at 1236 Å). Driscoll and Warneck (1968) have studied the photolysis of SO_2 at 1849 Å and have deduced an upper limit to the branching ratio for process (R4) of $y_4 \leq 0.50$. In section 5 we will consider the sensitivity of the calculated chemical state of Io's atmosphere to uncertainties in y_4.

The ground state ($X^3\Sigma^-$) of SO has a bond energy of D(S-O) = 5.34 $\pm$ 0.02 eV (Okabe, 1978). The cross sections for SO photolysis

$$SO + h\nu \rightarrow S + O \qquad \lambda \leq 2320 \text{ Å} \qquad (R2)$$

have been measured by Phillips (1981). The difficulties associated with laboratory determination of cross sections for (R2) are formidable due

to the need to know the absolute concentrations of SO and SO_2 in the absorption cell, and to know the energy state(s) of SO from which dissociation proceeds (as discussed by Phillips, 1981). However, using the cross sections obtained by Phillips (1981) we find a zero optical depth photolysis rate of $J_2 = 1.1 \times 10^{-5}$ s^{-1}, about 2 orders of magnitude larger than the photolysis rate for O_2 (reaction R1), even though the $B^3\Sigma^- - X^3\Sigma^-$ band system (1900 Å - 2400 Å) of SO is analogous to the Schumann-Runge band system of O_2 which lies between 1300 Å and 2000 Å. The reason for the large difference in photodissociation rates is due to the difference in spectral locations of the absorption band systems. Absorption by SO occurs at longer wavelengths where the solar flux πF_λ is larger.

Molecular oxygen (O_2) is photodissociated (R1) primarily by absorption in the Schumann-Runge continuum. The oxidation of sulfur compounds also results in a loss of atmospheric O_2. The chemical exchange reaction

$$S + O_2 \rightarrow SO + O + \Delta_6 \qquad \text{(R6)}$$

is exothermic ($\Delta_6 \simeq 0.22$ eV) and is important for determining the oxidation state of sulfur in the atmosphere of Venus (Winick and Stewart, 1980; Yung and DeMore, 1982). The measured values for the rate coefficient for (R6) have been evaluated by Baulch and Drysdale (1976) and more recently by DeMore et al. (1983). The recommended value of $k_6 = 2.3 \times 10^{-12}$ cm^3 $molecule^{-1}$ s^{-1} is based upon the laboratory measurements of Davis et al. (1972) which covered a temperature range 252-423 K and

showed zero activation energy for (R6) with the limits of determination, i.e., $E_6 = 0.0 \pm 0.005$ eV. This value for k_6 is in good agreement with four other measurements made near room temperature (DeMore et al., 1983). The value of k_6 used by Kumar (1981) to model SO_2 photochemistry on Io was based on the combustion data of Von Homann et al. (1968) and had an activation energy $E_6 = 0.25$ eV. Extrapolation of the Von Homann et al. (1968) expression for k_6 to 298 K gives a value for k_6 which is approximately 3 orders of magnitude smaller than the room temperature rate measured by several independent researchers (DeMore et al., 1983). For this reason, we will follow the recommendation of DeMore et al. (1983) and use the value for k_6 obtained by Davis et al. (1972).

The relative abundances of S, O, SO, and O_2 are also affected by the exchange and disproportionation reactions

$$SO + O_2 \rightarrow SO_2 + O + \Delta_7 \qquad \text{(R7)}$$

and

$$SO + SO \rightarrow SO_2 + S + \Delta_8 \quad . \qquad \text{(R8)}$$

These reactions are exothermic ($\Delta_7 \simeq 0.53$ eV, $\Delta_8 \simeq 0.31$ eV) and have activation energies, $E_7 = 0.20$ eV and $E_8 = 0.15$ eV, and rate constants $k_7 = 2.4 \times 10^{-13}\ e^{-2730/T}$, and $k_8 = 5.8 \times 10^{-12}\ e^{-1760/T}$ (Okabe, 1978; DeMore et al., 1983; Herron and Huie, 1980). At temperatures characteristic of the surface temperature of Io ($T \simeq 100$ K) it is clear that for $n_{SO} \sim n_S$, (R6) will dominate over (R7) as a loss mechanism for O_2.

The extended reaction set listed in Table 1 contains many 2-body and 3-body reactions which have an insignificant influence on the overall chemical structure of Io's predominantly SO_2 atmosphere at the terminator ($N(r_o) \sim 10^{10}$ cm^{-3}) but which may be marginally important near Io's subsolar region ($N(r_o) \sim 10^{13}$ cm^{-3}) and are included here for completeness. The reactions important for formation of Io's dayside ionosphere are discussed in section 4, and the chemistry of Na compounds is described in section 6.

(c) Diffusion

The radial variation of the abundances of chemical species in Io's atmosphere is influenced by molecular diffusion and possibly by eddy diffusion. The time and spatial variation of the abundance of constituent i is determined by the radial continuity equation

$$\frac{\partial n_i}{\partial t} + \frac{1}{r^2}\frac{\partial}{\partial r}\left(r^2 F_i(r)\right) = P_i(r) - L_i(r) \quad , \qquad (8)$$

where $F_i(r) = n_i(r)\, u_i(r)$ is the radial flux of constituent i, $u_i(r)$ is the diffusion velocity, $P_i(r)$ and $L_i(r)$ are the local production and loss rates for constituent i, respectively. The subject of molecular and eddy diffusion with application to planetary upper atmospheres has an extensive literature (Chamberlain, 1978; Hunten, 1973a; Hunten, 1973b). Briefly, diffusion is caused by concentration gradients, pressure gradients, temperature gradients, and turbulence.

The diffusion velocity u_i for the i^{th} minor constituent in a multicomponent gas is given by

$$u_i = -D_i\left(\frac{d\ \ln\ n_i}{dr} + \frac{1}{H_i} + \frac{d\ \ln\ T}{dr}\right) - K\frac{d\ \ln\ f_i}{dr} \qquad (9)$$

where $f_i = n_i/n$ is the mixing ratio of constituent i, n is the total number density of the gas, K is the eddy diffusion coefficient, and D_i is the average diffusion coefficient. The binary diffusion coefficient $D_{ij} = b_{ij}/n$ where b_{ij} is the binary collision coefficient for constituents i and j. In writing (9) we have neglected the effects of thermal diffusion which is small for heavy atoms and molecules.

An extensive study of binary diffusion coefficients for many pairs of gases has been performed by Mason and Marrero (1970); however, little research has been performed on the relative diffusion of sulfur and oxygen compounds such as S, SO, SO_2, O, and O_2. We have utilized results from classical gas kinetic theory along with calculations and data on the viscosity of pure gases (S, O, O_2, SO_2) to estimate several binary diffusion coefficients. According to gas kinetic theory (Chapman and Cowling, 1970), the first approximation (assuming the molecules are rigid elastic spheres) to D_{12} (diffusion of constituent 1 through background gas 2) is given by

$$D_{12} = \frac{3}{8nQ}\left(\frac{\pi kT}{2m_r}\right)^{1/2}, \qquad (10)$$

where $m_r = m_1m_2/(m_1 + m_2)$ is the reduced mass and

$$Q = \frac{\pi}{2} (\sigma_1 + \sigma_2) \qquad (11)$$

is the collision cross section. The collision diameters for molecules 1 and 2 are σ_1 and σ_2, respectively. The self diffusion coefficient D_{11} is given by (10) when constituent 1 is the same as constituent 2. The self diffusion coefficient D_{11} is related to the gas dynamic viscosity η by $D_{11} = 3A\eta/\rho$ (Chapman and Cowling, 1970), where A is a numerical coefficient which depends on the type of molecular interaction. For rigid elastic spheres 3A = 1.2. The dynamic viscosity of pure SO_2 and pure O_2 has been determined experimentally (Chapman and Cowling, 1970), and that for pure S and pure O by theoretical means (Konowalow et al., 1959). We have used these results to determine $\sigma(T)$ for O, S, O_2, and SO_2. Given the temperature variation of the collision diameter we then used (10) and (11) to determine $b_{ij}(T)$ for several pairs of molecules. The numerical results were then fitted to the functional form $b = AT^s$ for each pair of gases individually. A summary of these estimates are presented in Table 2. As a check on this method, results for diffusion of O through O_2 were calculated by the above procedure and compared to experimental results (Mason and Marrero, 1970). The agreement was better than 15% over the temperature range 200 K to 1000 K.

Turbulence gives rise to mixing, and the component of diffusion velocity due to atmospheric turbulence is parameterized by an eddy diffusion coefficient K (see Banks and Kockarts, 1973). Unfortunately, no adequate theory exists for determining K in a planetary atmosphere.

TABLE 2

Binary Diffusion Parameters

Gas Pairs*	10^{-16} A	S
O, S	4.45	0.794
O, O_2	9.39	0.751
O, SO_2	1.84	0.934
O_2, SO_2	1.20	0.939
S, SO_2	0.81	0.943

*Constants in the formula $b = AT^s$, where $D = b/n$ (D has units $cm^2\ s^{-1}$).

Usually K is found by semi-empirical methods. In some studies, K is left as an adjustable parameter in modeling the vertical variation of atmospheric constituents; the value of K is chosen so as to give the best agreement between model and observations. Values for K used in modeling the atmospheres of Mars, Venus, and the Earth generally lie in the range 10^5 to 10^8 cm^2 s^{-1} (McElroy et al., 1976; Yung and DeMore, 1982; Allen et al., 1981). In section 5 we will consider the effects of eddy diffusion on the calculated atmospheric compositional structure.

The specification of boundary velocities at Io's surface and at the critical level (exobase) allows one to obtain a solution of (8) for $n_i(r)$. Integrating (8) between $r = r_o$ and $r = r_c$ (r_c = critical level radius) gives, in a steady state,

$$\int_{r_o}^{r_c} [P_i(r) - L_i(r)]\, r^2\, dr = r_c^2\, F_i^c(r_c) - r_o^2\, F_i^o(r_o) \quad , \quad (12)$$

where $F_i^c(r_c) = n_i(r_c)\, u_i(r_c)$ and $F_i^o(r_o) = n_i(r_o)\, u_i(r_o)$ are the boundary fluxes (molecules cm^{-2} s^{-1}) of constituent i at the critical level and surface, respectively. In the next section we discuss the specification of boundary diffusion velocities.

3. Boundary Conditions

(a) The critical level

The uppermost region of a planet's atmosphere is the exosphere (sometimes called the planetary corona). The base of this region is the critical level (or equivalently the exobase) defined to be at the radius, r_c, at which the radially outward integrated density provides 1 collision mean free path to an atom or molecule, i.e.,

$$\int_{r_c}^{\infty} n(r)\, Q\, dr = 1 \qquad (13)$$

If Io's atmosphere and its interaction with Jupiter's corotating magnetospheric (low energy) plasma is spherically symmetric (it probably isn't!), then one would expect the strongest interaction to occur in the region $\simeq r_c \pm H$. This is because, in this region an impacting magnetospheric ion would begin to lose its kinetic energy, i.e., it experiences its first collision with an atmospheric atom. This is also the region from which atmospheric atoms with sufficient kinetic energy can escape to Jupiter's magnetosphere without impacting another atmospheric atom, on the average. Due to the asymmetric nature of the interaction, important processes probably occur at $r \gg r_c$. However, we choose to ignore this direct interaction and discuss two approximations to what may be happening at the exobase. In the first approximation we simply set the escape velocity equal to the average upward velocity of the

molecules at $r = r_c$. We will refer to this case as the non-thermal escape model.

In the absence of nonthermal processes, Io's atmosphere will lose mass by means of thermal evaporation (Jeans' escape) of molecules from the critical level. The discussion of this process is made simpler with a definition of the normalized potential energy of an atom i,

$$\lambda_i = \frac{GMm_i}{kTr} = \frac{r}{H_i}$$

$$= 6.31 \left(\frac{r_o}{r}\right) \left(\frac{1000}{T}\right) \left(\frac{m_i}{16\, m_H}\right) \qquad (14)$$

where $G = 6.67 \times 10^{-8}$ dynes cm^2 gm^{-2}, $M = 8.9 \times 10^{25}$ gm is the mass of Io, and m_H is the mass of a hydrogen atom.

The location of the critical level is determined by the density profile of the major constituent. We consider a single component exosphere which is isothermal. In the case of a plane-parallel atmosphere, equation (13) reduces to $n_c Q H_c = 1$. When (13) is evaluated for a spherically symmetric atmosphere one obtains

$$n_c\, H_c\, Q K_c(\lambda) = 1 \qquad (15)$$

where $K_c(\lambda)$ is the spherical correction factor (Chamberlain, 1961). The maximum value of K_c is 1.44 and occurs at $\lambda = 5$. Equation (15) determines the location of the critical level.

The thermal escape flux (Jeans' flux) for constituent i at r_c is

given by (Chamberlain, 1978)

$$F_i^J(r_c) = n_i(r_c)\ w_i(r_c)$$

$$= n_i(r_c)\ \frac{C_i}{\sqrt{2\pi}}\ (1 + \lambda_i(r_c))\ e^{-\lambda_i(r_c)} \qquad (16)$$

where the effusion velocity $w_i(r_c)$ is made up of two parts: $C/\sqrt{2\pi}$ is the average vertical velocity of particles directed upward, and $(1 + \lambda_c)$ $e^{-\lambda_c}$ is the probability that an atom which is directed upward will escape from the gravitational well. This equation should be approximately valid for $\lambda_c > 1.5$. Brinkmann (1970) has shown that for H and He escaping from the Earth's exobase, equation (16) gives results which agree to better than 30% with that obtained by detailed Monte Carlo investigations.

At $\lambda_c = 1.5$, $w_i \simeq C_i$, and the assumption of hydrostaticity breaks down. When $\lambda_c = 1.5$ the average kinetic energy of each atom at r_c is roughly equal to the escape energy. The bulk of the gas will then flow outward at speed $\sim C_i$, analogous to solar wind flow (Hunten, 1973).

(b) The surface of Io

Given a lack of information on the physical properties of Io's surface it is impossible to determine the details of the chemical interaction between the surface and the atmosphere. We consider four types of interaction, and, hence, four corresponding types of surface boundary conditions on atmospheric processes. In all cases we assume that SO_2 is provided by the surface at whatever rate is needed to supply the subsequent loss of S and O containing species to the magnetosphere or back to the surface. The different classes of boundary conditions are discussed below.

A. Chemically inert surface

For this class of boundary conditions we consider the atmospheric chemical structure that would obtain in the situation in which the surface diffusion velocity (and hence, flux) is zero for all constituents other than SO_2. Physically, this requires the atmosphere to be chemically uncoupled from the surface. This also is equivalent to assuming that the sticking coefficients for all atmospheric species (other than SO_2) is identically zero.

B. Surface as a chemical sink

Here we assume that all constituents (other than SO_2) that hit the surface stick to it, i.e., the sticking coefficient is unity. We assume

the surface does not release these gases. Only SO_2 is released by the surface.

The loss rate (i.e., surface flux) is determined by (9) and n_i evaluated at $r = r_o$. However, $(dn_i/dr)_o$ is not known a priori, so we have considered two possibilities for the velocity of material diffusing to Io's surface.

The characteristic diffusion time scale of an atom in an atmosphere is the time it takes the atom to random walk a scale height, i.e., $\tau_D \sim H^2/D$. A characteristic diffusion velocity is then $u_D \sim H/\tau_D \sim D/H$. Using this as a guide we set the diffusion velocity of atoms or molecules to Io's surface equal to

$$u_i(r_o) = -\frac{D_i}{H_a} , \tag{17}$$

where H_a is the scale height of the background atmosphere.

To calculate the maximum diffusion velocity possible near Io's surface we consider the diffusing atoms or molecules that are closer than one collision mean free path to the surface. We assume that the particles have a Maxwellian distribution of velocities. Then it can be shown that the average vertical velocity of particles of constituent i that are moving downward is

$$u_i^{max}(r_o) = -\frac{C_i}{\sqrt{2\pi}} \tag{18}$$

were $C_i^2 = kT/m_i$. We will use equations (17) and (18) for possible

boundary diffusion velocities in this class of boundary conditions.

C. Eddy transport to surface sink

Here the chemical interaction with the surface is identical to that in class B boundary conditions, i.e., the constituents other than SO_2 that hit the surface stick to it and are not released. In this class of boundary conditions (C) the character of atmospheric diffusion near the surface is different. We assume here that eddy diffusion in the atmosphere dominates over molecular diffusion near the surface. If $n(r_o) \sim 10^{10}$ cm^{-3}, then $D \sim 10^7$ cm^2 s^{-1}. Thus, for eddy diffusion to dominate we must have $K > 10^7$ cm^2 s^{-1}. By analogy to the derivation of the molecular diffusion velocity in (17) we can define an eddy diffusion velocity at Io's surface, (see Banks and Kockarts, 1973) i.e.,

$$u_e(r_o) = -\frac{K}{H_a} \qquad (19)$$

Note that now the loss velocity at the surface is the same for all constituents.

D. Surface as catalyst for O_2 formation

The surface of Io may act as a catalyst for the recombination of atomic oxygen to form O_2 (see schematic diagram of atmospheric chemistry, Figure 1). In this scenario, atomic oxygen is first produced in

the atmosphere by photolysis of SO_2 and diffuses to Io's surface. The O atoms stick and begin to thermally migrate along the surface. When two O atoms encounter they can possibly recombine to form O_2, the excess energy released in the recombination being sufficient to eject the O_2 from the surface. In this scenario the surface of Io performs two functions. The first function is to decrease the average distance between O atoms, i.e., increase the effective O atom density. The second function is to act as a third body to conserve energy and momentum during the recombination to form O_2. This is analogous to the function performed by the third body M in the reaction

$$O + O + M \rightarrow O_2 + M \qquad \text{(R13)}$$

This type of scenario has been invoked to explain the high abundance of H_2 in the instellar medium, i.e., H recombines on dust grains to form H_2 (Watson and Salpeter, 1972).

In this case for Io we assume perfect efficiency in converting atomic oxygen to molecular oxygen. In a steady state this implies

$$F^{\downarrow}(O) = 2\, F^{\downarrow}(O_2) \qquad (20)$$

as $r = r_o$. In order to obtain the maximum rate for this process we assume that O diffuses to the surface at the maximum molecular diffusion velocity given by (18).

4. Formation of the dayside ionosphere

Here we discuss the formation of the dayside ionosphere on Io. Solar EUV radiation can create ion-electron pairs when an atom or molecule absorbs a photon which has an energy greater than the ionization threshold. The photoionization reactions and rates important for the ionosphere of Io are listed in Table 3. Of the atoms and molecules listed SO has the lowest ionization threshold at E = 10.2 eV which corresponds to a photon wavelength of 1215 Å. For wavelengths shortward of this threshold we have used the extreme ultraviolet solar flux tabulated by Hinteregger (1970) to calculate ionization rates.

The photoionization of SO_2 has been studied by Dibeler and Liston (1968) in the wavelength range of 1050 Å to 600 Å. They find an ionization threshold at photon energy 12.32 eV. Wu and Judge (1981) have measured the photoabsorption cross sections for SO_2 in the range 175 Å to 760 Å region. For our ionization rate calculations we have used these results assuming that the ionization yields and cross sections from the two sets of data match at 700 Å.

The ionization threshold of SO is 10.2 eV (Dibeler and Liston, 1968). Since there are no data available on the ionization cross sections of SO we have assumed that the cross sections of SO are equal to those of O_2 but shifted 190 Å longward in wavelength so as to match thresholds.

For S and O the photoabsorption cross sections are equal to the ionization cross sections. We have used the ionization cross sections

TABLE 3

List of Essential Reactions for the Ionosphere of Io
with Their Preferred Rate Coefficients

	Reaction	Rate Coefficient	Reference
(R23)	$SO_2 + h\nu \rightarrow SO_2^+ + e$	$J_{23} = 3(-8)$	Wu and Judge (1981), Debeler and Liston (1968)
(R24)	$O_2 + h\nu \rightarrow O_2^+ + e$	$J_{24} = 2.3(-8)$	Brandt and McElroy (1967)
(R25)	$SO + h\nu \rightarrow SO^+ + e$	$J_{25} = 1.1(-7)$	same as O_2
(R26)	$O + h\nu \rightarrow O^+ + e$	$J_{26} = 1.4(-8)$	McGuire (1968)
(R27)	$S + h\nu \rightarrow S^+ + e$	$J_{27} = 2.8(-8)$	McGuire (1968)
(R28)	$Na + h\nu \rightarrow Na^+ + e$	$J_{28} = 3.7(-8)$	Peach (1973)
(R29)	$SO_2^+ + O \rightarrow SO^+ + O_2$	$k_{29} = 1.0(-10)$	estimated
(R30)	$SO_2^+ + O_2 \rightarrow O_2^+ + SO_2$	$k_{30} = 2.8(-10)$	estimated
(R31)	$SO_2^+ + S \rightarrow SO^+ + SO$	$k_{31} = 5.0(-10)$	Albritton(1978)
(R32)	$SO_2^+ + S \rightarrow S^+ + SO_2$	$k_{32} = 1.0(-10)$	estimated
(R33)	$SO_2^+ + SO \rightarrow SO^+ + SO_2$	$k_{33} = 5.0(-10)$	Albritton(1978)
(R34)	$SO_2^+ + SO \rightarrow S^+ + SO_3$	$k_{34} = 1.0(-10)$	estimated
(R35)	$SO_2^+ + Na \rightarrow Na^+ + SO_2$	$k_{35} = 1.0(-11)$	estimated
(R36)	$SO_2^+ + Na \rightarrow NaO^+ + SO$	$k_{36} = 1.0(-11)$	estimated
(R37)	$SO^+ + SO \rightarrow S^+ + SO_2$	$k_{37} = 5.0(-10)$	estimated
(R38)	$SO^+ + Na \rightarrow Na^+ + SO$	$k_{38} = 1.0(-11)$	estimated
(R39)	$SO^+ + Na \rightarrow NaO^+ + S$	$k_{39} = 1.0(-11)$	estimated
(R40)	$S^+ + SO \rightarrow SO^+ + S$	$k_{40} = 2.0(-9)$	estimated
(R41)	$S^+ + O_2 \rightarrow SO^+ + O$	$k_{41} = 1.6(-10)$	Prasad and Huntress (1980)
(R42)	$S^+ + Na \rightarrow Na^+ + S$	$k_{42} = 1.0(-11)$	estimated

TABLE 3 - Continued

	Reaction	Rate Coefficient	Reference
(R43)	$O^+ + SO_2 \rightarrow O_2^+ + SO$	$k_{43} = 1.0(-10)$	estimated
(R44)	$O^+ + SO_2 \rightarrow SO^+ + O_2$	$k_{44} = 1.0(-10)$	estimated
(R45)	$O^+ + SO \rightarrow SO^+ + O$	$k_{45} = 1.0(-10)$	estimated
(R46)	$O^+ + SO \rightarrow S^+ + O_2$	$k_{46} = 1.0(-10)$	estimated
(R47)	$O^+ + SO \rightarrow O_2^+ + S$	$k_{47} = 1.0(-10)$	estimated
(R48)	$O^+ + O_2 \rightarrow O_2^+ + O$	$k_{48} = 3.0(-12)$	Albritton (1978)
(R49)	$O^+ + S \rightarrow S^+ + O$	$k_{49} = 5.0(-10)$	estimated
(R50)	$O^+ + Na \rightarrow Na^+ + O$	$k_{50} = 1.0(-11)$	estimated
(R51)	$O_2^+ + S \rightarrow S^+ + O_2$	$k_{51} = 5.4(-10)$	Prasad and Huntress (1980)
(R52)	$O_2^+ + S \rightarrow SO^+ + O$	$k_{52} = 5.4(-10)$	Prasad and Huntress (1980)
(R53)	$O_2^+ + SO \rightarrow SO^+ + O_2$	$k_{53} = 1.0(-10)$	estimated
(R54)	$O_2^+ + Na \rightarrow Na^+ + O_2$	$k_{54} = 6.4(-10)$	Albritton (1978)
(R55)	$O_2^+ + Na \rightarrow NaO^+ + O$	$k_{55} = 7.1(-11)$	Albritton (1978)
(R56)	$NaO^+ + O \rightarrow Na^+ + O_2$	$k_{56} = 5.0(-11)$	estimated
(R57)	$Na^+ + e \rightarrow Na$	$k_{57} = 4.7(-11)T^{-0.69}$	Prasad and Huntress (1980)
(R58)	$NaO^+ + e \rightarrow Na + O$	$k_{58} = 3.5(-6)T^{-0.5}$	estimated
(R59)	$S^+ + e \rightarrow S$	$k_{59} = 6.8(-11)T^{-0.63}$	Prasad and Huntress (1980)
(R60)	$O_2^+ + e \rightarrow 2O$	$k_{60} = 3.5(-6)T^{-0.5}$	estimated
(R61)	$SO^+ + e \rightarrow S + O$	$k_{61} = 3.5(-6)T^{-0.5}$	estimated
(R62)	$SO_2^+ + e \rightarrow SO + O$	$k_{62} = 5.2(-6)T^{-0.5}$	estimated

Note: The units for photoionization rates (J), and two-body rates are sec^{-1}, and $cm^3\ sec^{-1}$, respectively.

obtained by McGuire (1973) for S and O.

Ionic species are lost by recombination and charge transfer processes. The peak electron density (which by charge neutrality is equal to the ion density if all ions are singly charged) in the dayside ionosphere is $n_e^{max} = 6 \times 10^4$ cm^{-3}. If we assume that the dominant ion is molecular, then the recombination of ion-electron pairs proceeds primarily by dissociative recombination, as for example

$$SO_2^+ + e \longrightarrow SO + O. \qquad (R62)$$

The characteristic time scale for changes in ion densities due to dissociative recombination is

$$\tau_{DR} \sim \frac{1}{\alpha_{DR} n_e}. \qquad (21)$$

A typical value for the dissociative recombination rate coefficient is $\alpha_{DR} \sim 3 \times 10^{-7}$ cm^3 s^{-1}. At the ionospheric electron density peak $\tau \sim 10^2$ s.

Due to the low densities in Io's atmosphere and the large values for the SO_2 and SO photodissociation rates, it is likely that large mixing ratios of S and O exist. If this is true then a large value for the production of atomic ions could obtain. Charge transfer and rearrangement reactions are very efficient for removing atomic ions in the presence of a predominantly molecular background neutral gas. For example, the reactions

$$O^+ + SO_2 \longrightarrow SO^+ + O_2 \qquad \text{(R43)}$$

and

$$S^+ + SO \longrightarrow SO^+ + S \qquad \text{(R40)}$$

will act to remove atomic ions and increase the molecular ion density. The characteristic time scale for changes in the density of atomic ions due to their loss by ion-atom interchange reactions is

$$\tau_{CT} \sim \frac{1}{k_{CT} n_a}, \qquad (22)$$

where k_{CT} is the charge exchange and rearrangement rate coefficient and n_a is the number density of the background neutral gas, in this case the number density of SO_2. A typical value for k_{CT} is 10^{-9} cm^3 s^{-1}, and if we take $n_a = 10^9$ cm^{-3} for the number density of SO_2 near the ionospheric peak then we get $\tau_{CT} \sim 1$ second.

The characteristic time scale for changes in the density of atomic ions due to direct radiative recombination is

$$\tau_{RR} \sim \frac{1}{\alpha_{RR} n_e}. \qquad (23)$$

A typical value for the radiative recombination rate coefficient for atomic ions is $\alpha_{RR} \sim 4 \times 10^{-12}$ cm^3 s^{-1}, giving $\tau_{RR} \sim 10^7$ seconds.

A comparison of these timescales shows that most of the positive charges probably end up on molecular ions, and that molecular ions probably dominate atomic ions in Io's dayside ionosphere.

Ambipolar diffusion of ions and electrons can in principle act as a

local source or sink for ionization. The plasma scale height as deduced by Pioneer 10 (Kliore et al., 1975) is $H_p \simeq 200$ km. The characteristic time scale for ambipolar diffusion is

$$\tau_{AD} \sim \frac{H_p^2}{D_{AD}}, \qquad (24)$$

where D_{AD} is the ambipolar diffusion coefficient. A typical value for D_{AD} is $10^{19}/n_a$ cm^2 s^{-1}, where n_a is the total number density of the background neutral gas through which the plasma is diffusing. For the case we are considering D_{AD} is of order 10^{10} cm^2 s^{-1}, and hence $\tau_{AD} \sim 4 \times 10^4$ seconds. Since τ_{AD} is much larger than the characteristic time scales for loss of ionization by charge transfer and recombination processes we expect plasma transport to be of secondary importance as an effective local source or sink of plasma at least near the ionosphere peak.

5. Numerical Results

The time dependent continuity equation (8) was solved for the radial variation of species concentration $n_i(r)$. The numerical method has been described elsewhere (Allen et al., 1981; Logan et al., 1978). In all of our calculations we time marched the solution into a steady state with starting conditions at t = 0 being that all concentrations, except that of SO_2, were equal to zero. In the altitude region where photochemistry is most important, integrating forward in time to $t \sim 3 \times 10^4$ seconds would generally bring the calculated concentrations to within 10% or less of their steady state ($t \rightarrow \infty$, $\partial n_i/\partial t \rightarrow 0$) values. Below we discuss the various cases considered. Tables 4 and 5 summarize some of the major results.

Solution of equation (8) requires specification of boundary fluxes of atmospheric constituents. A rigorous specification of these fluxes is impossible since the atmospheric escape mechanism and the details of the chemical interaction between Io's atmosphere and the surface are not known. The rationale that we follow for modeling the chemical structure of the atmosphere is as follows. We begin with an oversimplified model for the atmosphere (Model 1). The results from the Model 1 calculations will give us an estimate for the atmospheric model parameters that allows a match to the observations (downstream ionosphere). Using these results as a starting point we will then consider the effects which variations in the parameters have in atmospheric structure. Each model will be discussed in detail. Since it would be impossible to investigate all parameter combinations, we consider a range which we feel encompasses those conditions likely to obtain on

Io. The various sensitivity tests will allow us to determine those parameters which must be known accurately in order to reliably model Io's atmospheric chemical structure.

Model 1 -- Reference Case (B)

We first consider an isothermal atmosphere ($T(r) = T_\infty$ = constant). This ignores the fact that there will be some type of thermal boundary layer between the atmosphere and surface of Io. We assume that the eddy diffusion coefficient K = 0, i.e., that molecular diffusion completely controls the vertical transport of atmospheric constituents.

We treat the surface of Io in our model as a perfect "sponge", i.e., the surface is a sink to all the constituents which impact it (type B boundary conditions). Upon impact all constituents, other than SO_2, stick and are never released. In this model the downward surface diffusion velocity is specified to be the equal to the characteristic diffusion velocity, equation (17). Banks and Kocharts (1979) have shown that for the upper atmosphere of the earth this relation gives better than an order of magnitude estimate for the actual diffusion velocity. The downward diffusive flux is then

$$F^i(z = 0) = n_i(r_0)\, u_i(r_0) \quad . \qquad (25)$$

The specification of boundary conditions at the top of Io's atmosphere is made difficult since the escape mechanism, escape flux, and even the exobase level are unknown. Various escape mechanisms have been proposed such as an thermal evaporation, atmospheric sputtering, and ionization of atmospheric constituents and subsequent pick up by the

Figure 2. The composition of Io's neutral atmosphere as calculated under the assumptions specified in model 1 (Reference Case (B)).

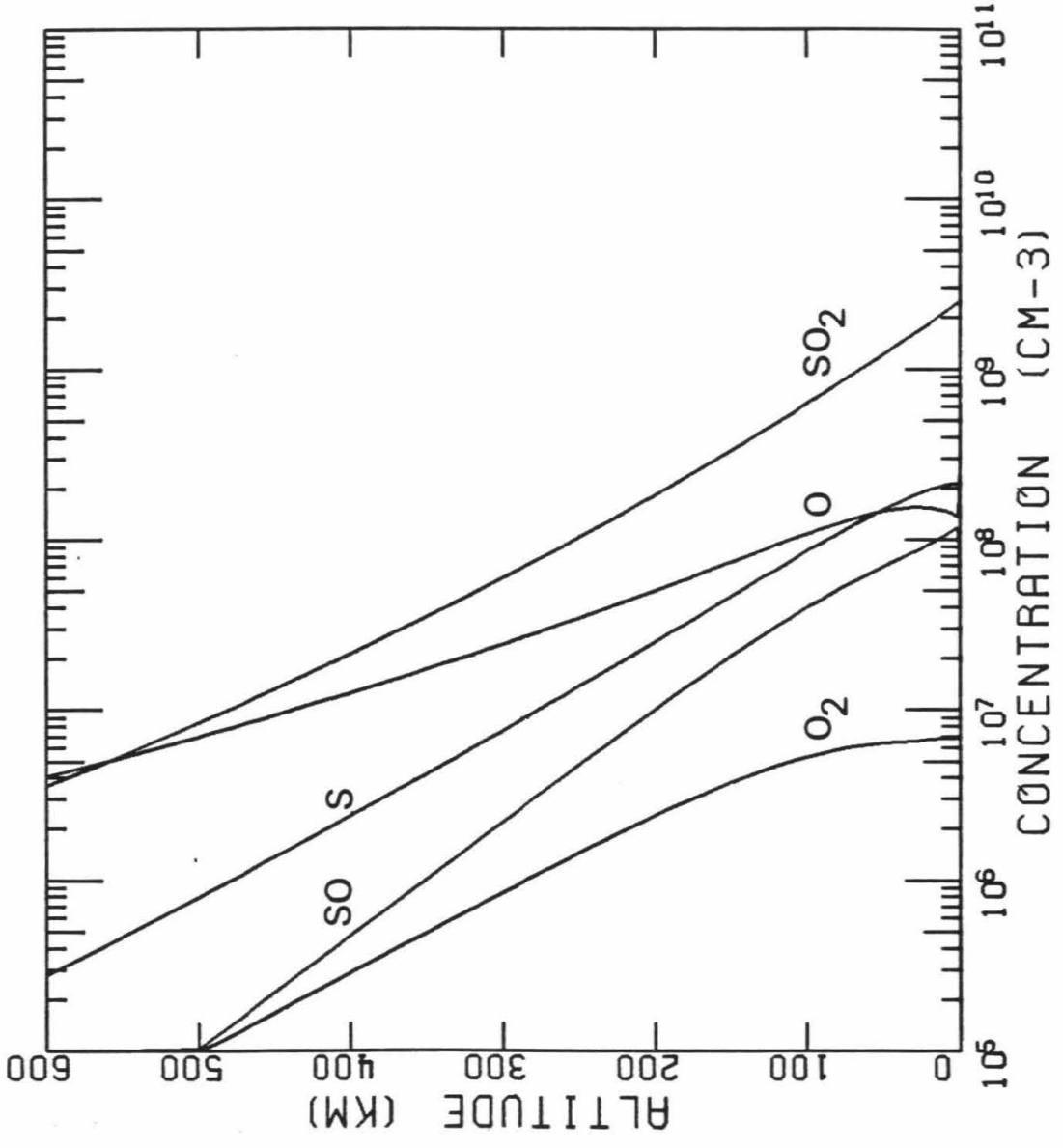
ALTITUDE (KM)
0
100
200
300
400
500
600
CONCENTRATION (CM-3)
10^5
10^6
10^7
10^8
10^9
10^{10}
10^{11}
SO_2
O
S
SO
O_2

Figure 3. The electron and ion densities in Io's ionosphere as calculated for model 1 (Reference Case (B)).

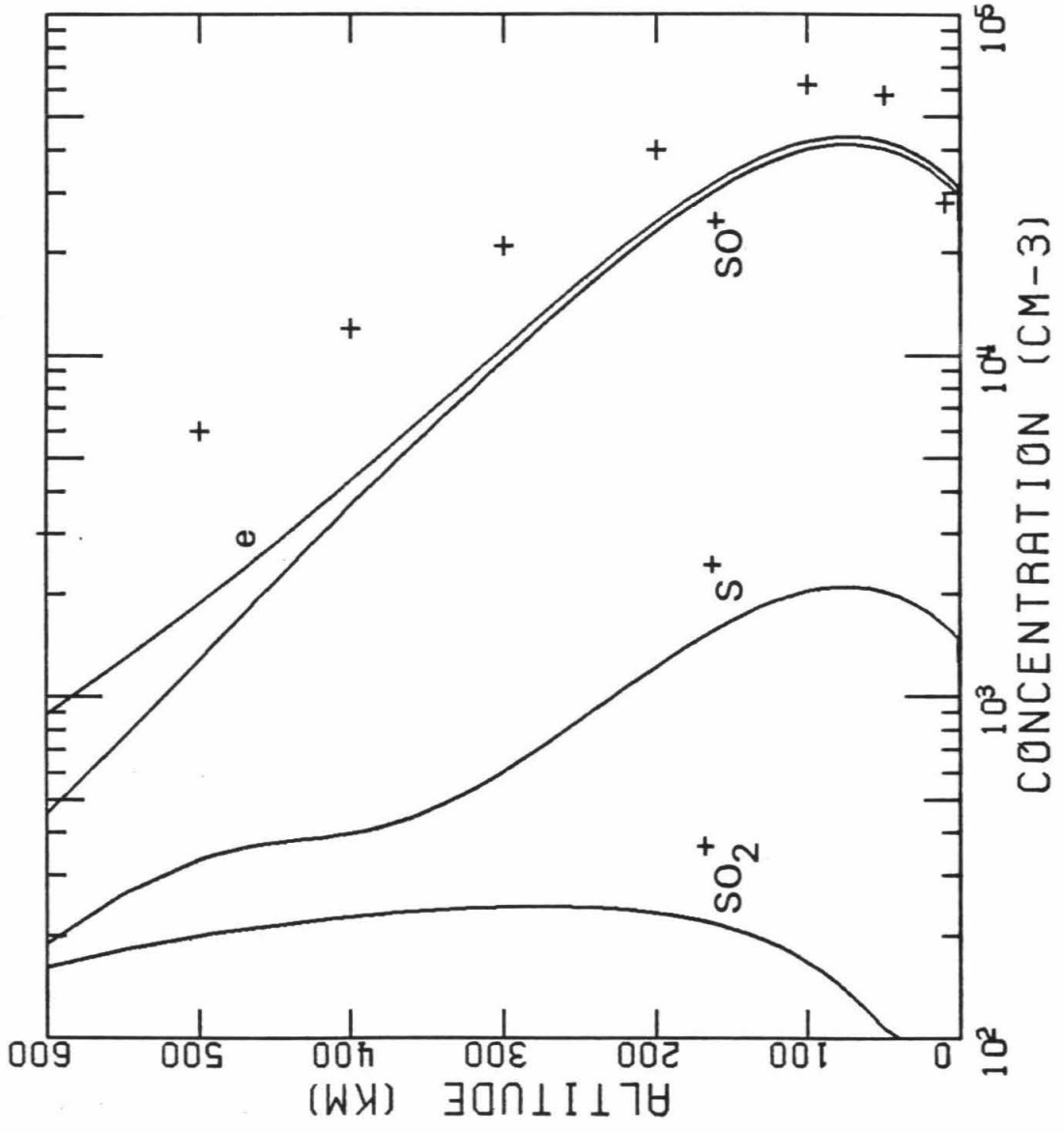
ALTITUDE (KM)
0
100
200
300
400
500
600
CONCENTRATION (CM-3)
10^2
10^3
10^4
10^5
e
SO^+
S^+
SO_2^+

corotating Jovian magnetic field. If the observed properties of the near Io neutral Na and K clouds are an indication, then a non-thermal escape mechanism is probably operative (the characteristic velocity of the atoms in the clouds is a few km s^{-1}). The total escape flux is unknown but probably lies in the range of 10^{10}-10^{11} cm^{-2} s^{-1}. For the sake of argument if we here take the atmospheric density and temperature at the exobase equal to 10^7 cm^{-3} and 1000 K, respectively, then the inferred range for the escape flux implies that the bulk upward velocity just below the exobase can be up to 10% of the speed of sound.

In this model (1) we treat the exobase as a surface which absorbs the atoms or molecules which hit it. The neutral species velocities at the exobase is set equal to the average upward velocity of molecules just below that level, i.e.

$$u_i(r_{ex}) = \frac{C_i}{\sqrt{2\pi}} \quad . \tag{26}$$

Figure 2 shows the concentrations of neutral species as a function of altitude calculated under these model assumptions, while Figure 3 shows the ion and electron concentration profiles. The results for this model are discussed below.

The best fit to the Pioneer 10 ionospheric data is obtained with a surface density for SO_2 of $n_o(SO_2) = 2.5 \times 10^9$ cm^{-3} and an atmospheric temperature of 960 K. The vertical column density of SO_2 is 1.9×10^{16}, or about 1.5 times the column density required for the locally buffered atmosphere at $\theta = 90°$ if the terminator temperature is 110 K. Considering the range of uncertainities, the column density corresponds

quite well.

The total photolysis rate of SO_2 is 1.68 x 10^{11} cm^{-2} s^{-1} (R3 + R4). R3 dominates over R4 by a factor 4.1 for column rates. The dominant photochemical source of SO_2 is R8 at a rate of 6.08 x 10^{10} cm^{-2} s^{-1}, giving a net SO_2 destruction rate of 1.07 x 10^{11} cm^{-2} s^{-1}. The total number of photons available for SO_2 photodissociation is ~2.5 x 10^{11} cm^{-2} s^{-1}, thus about 3 photons in every 5 contribute directly to breaking apart SO_2 molecules. The remaining photons penetrate the atmosphere to the surface or else contribute to photolysis of SO. The characteristic time to reach steady concentrations in this model is ~4 x 10^4 s.

The mixing ratios at the base of the atmosphere for O, S, SO, O_2, and SO_2 are 1.16 x 10^{-1}, 8.19 x 10^{-2}, 2.03 x 10^{-2}, 2.63 x 10^{-3}, and 7.79 x 10^{-1}, respectively. SO is produced by photolysis of SO_2 at about the same rate at which O is produced. However, O is lost from the atmosphere primarily by diffusion while SO is lost mainly via R8 and R2 in a column ratio of 5.4:1. The lower mixing ratio of SO reflects these additional local loss processes. The very low mixing ratio of 3 x 10^{-3} for atmospheric O_2 is due to the large rate constant for R6. The column density of O_2 is 1.2 x 10^{14}, not enough by itself to produce a collisionally "thick" atmosphere if all other atmospheric constituents were to magically vanish. The column density in this model is lower by a factor of order 10^2 than that found by Kumar (1981) in his model of Io's atmosphere.

The exobase is located at an altitude of approximately 650 km and the major constituent is O. The exospheric escape fluxes $\phi_e(i)$ (ϕ

normalized in all cases to Io's surface) are listed in Table 5. The surface flux of constituent i is defined by $\phi_o(i)$, and the total atmospheric boundary loss of species i is $\phi = -\phi_o + \phi_e$. Mass conservation implies that

$$\phi(S) + \phi(SO) \cong \phi(O_2) + \frac{1}{2}[\phi(O) + \phi(SO)] \qquad (27)$$

and

$$\phi_o(SO_2) \cong \phi_e(SO_2) + \phi(S) + \phi(SO). \qquad (28)$$

The SO_2 supply rate to the atmosphere is $\phi_o(SO_2) = 1.69 \times 10^{11}$ cm^{-2} s^{-1}. This is of order a factor of 10^2 smaller than the maximum one-way evaporation flux of SO_2 molecules from a surface frost at T = 110 K.

Of particular interest is the relative atmospheric escape rates for S and O. At the exobase the total number of O atoms (in all forms escaping is approximately 2.9 times the corresponding number of S atoms. As a result of this the surface depositional fluxes of O and S are in the ratio of 1.4:1. Thus, the surface deposition tends to increase the relative S content of the surface (relative to that of pure SO_2). This is a feature common to this class of models of Io's atmosphere. The consequences of this S enrichment of Io's surface will be discussed more in section 7.

The source of ionization for the ionosphere is solar UV radiation. The molecule SO has the lowest ionizaiton potential (10.2 eV) of any of the species made up of SO_2 and it's photochemical products. Thus photons of this energy or greater can produce ionization in Io's

atmosphere. The column solar UV ion production rates are as follows:

$$q(O^+) = 3.9 \times 10^7 \text{ cm}^{-2} \text{ s}^{-1}$$
$$q(S^+) = 2.8 \times 10^7 \quad "$$
$$q(SO^+) = 3.9 \times 10^7 \quad "$$
$$q(O_2^+) = 2.3 \times 10^6 \quad "$$
$$q(SO_2^+) = 1.9 \times 10^8 \quad "$$

The peak in the SO_2^+ production rate occurs at an altitude of 80 km, which corresponds to the peak of the electron density. Charge transfer reactions such as

$$SO_2^+ + S \longrightarrow SO^+ + SO \qquad \text{(R31)}$$
$$SO_2^+ + S \longrightarrow S^+ + SO_2 \qquad \text{(R32)}$$
$$SO_2^+ + SO \longrightarrow SO^+ + SO_2 \qquad \text{(R33)}$$

act to transfer the charge from SO_2^+ to atoms or molecules with lower ionization thresholds. R31, R32, and R33 are exothermic with exothermicities 1.79, 3.3, and 2.1 eV respectively and are expected to be quite fast. The reaction

$$S^+ + SO \longrightarrow SO^+ + S \qquad \text{(R40)}$$

is near resonant (ΔE = 0.2 eV). The rate for R40 has not been measured. We will assume that it has a fast rate coefficient (Bauer, 1973; Huntress, 1977). Most of the positive charges in model 1 end up on SO through these charge exchange reactions. The complete set of reactions used in the model are listed in Table 3.

The electron and ion concentrations calculated from model 1 are shown in figure 3. The peak electron density in the ionosphere occurs near 80 km altitude and has a value of 4.4×10^4 cm^{-3}, or about 30 % less than that observed by Pioneer 10. The dominant ion everywhere from the surface to the exobase (650 km) is SO^+. The secondary ion S^+ makes up about 5 % of the ions near the surface and 40 % near the exobase. Even though the column production rate of SO_2^+ is the largest, the concentration of SO_2^+ is of order 10^2 cm^{-3} in this model, due to the reasons mentioned above.

The characteristic time scale for the ions to reach steady state conditions in this model is of order 10^3 seconds, about a factor of 20 less than the time needed for the neutral constituents to reach steady state values.

Model 2 - Bates' Temperature Profile (B)

The temperature profile given by equation (3) takes into account the fact that there probably exists an atmospheric thermal boundary layer near Io's surface. This can have a major effect on atmospheric structure as will be seen. The atmoshperic scale height at the surface in model 1 is 69 km. If the atmospheric temperature at the surface is the same as the surface temperature (about 100 K), then the scale height at z = 0 km is 8 km. The Bates' temperature profile gives an atmospheric temperature which increases exponentially with altitude, with an e-folding length ~ H. We expect the atmospheric density to decrease much more rapidly with altitude for the Bates' profile than for the isothermal profile (at least in the first few scale heights above

Figure 4. The composition of Io's neutral atmosphere as calculated for model 2 (Bates' temperature profile (B)).

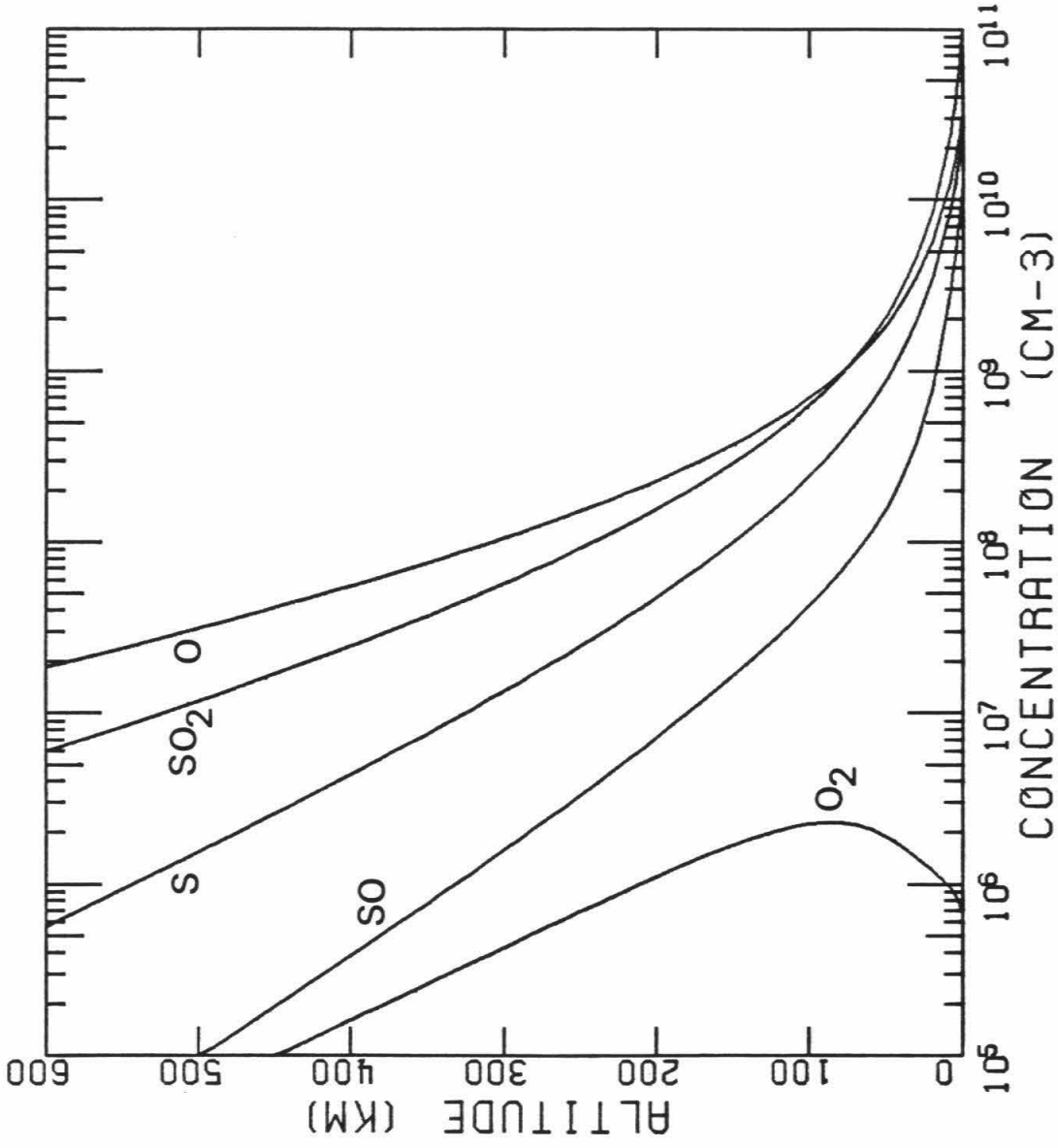
ALTITUDE (KM)
0
100
200
300
400
500
600
CONCENTRATION (CM-3)
10^5
10^6
10^7
10^8
10^9
10^{10}
10^{11}
O
SO_2
S
SO
O_2

Figure 5. The electron and ion densities in Io's ionosphere as calculated for model 2 (Bates' temperature profile (B)).

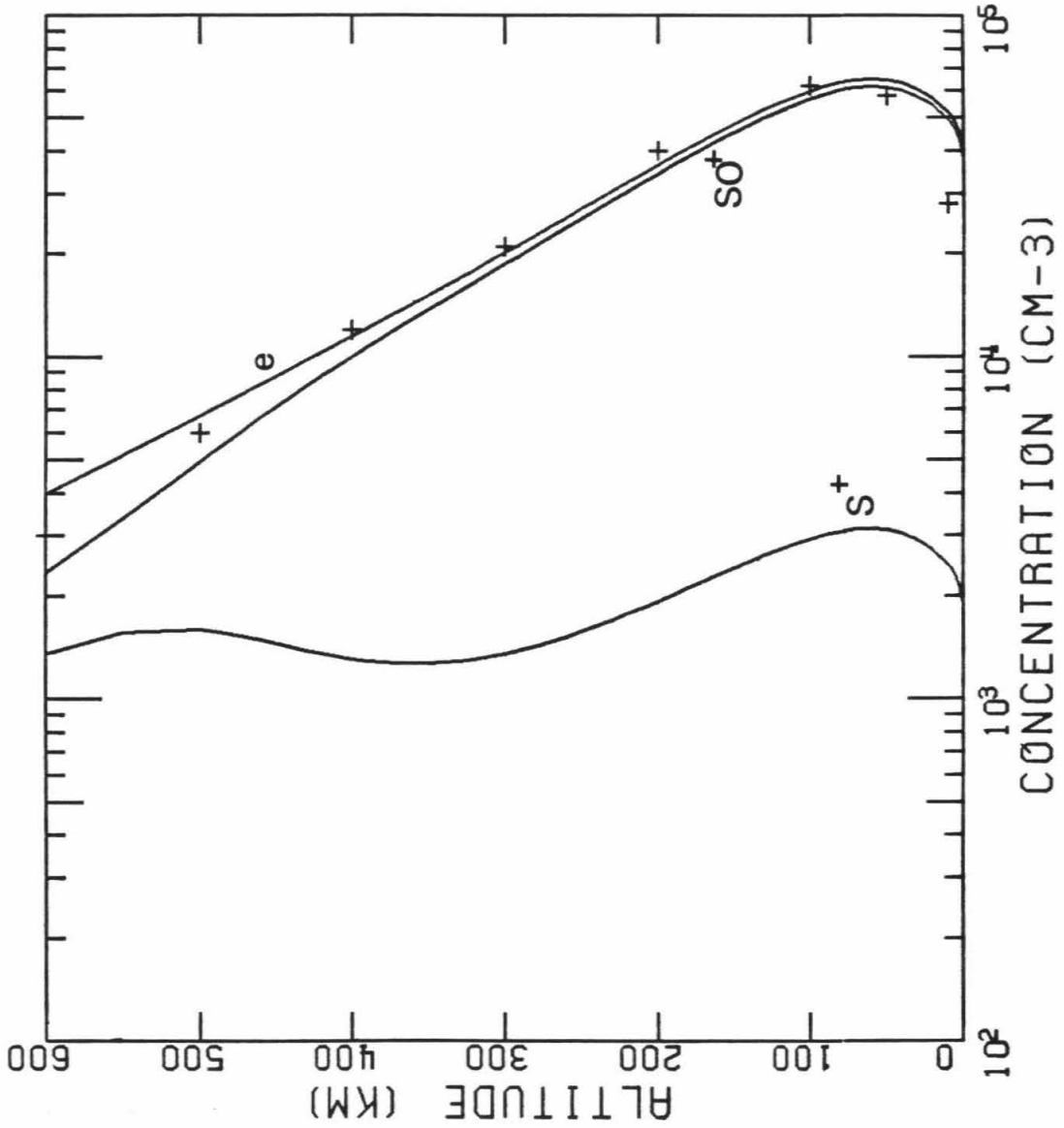
ALTITUDE (KM)
0
100
200
300
400
500
600
CONCENTRATION (CM-3)
10^2
10^3
10^4
10^5
e
SO+
S+

the surface).

In Model 2 we assume B-type surface boundary conditions and the same type of exobase non-thermal escape conditions as in Model 1. We use the Bates' T(r) and vary T_∞ and $n_o(SO_2)$ to obtain the best match ionosphere to the Pioneer 10 determination. The neutral constituents profiles' are shown in figure 4, and the ion concentrations in figure 5.

The best match in this case requires a surface number density of SO_2 of 1×10^{11} cm^{-3}, and an exospheric temperature of 1230 K. The peak ionization rate in model 1 occurs at an SO_2 concentration near 10^9 cm^{-3}, at Z_p = 80 km. With specified T(r) in model 2 a much larger surface density of SO_2 is required in order to have a concentration near 10^9 at the same Z_p. Of immediate prominence in figure 4 is the rapid decrease with altitude of concentrations of all species. Atomic oxygen becomes the dominant constituent above about 80 km as opposed to ~ 550 km in model 1. There are two main reasons for this. First, in model 2 the column densities of SO and SO_2 are sufficiently large as to present an optically thick target to the photons which cause dissociation in both molecules, so that the total production rate of O is larger in model 2 than in model 1. Second, with a higher surface density of SO_2 the diffusion velocity of O to the surface is smaller than in model 1.

The column density of O_2 in this model is 4.6×10^{13} cm^{-3}, about a factor of 3 less than in model 1, due to the large column production of S with subsequent reaction R6 to remove the O_2.

The exobase in this model lies at Z = 1160 km, i.e., at a higher altitude than in model 1 because of the larger production rate of O and hence a higher concentration of O. The exobase escape flux of O is 3.3

x 10^{11} cm^{-2} s^{-1}, about 30 times the atomic sulfur flux. The ratio of the total escape rate of O relative to the total S (in all atomic and molecular forms) is 6.4, more than twice the ratio found in model 1. The relative surface depositional (excluding SO_2) flux of O to S is also higher in model 2, at a value of 1.16.

The peak in the calculated electron density profile is 6.5 x 10^4 cm^{-3} at an altitude of 82 km, giving a good match to the Pioneer 10 downstream peak. The overall match between this model and the measured electron density distribution is better than in model 1. The scale height of the ionosphere matches to better than 5 % between 300 km and 400 km, but the calculated H_p (at 600 km) is about 40 % too high. Also, the calculated surface electron density is about 45 % too high. The relative concentration of ions is very similar to that of model 1.

Model 3 - Maximum Surface Loss (B)

This model has only one change from model 2, i.e., we here set the surface loss velocity equal to the maximum velocity given by equation (18). This is done in order to determine the sensitivity of the calculated compositional structure to the surface loss fluxes. We here keep the surface concentration of SO_2 and the exospheric temperature the same as in the previous model (We keep the same values for models 3 through 7).

Using the maximum loss velocity (18) for the surface boundary condition produces concentration boundary layers near the surface. The boundary layers are confined to the first scale height, i.e., about 10 km above the surface, as seen in figure 6. Over an altitude range of

Figure 6. The composition of Io's neutral atmosphere as calculated for model 3 (Maximum Surface Loss Velocity (B)).

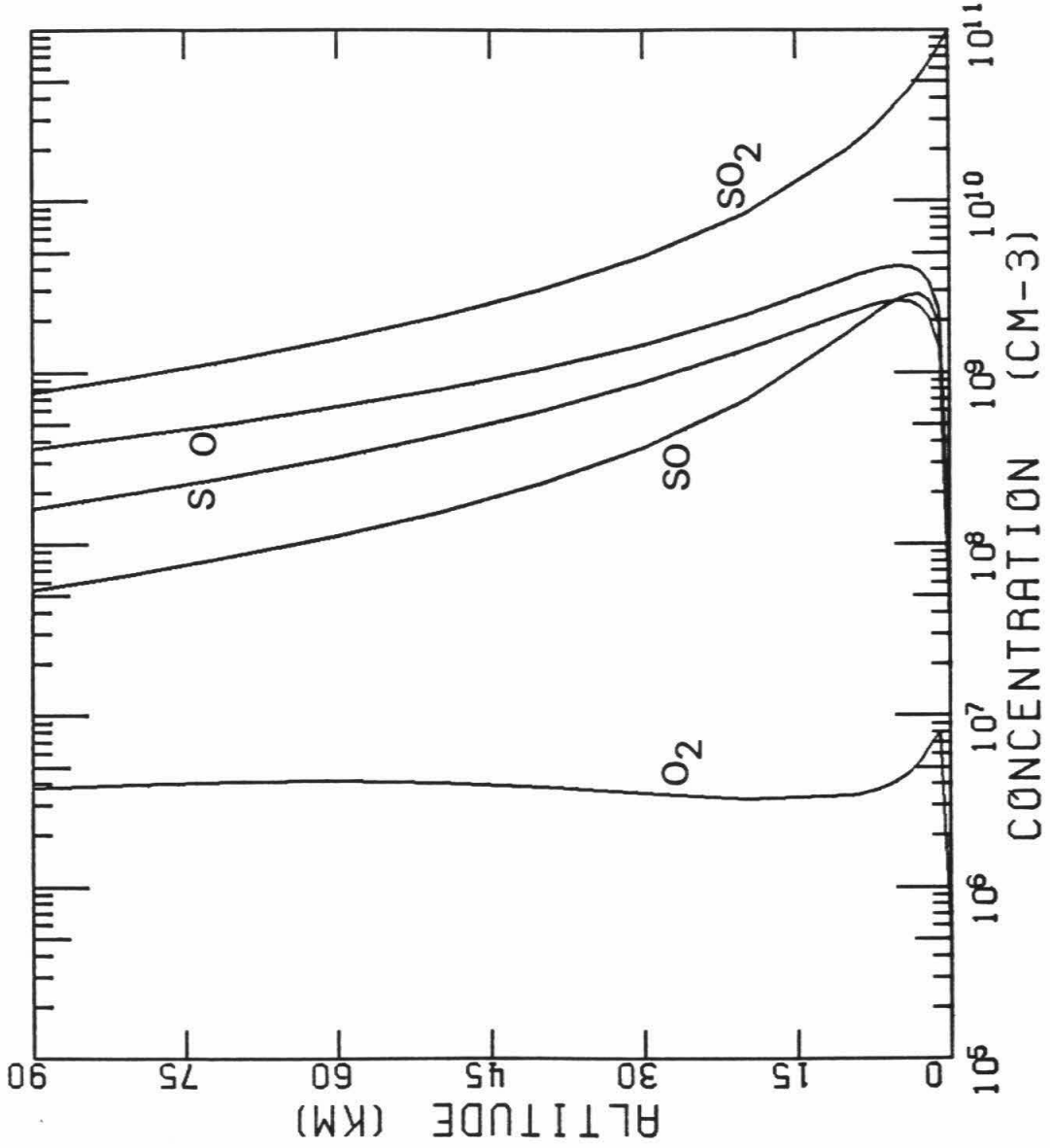
ALTITUDE (KM)
0
15
30
45
60
75
90
CONCENTRATION (CM-3)
10^5
10^6
10^7
10^8
10^9
10^{10}
10^{11}
SO_2
S O
SO
O_2

Figure 7. The electron and ion densities in Io's ionosphere as calculated for model 3 (Maximum Surface Loss Velocity (B)).

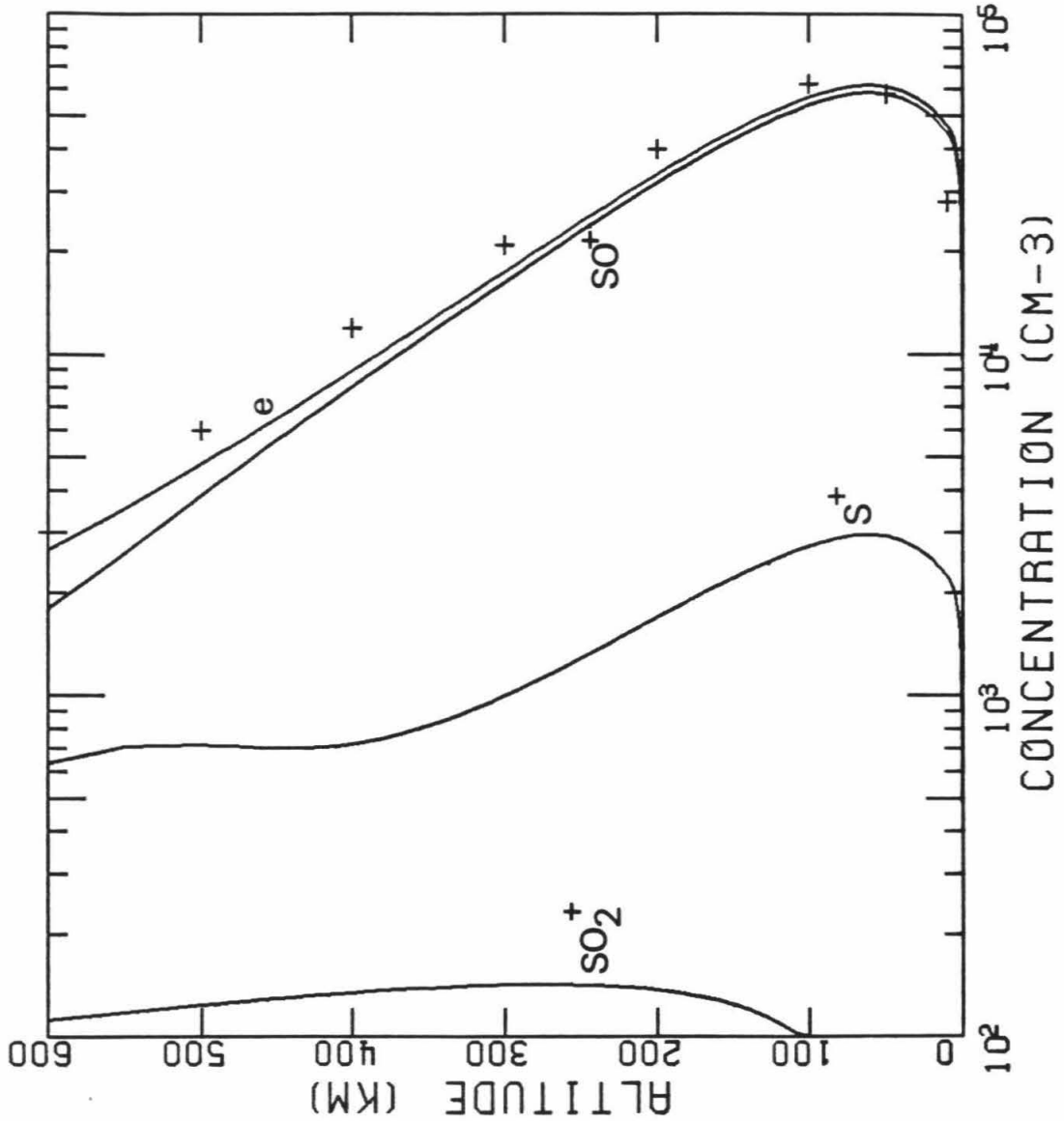
ALTITUDE (KM)
0
100
200
300
400
500
600
CONCENTRATION (CM-3)
10^2
10^3
10^4
10^5
SO_2^+
S^+
SO^+
e

just a few kilometers the concentrations of minor species can change by as much as two orders of magnitude. On the other hand, the surface flux of the minor species O, S, and SO change by less than 45 % , as can be seen in Table 5. Even the exobase escape fluxes have changed by less than a factor of 2. Above about 100 km altitude the concentrations of O and S are typically about 50 % less than in model 2, leading to slightly lower electron densities as shown in figure 7. The lower O density implies a lower exobase, in this case located at 890 km.

Model 4 - O_2 Surface Catalysis (D)

Model 4 has the same boundary conditions as in Model 3 except that at the surface the fluxes of O and O_2 satisfy equation (20). This is done in order to determine the effect that surface recombination of O to form O_2 (as discussed in section 3.(b)) has on atmospheric compositional structure. Using models 2 and 3 as guides, we choose the downward flux of O to be 3×10^{11} cm^{-2} s^{-1}.

The return flux of O_2 into the atmosphere results in a concentration boundary layer aporoximately 10 km thick as seen in figure 8. However, the O_2 density distribution above this layer is largely unaffected. The column denisty for O_2 is 3.3×10^{14} cm^{-2}, only a factor of 7 greater than that found in model 2, and just barely enough to provide a collisionally thick atmosphere if all the other atmospheric components were to magically disappear. The O_2 returned to the atmosphere is rapidly attacked by S through the fast reaction R6 to form SO + O. The extra O supply to the atmosphere pushes the exobase to 2300 km altitude. Atomic oxygen is the dominant constituent above about 70

Figure 8. The composition of Io's neutral atmosphere as calculated for model 4 (O_2 Surface Catalysis (D)).

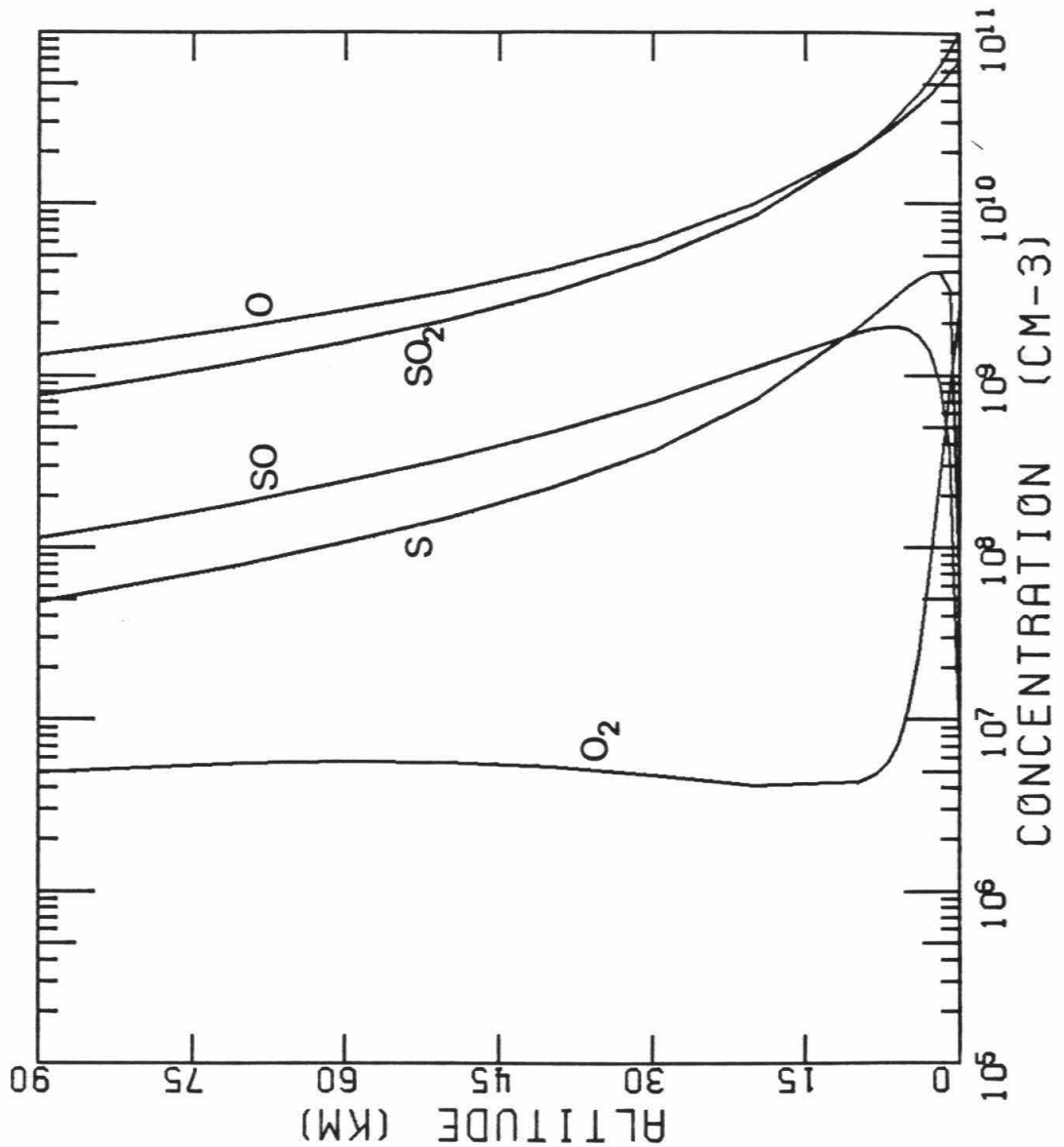
ALTITUDE (KM)
0
15
30
45
60
75
90
CONCENTRATION (CM-3)
10^5
10^6
10^7
10^8
10^9
10^{10}
10^{11}
O
SO_2
SO
S
O_2

Figure 9. The electron and ion densities in Io's ionosphere as calculated for model 4 (O_2 Surface Catalysis (D)).

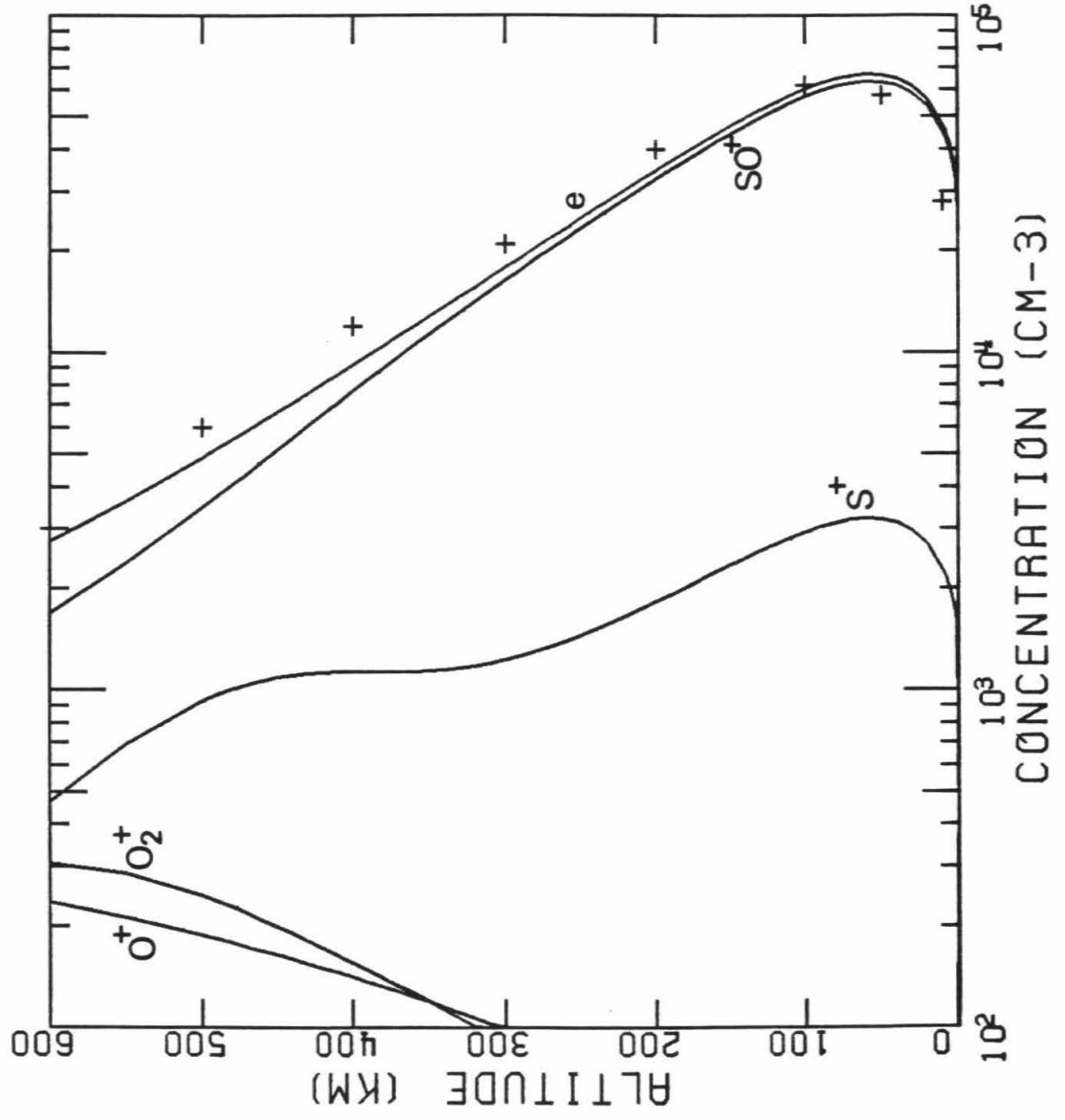
ALTITUDE (KM)
0
100
200
300
400
500
600
CONCENTRATION (CM-3)
10^2
10^3
10^4
10^5
O^+
O_2^+
S^+
e
SO^+

km. The characteristics of the ionosphere (figure 9) are largely the same as in model 3.

Model 5 - Eddy Mixing (C)

In this model we set the eddy diffusion coefficient $K = 10^8$ cm^2 s^{-1} in order to ascertain the effect that eddy mixing has on atmospheric structure. In other respects this model is the same as model 4. The boundary fluxes in Table 5 are similar to those of Model 4. The effect of eddy mixing on the concentration profiles is limited to the region less than 20 km from the surface, and tends to produce constant mixing ratios for the minor constituents in this region.

Model 6 - Chemically Inert Surface (A)

The extreme case for no chemical interaction between Io's atmosphere and its surface is investigated in this model. We set the surface velocity, and hence the surface flux, of atmospheric constituents other than SO_2 equal to zero.

The calculated concentration profiles are shown in figures 10 and 11. S and O have concentrations greater than that of SO_2 at all altitudes. The exobase escape fluxes of O and S (in all forms) are constrained to be in the ratio of 2:1. Dur to the large atmospheric concentration of O, the exobase is located much further from the surface than than in previous models, at Z = 4370 km.

Model 7 - Thermal Escape (B)

In the absense of non-thermal interactions between Io's atmosphere

Figure 10. The composition of Io's neutral atmosphere as calculated for model 6 (Inert Surface (A)).

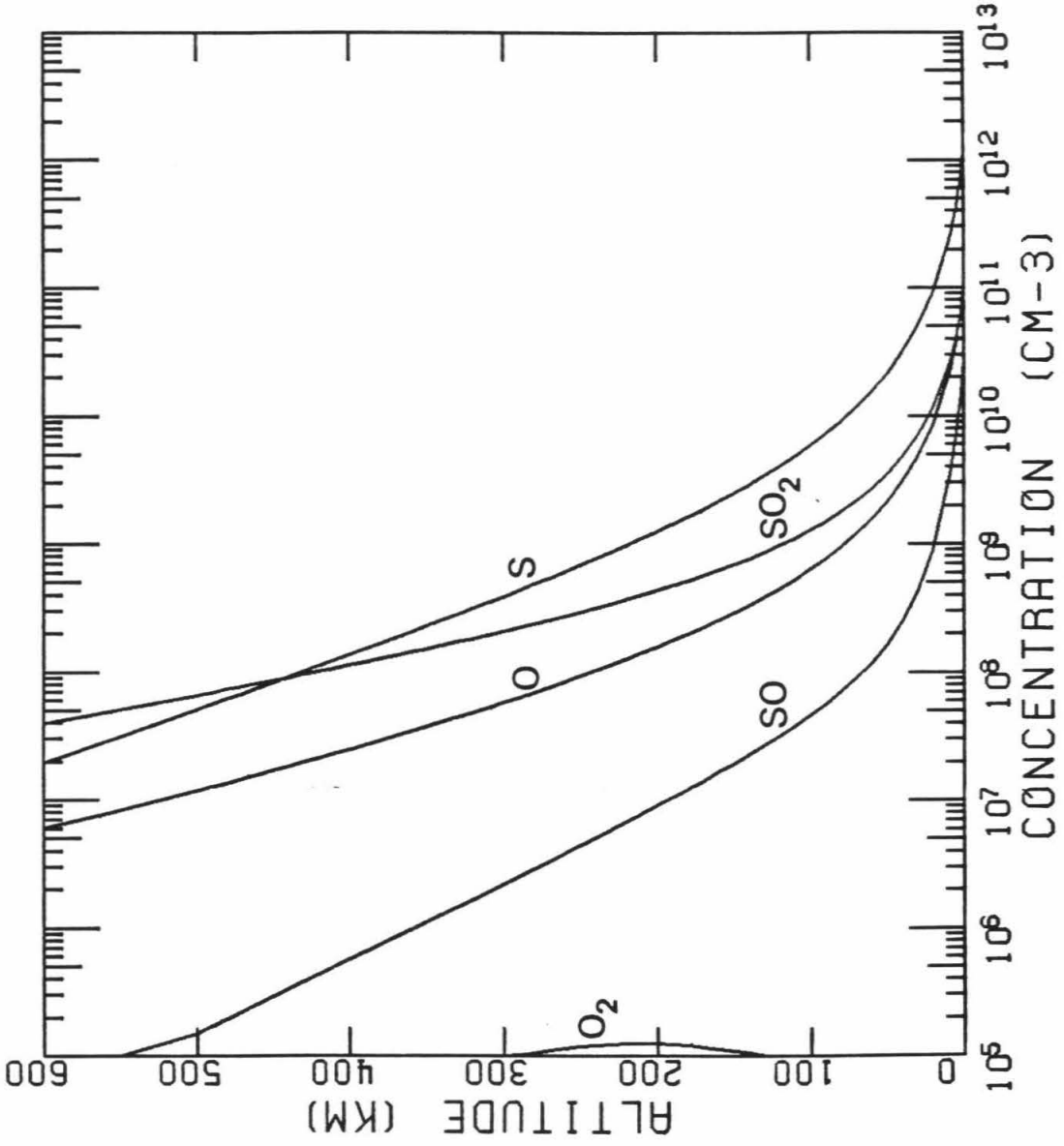
ALTITUDE (KM)
0
100
200
300
400
500
600
CONCENTRATION (CM-3)
10^5
10^6
10^7
10^8
10^9
10^{10}
10^{11}
10^{12}
10^{13}
O_2
SO
O
SO_2
S

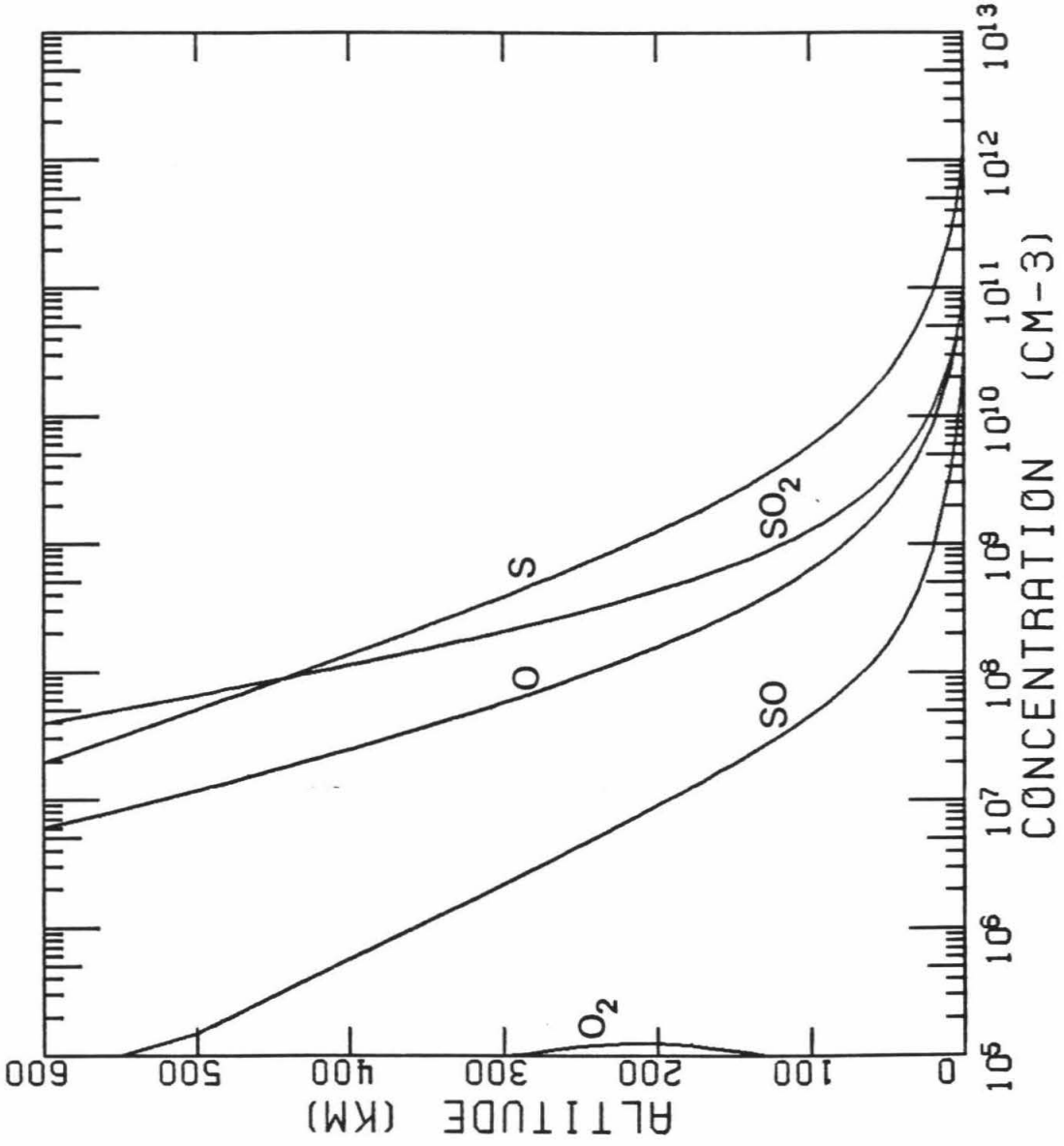
ALTITUDE (KM)
0
100
200
300
400
500
600
CONCENTRATION (CM-3)
10^5
10^6
10^7
10^8
10^9
10^{10}
10^{11}
10^{12}
10^{13}
O_2
SO
O
SO_2
S

Figure 11. The electron and ion densities in Io's ionosphere as calculated for model 6 (Inert Surface (A)).

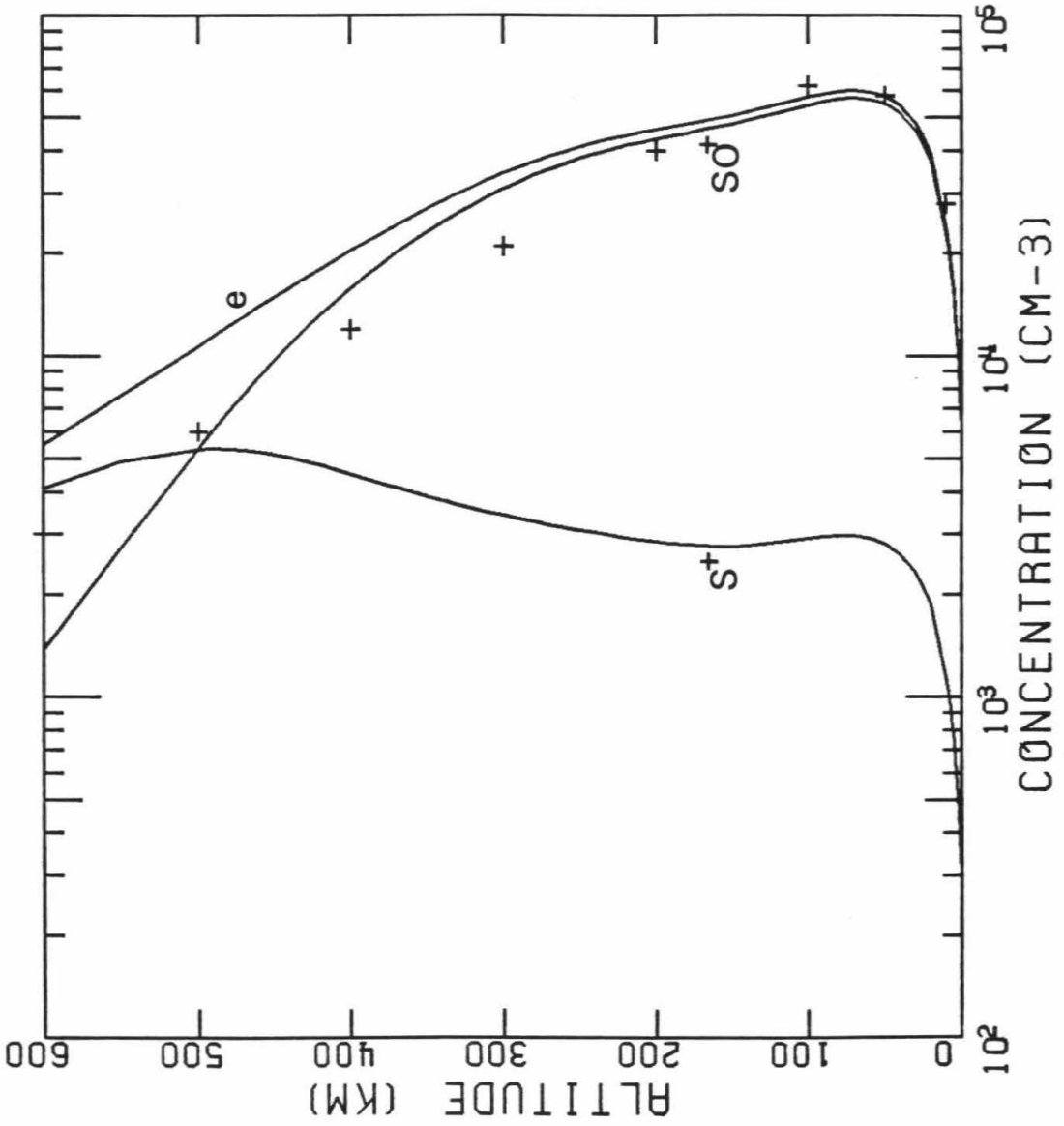
ALTITUDE (KM)
0
100
200
300
400
500
600
CONCENTRATION (CM-3)
10^2
10^3
10^4
10^5
e
SO^+
S^+

and Jupiter's magnetosphere, mass will be lost from the top of Io's atmosphere by means of thermal evaporation (Jean's Escape). In this model the escape flux is give by the Jean's expression, equation (16). The surface boundary conditions for minor species are given by equation (17).

The results are presented in figures 12 and 13. Atomic oxygen is dominant at all altitudes. The escape flux of O is more than a factor of 10^5 greater than that for S. The exobase in this case is located at Z = 5150 km. At the exobase the value of the reduced potential energy λ = 1.34. If this were the physical situation in the atmosphere of Io, then the escape would become hydrodynamic (Watson et al., 1981).

Figure 12. The composition of Io's neutral atmosphere as calculated for model 7 (Thermal Jeans' Escape (B)).

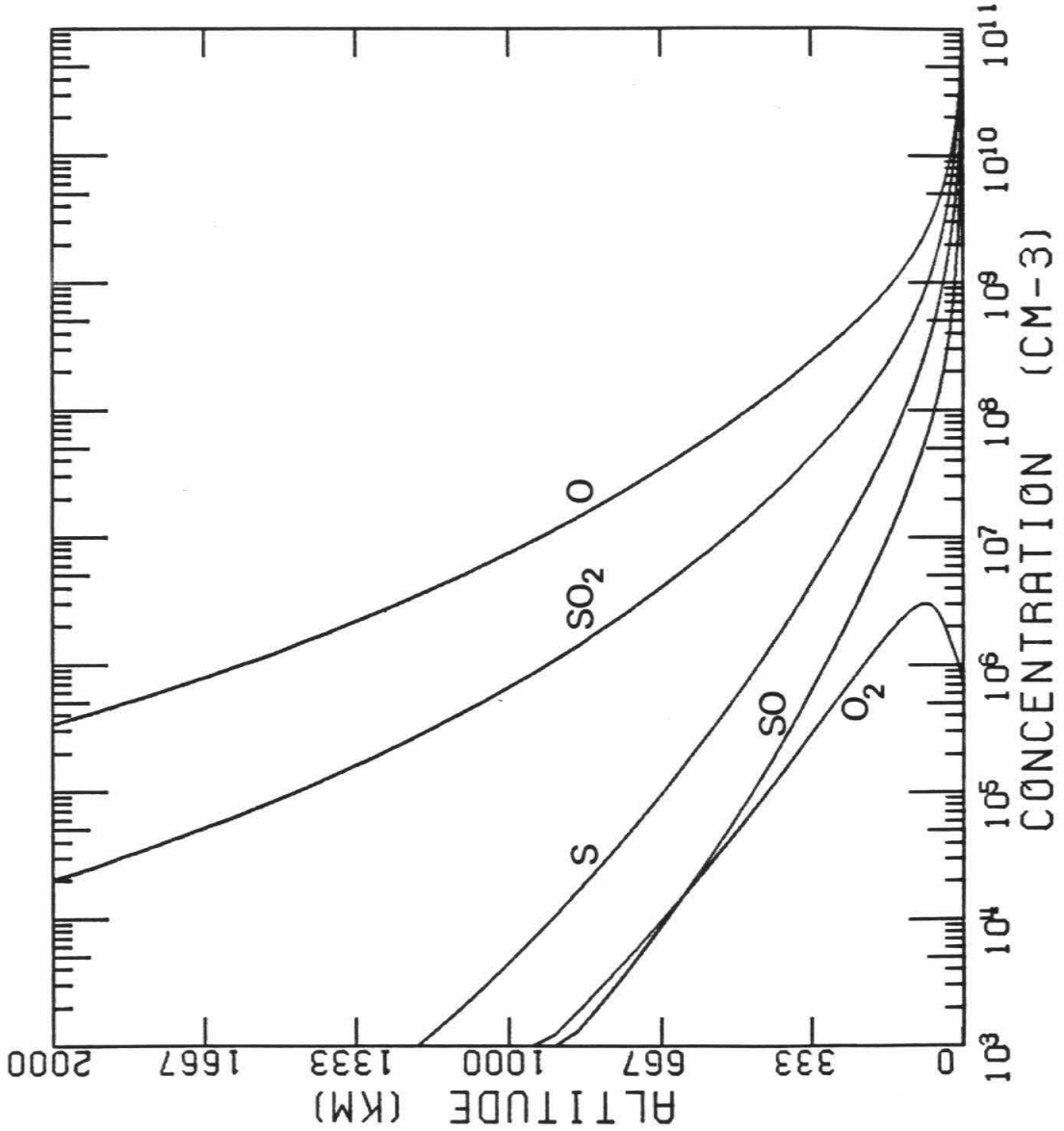
ALTITUDE (KM)
0
333
667
1000
1333
1667
2000
CONCENTRATION (CM-3)
10^3
10^4
10^5
10^6
10^7
10^8
10^9
10^{10}
10^{11}
O
SO_2
S
SO
O_2

Figure 13. The electron and ion densities in Io's ionosphere as calculated for model 7 (Thermal Jeans' Escape (B)).

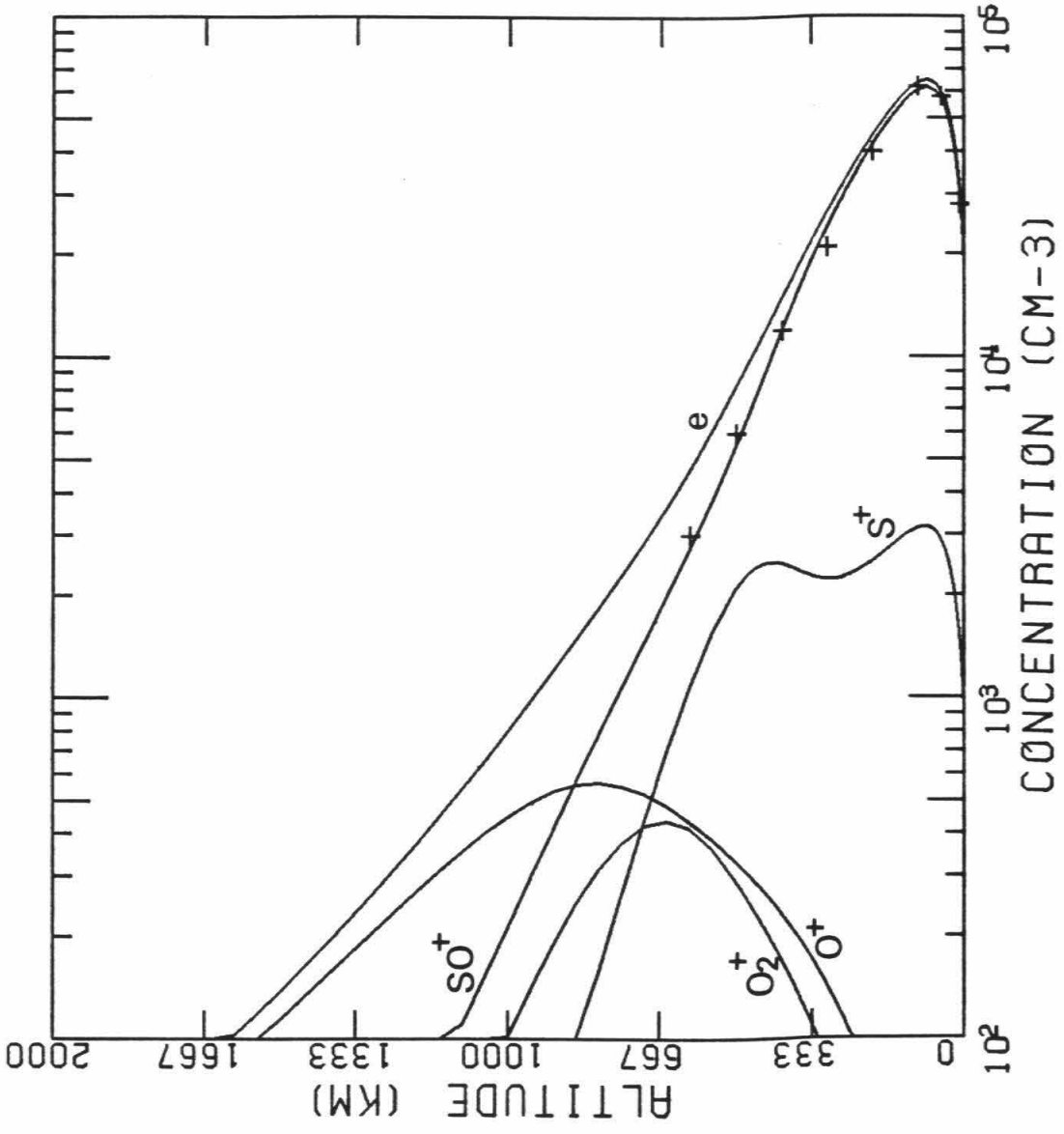
ALTITUDE (KM)
0
333
667
1000
1333
1667
2000
CONCENTRATION (CM-3)
10^2
10^3
10^4
10^5
e
S^+
O_2^+
O^+
SO^+

Table 4

Summary of Important Parameters for each

Model of the Ionian Atmosphere

Model	Z_{peak}(km)	$n_e^{max}(cm^{-3})$	r_{ex}/r_{Io}
1. Reference Case	78	4.4×10^4	1.36
2. Bates' T(r)	82	6.5×10^4	1.64
3. Max. Surf. Flux	65	6.1×10^4	1.49
4. O_2 Surface Catalysis	58	6.7×10^4	2.26
5. Eddy Mixing	54	6.6×10^4	2.18
6. Inert Surface	79	6.0×10^4	3.40
7. Thermal Escape	85	6.5×10^4	3.82
8. Na_2O Injection	50	5.8×10^4	1.53

Table 5

Boundary Fluxes*

Model	Level (alt)	O	S	SO	O_2	SO_2
1. Reference case	0	-1.2(11)	-8.2(10)	-2.0(10)	-2.6(9)	1.7(11)
	650	7.1(10)	4.8(9)	8.8(7)	5.3(8)	6.2(10)
2. Bates' T(r)	0	-3.1(11)	-2.5(11)	-1.2(11)	-6.8(6)	4.4(11)
	1160	3.3(11)	9.9(9)	1.7(7)	2.6(8)	6.1(10)
3. Max. Surface Flux	0	-4.0(11)	-1.8(11)	-2.2(11)	-2.5(9)	4.9(11)
	890	1.8(11)	8.8(9)	2.2(8)	5.4(8)	8.1(10)
4. Surface Catalysis	0	-3.0(11)	-3.8(11)	-3.6(11)	1.5(11)	4.4(11)
	2300	4.4(11)	2.6(9)	2.1(8)	2.5(8)	4.2(10)
5. Eddy Mixing	0	-3.0(11)	-1.0(10)	-4.0(10)	1.5(11)	4.6(11)
	1970	4.2(11)	1.6(9)	2.1(8)	3.2(8)	5.2(10)
6. Inert Surface	0	0	0	0	0	3.6(11)
	4370	7.0(11)	3.5(11)	1.9(8)	3.3(7)	8.0(9)
7. Thermal Escape	0	-6.3(11)	-2.6(11)	-1.3(11)	-6.6(6)	3.9(11)
	5150	1.3(10)	1.3(4)	9.0(1)	1.6(3)	2.6(4)

* The notation is as follows: $A(B) = A \times 10^{B}$. The units are cm^{-2} s^{-1}. All fluxes are normalized to Io's surface.

6. Atmospheric Sodium

Neutral sodium atoms have been observed in a cloud in the near-Io spatial region (Matson et al., 1977). Spectral and theoretical studies indicate that the sodium atoms are streaming away from Io with velocities characteristic of Io's surface escape velocity (Carlson, 1978; Smyth and McElroy, 1978). Estimates of the Na escape flux from Io range from 10^7 to 10^9 cm^{-2} s^{-1} (Brown et al., 1983). Presumably Na, or Na compounds, exist on Io's surface and in the atmosphere. Summers et al. (1983) present a mechanism whereby Na may be injected from Io's surface into the atmosphere. In this section we speculate on the fate of atmospheric sodium.

Very little in known concerning the chemical composition of Io's surface. In particular, it is not known in what form(s) or quantity that Na exists on the surface (Fanale et al., 1982). Furthermore, it is almost impossible to guess in what chemical form Na will be injected into the atmosphere. To make matters worse, very little is known regarding gas phase reactions of sodium and oxygen species, and virtually nothing concerning sodium and sulfur species. Be that as it may, we here present a model of a possible scenario for the source and fate of atmospheric sodium.

We assume that the surface is a source of Na_2O, the upward flux of which we take to be 5×10^7 molecules cm^{-2} s^{-1}. We propose that atomic sodium is produced as a result of

$$Na_2O + O \longrightarrow 2\ NaO \qquad (R20)$$

followed by

$$NaO + O \longrightarrow Na + O_2 \qquad (R18)$$

It is known that R18 is exothermic and fast (Lui and Reed, 1979).

Atomic sodium has an ionization potential of 5.14 eV and is ionized via R28. Charge transfer from SO_2^+ and SO^+ can conceivably produce Na^+ and NaO^+. The rate constants are not known for these reactions so we choose rates that are typical for ion-molecule reactions involving comparable amounts of exothermicity. The set of speculative reactions is included in Table 3.

The model we present has boundary conditions identical with the Maximum Surface Loss model (3). We set $N_o(SO_2) = 1 \times 10^{11}$ cm^{-3} and T_∞ = 1230 K. The calculated chemical structure is shown in figures 14 and 15.

The surface source of Na_2O is about 3 orders of magnitude smaller than the surface source of SO_2. The conversion of Na_2O to Na and O_2 is so rapid that only very small steady state atmospheric concentrations of Na_2O can exist. In this model the concentrations of Na_2O and NaO near the surface are 1.8×10^4 cm^{-3} and 4.4×10^3 cm^{-3}, respectively. The concentrations of Na_2O and NaO decrease with altitude with a length scale of approximately 1 km due to the rapid processes R20 and R18. The surface concentration of Na is 1×10^6 cm^{-3}. Approximately 10 % of the sodium atoms injected into the atmosphere escape from the top of the atmosphere, the remaining are deposited back on the surface in the form of NaO and Na. Overall the influence of Na compounds on the major

atmospheric properties is minimal.

The ion mixing ratio for Na^+ is about 0.1 at the surface and decreases with altitude. The concentration of Na^+ is a function of the surface source flux of Na_2O. If the surface source is an order of magnitude larger than the value we have assumed, then Na^+ could possibly have an important influence on ionospheric properties.

Figure 14. The composition of Io's neutral atmosphere as calculated assuming surface injection of Na_2O (see section 6).

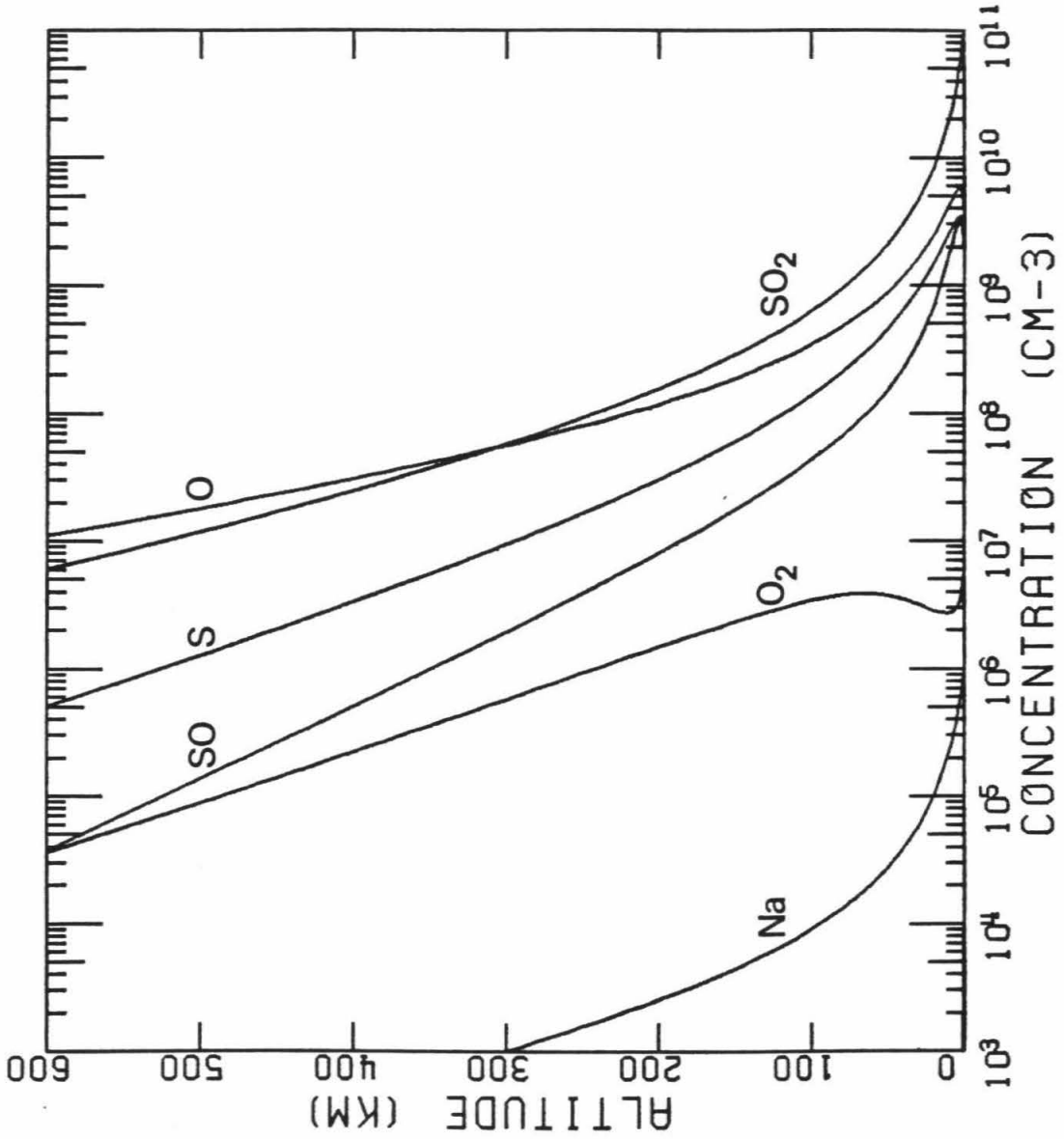
ALTITUDE (KM)
0
100
200
300
400
500
600
CONCENTRATION (CM-3)
10^3
10^4
10^5
10^6
10^7
10^8
10^9
10^{10}
10^{11}
O
S
SO
SO_2
O_2
Na

Figure 15. The electron and ion densities in Io's ionosphere as calculated assuming a surface source of Na_2O (see section 6).

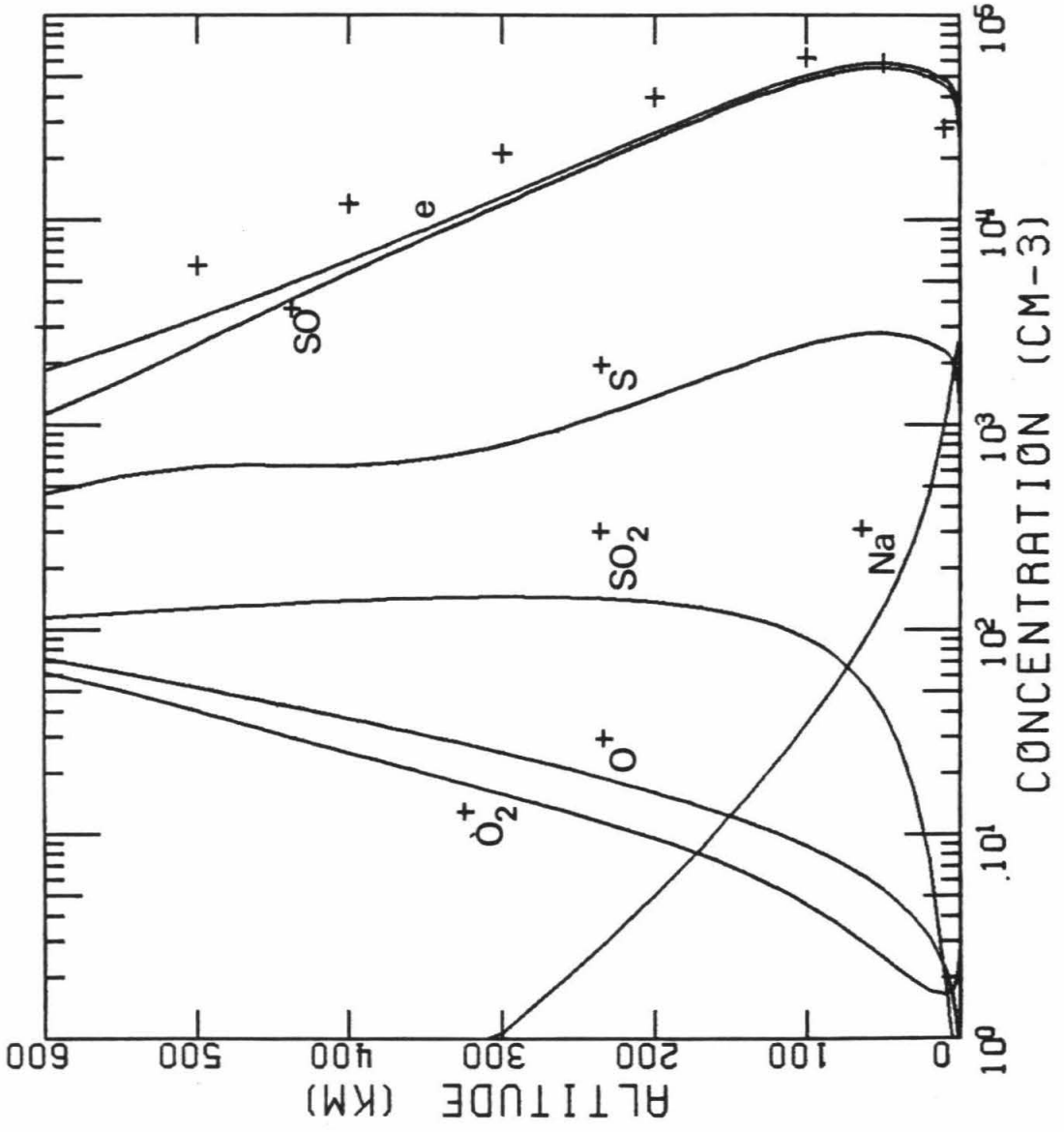
ALTITUDE (KM)
0
100
200
300
400
500
600
CONCENTRATION (CM-3)
10^0
10^1
10^2
10^3
10^4
10^5
O_2^+
O^+
SO_2^+
S^+
SO^+
e
Na^+

7. Dicussion

The atmosphere of Io can be viewed as a system that (1) modulates the interaction between Jupiter's magnetosphere and Io's surface, and (2) processes material as it moves outward from Io's surface and into the magnetosphere. SO_2 is supplied to the atmosphere by sublimation. Once the SO_2 is in the atmosphere photochemical processes act to produce large concentrations of atomic oxygen and sulfur which, having a scale height larger than that of SO_2, can become dominant constituents at the exobase and escape with relative ease. Surface sputtering by high energy magnetospheric ions (Summers et al., 1983) may inject Na compounds into the atmosphere which may subsequently diffuse to the exobase. Atmospheric sputtering from the exobase region can then remove the atmospheric constituents out of Io's gravitational control. Atmospheric processes can also affect the composition and geochemistry of the surface. The models of Io's atmosphere presented in this paper help elucidate some of the processes which may be important for determining the physical properties of the atmosphere. Below we discuss some of the inferred properties of the Ionian Atmosphere.

(a) Neutral Atmosphere

In our theoretical study we have found that the calculated vertical compositional structure of Io's atmosphere and ionosphere are sensitive to the assumed temperature profile and the abundance of gaseous SO_2. We have investigated two extreme cases for the vertical temperature profile of the atmosphere (isothermal and the Bates' profile) each with one

undetermined parameter, i.e., the exospheric temperature. We have also left the surface density of SO_2 as an undetermined parameter in some of our models. Using solar UV radiation as the source of dissociation and ionization of atmospheric chemical species, the models can reproduce the main characteristics of Io's downstream (dayside) ionosphere as determined by the Pioneer 10 radio occultation experiment. From our models we infer that the surface density of gaseous SO_2 in the terminator region must be in the range of 2.5×10^9 to 1×10^{11} cm^{-3}, and that the exospheric temperature is in the range of 960 K to 1230K.

We have identified R8 as the dominant photochemical source of SO_2, but with a column rate at only about 30 % of the net surface sublimation rate needed to supply loss of minor species to the surface and exosphere. SO_2 is lost via dissociation reactions R3 and R4.

The dominant source of O_2 is R4 at a rate of about 25 % of the total photolysis rate of SO_2. The loss of O_2 is accomplished via R6, i.e., the rapid oxidation of S. The maximum column abundance of O_2 is of order 10^{14} cm^{-2}.

The location of the exobase is critically sensitive to the choice of surface and exospheric boundary conditions but probably lies at least above the 650 km altitude level, and may lie sufficiently far from the surface so that the gas flows hydrodynamically away from Io (see model 7).

The total atomic escape flux from the exobase in all models is greater than 10^{10} cm^{-2} s^{-1} (normalized to Io's surface).

(b) Ionosphere

The source of ionization in the models presented is solar UV radiation. As a consequence of this and the assumed ion-molecule reactions we can reproduce the major characteristice of the dayside ionosphere (as deduced by the Pioneer 10 radio occultation experiment). The dominant ion in all cases is SO^+. This result is a consequence of the assumed rates for R31, R32, R33, and R40. Better determinations of the rates for these reactions will allow the development of a more refined model of Io's ionosphere.

(c) Surface enrichment of S

Atomic oxygen is the lightest constituent and tends to float to the top of the atmosphere. O will preferentially escape from the top of the atmosphere if the escape mechanisms work as modeled in section 5. In every model except the Inert Surface Model (6), the relative exobase escape fluxes of O and S are in a ratio of $> 2:1$. The relative surface fluxes of O and S are therefore $< 2:1$. We thus have an enrichment of S on the surface relative to that found in pure SO_2 frost. The rate of deposition of this excess sulfur can be determined from the values in Table 5. The rates are in the range of 100 m to 1 km per billion year.

McEwen and Soderblom (1983) discuss the possibility that there are two classes of volcanoes on Io. One class has SO_2 as the driving volatile while the second class uses elemental sulfur. This second, Prometheus class of volcanoes requires a reservoir of liquid sulfur just under the surface. The size of the reservoir is not known but it may be as small as the equivalent of a few meters thickness spread over the

area of Io's surface (L.A. Soderblom, personal communication). We speculate that photochemical processing of atmospheric SO_2 may lead to surface enrichment of S and may supply a reservoir to power the Prometheus class of volcanoes.

(d) Atmospheric Sodium

We presented a scenario for the source and fate of atmospheric atomic sodium in section 6. In order to improve upon that model it is necessary to know the chemical form of Na on Io's surface. The rates for charge transfer to Na from other atmospheric ions also need to be better determined. If the model presented is in some sense isomorphic to the situation on Io, then it may indeed by a simple matter to get escape fluxes of Na of order 10^7 cm^{-2} s^{-1}.

(e) Escape Mechanism

All of the models presented have a total atomic escape rate comparable to that which has been inferred to be needed to supply the Io plasma torus (Brown et al., 1983). However, if it is necessary to have comparable (same order of magnitude) escape fluxes of O and S (Brown et al., 1983), then the nonthermal escape models presented stand a greater chance of being correct than the Thermal Escape model (7). It is known that atmospheric sputtering is a very efficient process for removing atoms from the top of an atmosphere (Haff et al., 1981; Summers et al., 1983).

REFERENCES

Albritton, D.L. (1978). Ion-neutral reaction rate constants measured in flow reactions through 1977. Atomic Data and Nuclear Data Tables **22**, 1-101.

Allen, M., Y.L. Yung, and J.W. Waters (1981). Vertical transport and photochemistry in the terrestrial mesosphere and lower thermosphere (50-120 km). J. Geophys. Res., **86**, 3617- .

Banks, P.M. (1969). The thermal structure of the ionosphere. Proceedings of the IEEE, **57**, 258-281.

Bates, D.R. (1959). Some problems concerning the terrestrial atmosphere above about the 100 km level. Proc. Roy. Soc. London, **A253**, 451-462.

Bauer, S.J. (1973). Physics of Planetary Ionospheres, Springer-Verlag, New York.

Baulch, D.L. and D.D. Drysdale (1976). Evaluated Kinetic Data for High Temperature Reactions, University of Leeds.

Brewer, L. and G.D. Brabson (1966). Ultraviolet Fluorescent and Absorption Spectra of S_2 Isolated in Inert-Gas Matrices. J. Chem. Phys. **44**, 3274-3278.

Brinkmann, R.T. (1970). Departures from Jeans' Escape Rate for H and ³He in the Earth's Atmosphere. Planet. Space Sci., **18**, 449-478.

Brown, R.A. (1974). Optical line emission from Io. In Exploration of the Planetary System (A. Woszczyk and C. Iwaniszewska, eds.), D. Reidel Pub. Co., Dordrecht, Holland, pp. 527-531.

Brown, R.A. (1981). The Jupiter hot plasma torus: Observed electron

temperature and energy flows. Astrophys. J., **244**, 1072-1080.

Brown, R.A., C.B. Pilcher, and D.F. Strobel (1983). Spectrophotometric studies of the Io torus. In Physics of the Jovian Magnetosphere (A. Dessler, ed.), Cambridge University Press, Cambridge, pp. 197-225.

Brown, R.A. and Y.L. Yung (1975). Io, its atmosphere and optical emissions. In Jupiter (T. Gehrels, ed.), University of Arizona Press, Tucson, pp. 1102-1145.

Carlson, R.A. (1978). Astrophys. J., **223**, 1082-1086.

Chamberlain, J.W. (1978). Theory of Planetary Atmospheres, Academic Press, New York.

Chapman, S. (1931). Proc. Phys. Soc., **43**, 26 .

Chapman, S. and T.G. Cowling (1970). The Mathematical Theory of Non-uniform Gases, 3rd edition, Cambridge University Press, London.

Cloutier, P.A., R.E. Daniell, Jr., A.J. Dessler, and T.W. Hill (1978). A cometary ionosphere model for Io. Astrophys. Sp. Sci., **55**, 93-112.

Davis, D.D., R.B. Klemm, and M. Pilling (1972). A flash photolysis-resonance kinetics study of ground-state sulfur atoms: I. Absolute rate parameters for reaction of $S(^3P)$ with $O_2(^3\Sigma)$. Int. J. Chem. Kinetics, **IV**, 367-382.

DeMore, W.B., M.J. Molina, R.T. Watson, D.M. Golden, R.F. Hampson, M.J. Kurylo, C.J. Howard, and A.R. Ravishankara (1983). Chemical Kinetics and Photochemical Data for Use in Stratospheric Modeling. Evaluation Number 6: NASA Panel for Data Evaluation. JPL Publication 83-62, Jet Propulsion Laboratory.

Doering, J.P. and B.H. Mahan (1961). Photolysis of nitrous oxide. I. 1236 Å. J. Chem. Phys., **34**, 1617-1620.

Driscoll, J.N. and P. Warneck (1968). Primary processes in the photolysis of SO_2 at 1849 Å. J. Phys. Chem., **72**, 3736-3740.

Durrance, S.T., P.D. Feldman, and H.A. Weaver (1982). Rocket detection of ultraviolet emissions from neutral oxygen and sulfur in the Io torus. B.A.A.S., **14**, 763.

Fanale, F.P., W.B. Banerdt, L.S. Elson, T.V. Johnson, and R.W. Zurek (1982). Io's surface: Its phase composition and influence on Io's atmosphere and Jupiter's magnetosphere. In Satellites of Jupiter (D. Morrison, ed.), University of Arizona Press, Tucson, pp. 756-781.

Fanale, F.P., R.H. Brown, D.P. Cruikshank, and R.N. Clarke (1979). Significance of absorption features in Io's IR reflectance spectrum. Nature, **280**, 761-763.

Fanale, F.P., T.V. Johnson, and D.L. Matson (1974). Io: A surface evaporite deposit? Nature, **186**, 922-925.

Golomb, D., K. Watanabe, and F.F. Marmo (1962). Absorption coefficients of sulfur dioxide in the vacuum ultraviolet. J. Chem. Phys., **36**, 958-960.

Haff, P.K., C.C. Watson, and Y.L. Yung (1981). Sputter Ejection of Matter from Io. J. Geophys. Res., **86**, 6933-6938.

Herron, J.T. and R.E. Huie (1980). Rate constants at 298 K for the reactions SO + SO + M -> $(SO)_2$ + M and SO + $(SO)_2$ -> SO_2 + S_2O. Chem. Phys. Lett., **76**, 322-324.

Hinteregger, H.E. (1970). The extreme ultraviolet solar spectrum and

its variation during a solar cycle. Ann. Geophys., **26**, 547-554.

Hirschfelder, J.D., C.F. Curtiss, and R.B. Bird (1954). Molecular Theory of Gases and Liquids, John Wiley and Sons, Inc., New York.

Houghton, J.T. (1977). The Physics of Atmospheres, Cambridge University Press, Cambridge.

Howell, R.R., D.P. Cruikshank, and F.P. Fanale (1983). Sulfur dioxide abundance and location on Io. Paper given at IAU Colloquium No. 77, Natural Satellites, at Cornell University, New York.

Hudson, R.D. (1971). Critical review of ultraviolet photoabsorption cross sections for molecules of astrophysical and aeronomic interest. Rev. Geophys. Space Phys., **9**, 305-406.

Huie, M.-H. and S.A. Rice (1972). Decay of fluorescence from single vibronic states of SO_2. Chem. Phys. Lett., **17**, 474-478.

Hunten, D.M. (1973). The escape of H_2 from Titan. J. Atmos. Sci., **30**, 726-772.

Hunten, D.M. (1973). The escape of light gases from planetary atmospheres. J. Atmos. Sci., **30**, 1481-1494.

Johnson, T.V., A.F. Cook, III, C. Sagan, and L.A. Soderblom (1979). Volcanic resurfacing rates and implications for volatiles on Io. Nature, **280**, 746-750.

Kliore, A.J., G. Fjeldbo, B.L. Seidel, D.N. Sweetnam, T.T. Sesplaukis, and P.M. Woiceshyn (1975). The atmosphere of Io from Pioneer 10 radio occultation measurements. Icarus, **24**, 407-410.

Konowalow, D.D., J.O. Hirschfelder, and B. Linder (1959). Low-temperature, low-pressure coefficients for gaseous oxygen and sulfur atoms. J. Chem. Phys., **31**, 1575-1579.

Kumar, S. (1979). The stability of the SO_2 atmosphere on Io. Nature, **280**, 758-760.

Kumar, S. (1980). A model of the SO_2 atmosphere and ionosphere of Io. Geophys. Res. Lett., **7**, 9-12.

Kumar, S. (1982). Photochemistry of SO_2 in the atmosphere of Io and implications on atmospheric escape. J. Geophys. Res., **87**, 1677-1684.

Kumar, S. and D.M. Hunten (1982). The atmosphere of Io and other satellites. In Satellites of Jupiter (D. Morrison, ed.), University of Arizona Press, Tucson, pp. 782-806.

Liu, S.C. and G.C. Reid (1979). Sodium and other minor constituents of meteoritic origin in the atmosphere. Geophys. Res. Lett. **6**, 283-286.

Logan, J.A., M.J. Prather, S.C. Wofsy, and M.B. McElroy (1978). Atmospheric chemistry: Response to human influence. Philos. Trans. Roy. Soc. London, **290**, 187-233.

Mason, E.A., and T.R. Marrero (1970). The diffusion of atoms and molecules. In Advances in Atomic and Molecular Physics, Vol. 6, (D.R. Bates and I. Esterman, eds.), Academic Press, New York.

McEwen, A.S. and L.A. Soderblom (1983). Two Classes of Volcanic Plumes on Io. Icarus, **58**, 197-226.

McGuire, E.J. (1968). Photoionization cross-sections of the elements helium to xenon. Phys. Rev. **175**, 20-48.

Matson, D.L., B.A. Goldberg, T.V. Johnson, and R.W. Carlson (1977). Images of Io's sodium cloud. Science, **199**, 531-533.

Morrison, D. and D.P. Cruikshank (1974). Physical properties of the

natural satellites. Space Sci. Rev., **15**, 641-739.

Mount, G.H., G.J. Rottman, and J.G. Timothy (1980). The solar spectral irradiance 1200-2550 Å at solar maximum. J. Geophys. Res., **85**, 4271-4274.

Nash, D.B. (1983). Laboratory IR spectral of SO_2 frost, absorbate, and gas over various substrates, and applications to Io's surface composition. Paper given at IAU Colloquium No. 77, Natural Satellites, Cornell University, New York.

Nash, D.B. and R.M. Nelson (1979). Spectral evidence for sublimates and adsorbates on Io. Nature, **280**, 763-766.

Okabe, H. (1971). Fluorescence and predissociation of sulfur dioxide. J. Am. Chem. Soc., **93**, 7095-7096.

Okabe, H. (1978). Photochemistry of Small Molecules, Wiley, New York.

Pearl, J., R. Hanel, V. Kunde, W. Maguire, K. Fox, S. Gupta, C. Ponnamperuma, and F. Raulin (1979). Identification of gaseous SO_2 and new upper limits for other gases on Io. Nature, **280**, 755-758.

Prasad, S.S. and W.T. Huntress (1980). A Model for Gas Phase Chemistry in Interstellar Clouds. Astrophys. J. Suppl. Ser. **43**, 1-35.

Phillips, L.F. (1981). Absolute absorption cross sections for SO between 190 nm and 235 nm. J. Phys. Chem., **85**, 3994-4000.

Smith, W.H. (1969). Absolute transition probabilities for some electronic states of CS, SO, and S_2. J. Quant. Spectrosc. Radiat. Transfer, **9**, 1191-1199.

Smith, W.H., and H.S. Liszt (1971). Franck-Condon factors and absolute oscillator strengths for NH, SiH, S_2, and SO. J. Quant. Spectros. Radiat. Transfer, **11**, 45-54.

Smyth, W.H. and M.B. McElroy (1978). Io's sodium cloud: Comparison of models and two-dimensional images. Astrophys. J., **226**, 336-346.

Smyth, W.H. and D.E. Shemansky (19828). Escape and ionization of atomic oxygen from Io.

Smythe, W.D., R.M. Nelson, and D.B. Nash (1979). Spectral evidence for SO_2 frost or adsorbate on Io's surface. Nature, **280**, 766.

Summers, M.E., Y.L. Yung, and P.K. Haff (1983). A Two-stage Mechanism for Escape of Na and K from Io. Nature, **304**, 710-712.

Thompson, B.A., P. Harteck, and R.R. Reeves, Jr. (1963). Ultraviolet absorption coefficients of CO_2, CO, O_2, H_2O, N_2O, NH_3, NO, SO_2, and CH_4 between 1850 Å and 4000 Å. J. Geophys. Res., **68**, 6431-6436.

Trafton, L. (1975). Detection of a potassium cloud near Io. Nature, **258**, 690-692.

Trafton, L. (19818). A survey of Io's potassium cloud. Astrophys. J., **247**, 1125-1140.

Von Homann, K.H., G. Krome, and H.G. Wagner (1968). Schwefelkahlanstuff-Oxydation, Geschwin digkeit von Elementarreaktion. Ber. Bunsen-ges. **22** 998.

Warneck, P., F.F. Marmo, and J.O. Sullivan (1964). Ultraviolet absorption of SO_2: Dissociation energies of SO_2 and SO. J. Chem. Phys., **40**, 1132-1136.

Watson, A.J., T.M. Donahue, and J.C.G. Walker (1981). The Dynamics of a Rapidally Escaping Atmosphere: Applications to the Evolution of Earth and Venus. Icarus, **48**, 150-160.

Watson, W.D. and E.E. Salpeter (1972). Astrophys. J. **174**, 321-334.

Welge, K.H. (1974). Photolysis of O_x, HO_x, CO_x, and SO_x compounds.

Can. J. Chem., 52, 1424-1435.

Winick, J.R. and A.I. Stewart (1980). Photochemistry of SO_2 in Venus' upper cloud layers. J. Geophys. Res., 85, 7849- .

Wu, C.Y.R. and D.L. Judge (1981). Study of sulfur-containing molecules in the EUV region. 1. Photoabsorption cross sections of SO_2. J. Chem. Phys., 74, 3804-3806.

Yung, Y.L. and W.B. DeMore (1982). Photochemistry of the stratosphere of Venus: Implications for atmospheric evolution. Icarus, 51, 199-247.

A Two-stage Mechanism for Escape of Na and K from Io

By

Michael E. Summers and Yuk L. Yung

Division of Geological and Planetary Science

California Institute of Technology, Pasadena, CA 91125

and

Peter K. Haff

Division of Physics, Mathematics and Astronomy

California Institute of Technology, Pasadena, CA 91125

Published in Nature, **304**, 710-712, 1983

Contribution number 3873 from the Division of Geological and Planetary Sciences, California Institute of Technology, Pasadena, CA 91125.

ABSTRACT

It is generally accepted that Io is the source of S, O, Na and K which, subsequent to ionization, form the constituents of the Io plasma torus. The escape of S and O from Io can be understood in terms of the photochemistry of a predominantly SO_2 atmosphere created by the high vapor pressure of SO_2 (refs. 1, 15). However, the vapor pressures of Na_2S, K_2S and other common compounds containing Na and K are negligible at the surface temperatures of Io. This has given rise to the suggestion that over part of Io's surface (the nightside) the atmosphere is thin enough so that surface sputtering by corotating ions can eject Na and K directly into the Io torus[2,3]. The main objection to this idea is that it implies a 'sun-locked' source for Na and K, while observations of the Na and K clouds around Io indicate a 'Jupiter-locked' ejection mechanism. We propose here that Na and K escape from Io in two stages. Atoms of Na and K are first sputtered into the atmosphere from the surface by high energy magnetospheric ions. Atmospheric sputtering[4] by low energy corotating ions then removes these constituents (along with others present) out of Io's gravitational field. We suggest that the observed Na and K ejection asymmetry is due to preferential sputtering of atmospheric particles on the hemisphere of Io facing Jupiter. The estimated injection rates are sufficiently large to maintain the observed K, Na, and O clouds observed around Io[5,6,7,18].

The SO_2 abundance of 0.2 cm atm detected by the Voyager I IRIS experiment in the subsolar region of Io corresponds to a SO_2 vertical column density $N_{IRIS} \simeq 5 \times 10^{18}$ cm^{-2} (ref. 8). This is approximately the atmospheric SO_2 abundance that would exist if the SO_2 gas were in thermodynamic equilibrium with SO_2 surface frost at T = 130 K. The globally averaged SO_2 vertical column density $\bar{N}$ is probably much less than this value since the vapor pressure of SO_2 decreases exponentially with decreasing temperature. An estimate of $\bar{N}$ may be obtained by assuming local pressure equilibrium between atmospheric SO_2 and surface frost. From an extrapolation of the SO_2 vapor pressure data of Wagman[21], and a surface temperature variation which approximates the IRIS observations[8], we obtain $\bar{N} \simeq 5 \times 10^{17}$ cm^{-2}. It should be noted that photochemical models of Io's atmosphere which reproduce the characteristics of the downstream ionosphere as observed by Pioneer 10 require $\bar{N} \sim 1 \times 10^{17}$ cm^{-2} (ref. 9).

Corotating S^+ and O^+ ions in the plasma torus impacting Io's atmosphere are unable to penetrate to Io's surface if $\bar{N} \sim 10^{16}$ cm^{-2} (ref. 10). In order for S^+ and O^+ ions to penetrate an SO_2 atmosphere characterized by $\bar{N} \simeq 5 \times 10^{17}$ cm^{-2}, their incident kinetic energies must be greater than 0.3 MeV and 0.1 MeV, respectively. The Voyager I Low Energy Charged Particle (LECP) and Plasma Science (PLS) experiments detected a flux $F \simeq 10^5$ cm^{-2} s^{-1} MeV^{-1} of ions in the vicinity of Io's orbit with energies greater than these minimum values[10].

The sputtering of frozen SO_2 frost by high energy ($0.08 \leq E$ (MeV/amu) ≤ 1.30) He and F ions has recently been studied by Melcher et al.[11] (see also ref. 10). The peak sputtering yield for incident F^+

was 7300 at energy Ep = 0.32 MeV/amu. The yield spectrum exhibited a rapid rise with increasing energy for E < Ep, and an exponential decrease for E > Ep. The qualitative character of the yield spectrum was previously predicted on the basis of a modified lattice potential model of high energy ion erosion developed by Watson and Tombrello[12]. The theory correctly predicts the energy at which the peak yield occurs; however, the magnitude of the predicted yields is approximately a factor of 3 too large. We have utilized this theory to estimate the sputtering yield due to impacting high energy O^+ and S^+ on SO_2. In Figure 1 we show the calculated yields as a function of incident ion energy, E, made using the same normalization factor that adjusted the calculated F^+ sputtering yields to agree with the data. The peak yield for O^+ on SO_2 frost is 8900 and occurs at E = 0.23 MeV/amu. The sputtering yield spectra for F^+ and O^+ are similar because they have similar masses. The peak yield for S^+ on SO_2 frost is 35,000 at E = 0.4 MeV/amu.

The surface sputtering rate due to impacting ions is given by the integral of the product of the yield and the differential ion flux incident on the surface. The differential ion flux in the vicinity of Io's orbit was measured by the Voyager I PLS and LECP experiments; however, the composition of the high energy plasma is uncertain. We have used the PLS and LECP data and data extrapolations of the high energy ion flux given by Lanzerotti et al. (ref. 10, and see Figure 2), to calculate the surface sputtering rate on Io. Assuming that the high energy ions consist of S^+ and O^+ in the ratio 1:2, we find a surface sputtering rate $\phi(SO_2) \simeq 8 \times 10^8$ cm^{-2} s^{-1}. This value of the flux of

Figure 1. The calculated SO_2 sputtering yield as a function of incident energy for S^+ and O^+ ions. The calculations were performed using the theory of Watson and Tombrello[12].

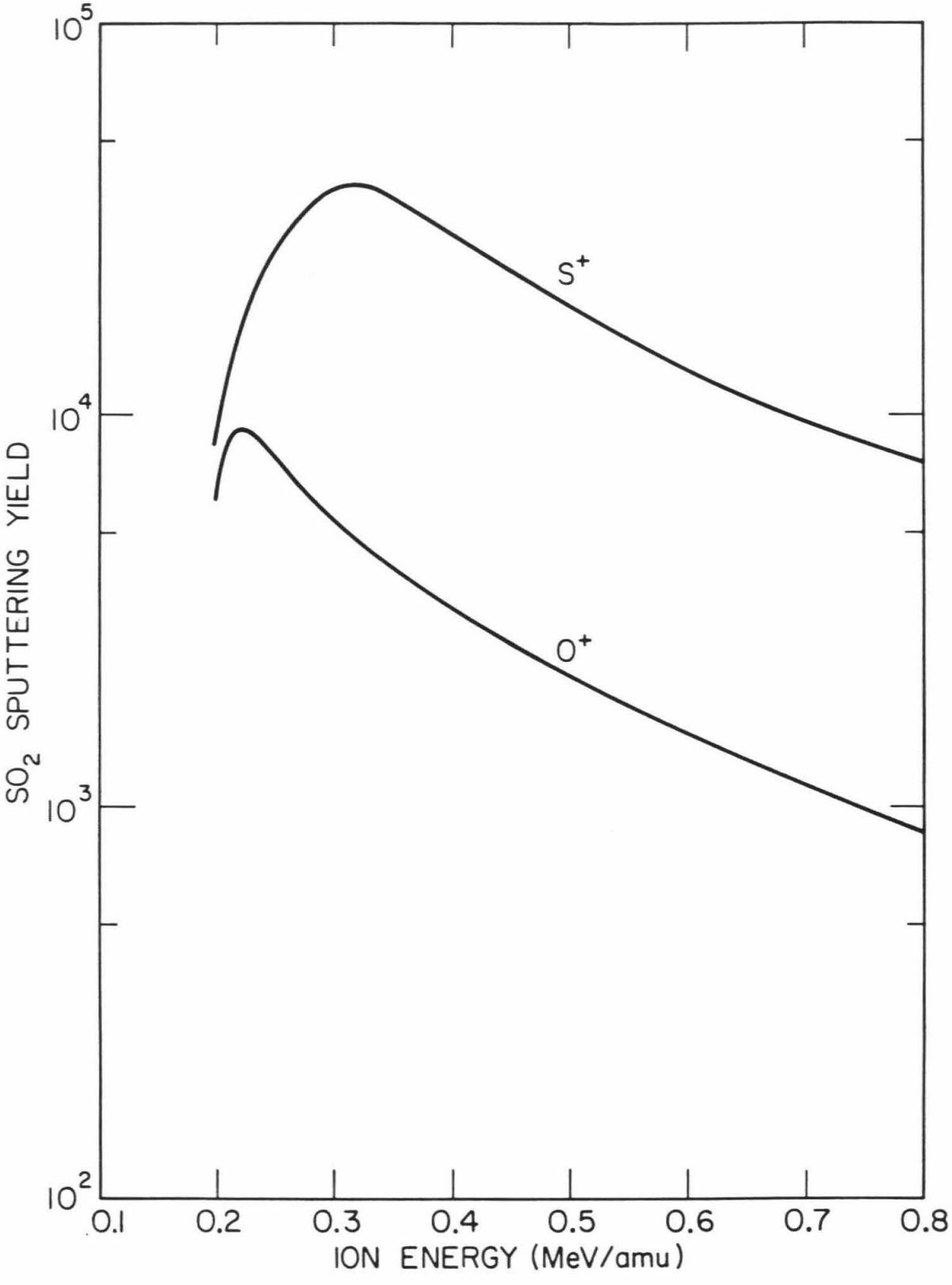
10^5
10^4
10^3
10^2
SO_2 SPUTTERING YIELD
S^+
O^+
0.1
0.2
0.3
0.4
0.5
0.6
0.7
0.8
ION ENERGY (MeV/amu)

Figure 2. The differential ion flux in the vicinity of Io's orbit, adopted from Lanzerotti et al.[10], and extrapolated to higher energies using the power law $d(\text{Flux})/dE = (E/E_0)^{-n}$, where E_0 is a reference energy and $n = 7$.

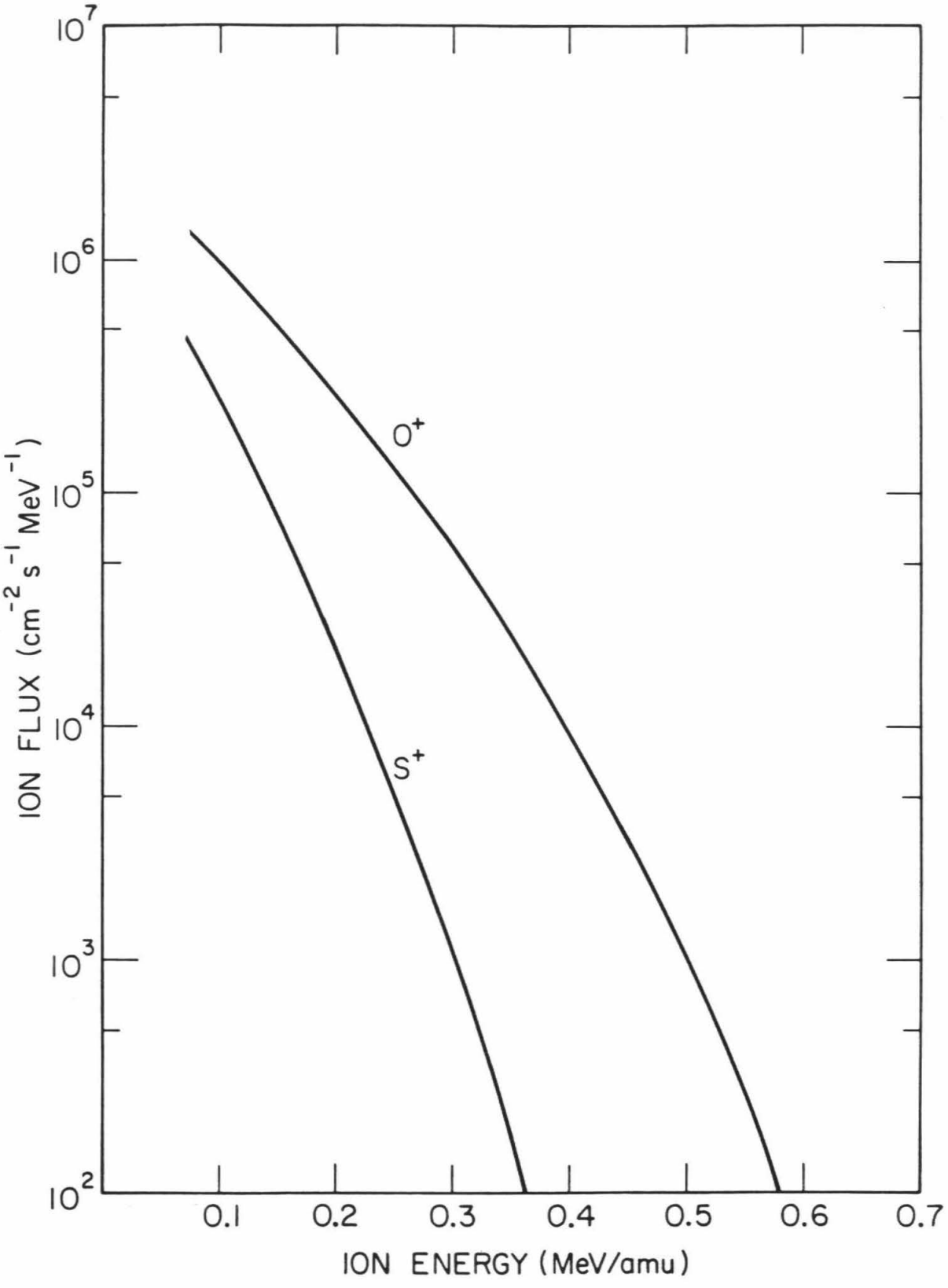
10^7
10^6
10^5
10^4
10^3
10^2
ION FLUX ($cm^{-2}\,s^{-1}\,MeV^{-1}$)
O^+
S^+
0.1
0.2
0.3
0.4
0.5
0.6
0.7
ION ENERGY (MeV/amu)

SO_2 molecules into the atmosphere is about 7 orders of magnitude smaller than the sublimation rate of SO_2 in the subsolar region of Io. Thus, surface sputtering by these high energy ions is insignificant for the overall mass balance of the atmosphere. If minor constituents such as Na and K are present on the surface with the SO_2 frost, then sputtering may be an important mechanism for mobilizing these constituents.

It has been suggested that Na and K exist on the surface of Io in the form of Na_2S and K_2S (ref. 13); however, the surface abundances of these salts are unknown. We consider the consequences of having K, Na, and S present on the surface in cosmic proportions. This assumption implies a number ratio of Na atoms to S atoms of 0.12, and a ratio of K to S of 0.008 (ref. 14). In the sputtering process we assume that each surface constituent is ejected in proportion to its surface abundance. Thus, we estimate the surface source of Na and K to be $\phi_{Na} \simeq 1 \times 10^8$ cm^2 s^{-1} and $\phi_K \simeq 6 \times 10^6$ cm^{-2} s^{-1}. These fluxes are of the correct magnitude to maintain in a steady state the Na and K clouds observed around Io[5,6,7].

Once in the atmosphere Na and K will escape from Io by the same mechanism that operates for S and O. Earth-based spectroscopic observations of the neutral Na and K clouds indicate particle injection velocities from Io $\approx$ 3 km s^{-1} (refs. 6, 7, 19). Thermal Jean's escape will produce escaping K with velocities greater than this minimum value only if the exosphere temperature $T_{ex} \approx$ 14,000 K, while models of Io's ionosphere indicate $T_{ex} \simeq$ 1000 K (ref. 1). Sputtering of atmospheric particles by impacting corotating S^+ and O^+ will produce an average velocity for the escaping particles $\geq$ 2.6 km s^{-1}. There are simple and

compelling reasons to believe that the exosphere of Io is dominated by neutral oxygen atoms[1], and that Io's exobase may lie at about 2.0 Io radii from the surface[15]. The yield for atmospheric sputtering by low energy ions is $Y \geq 1$ (ref. 4). The flux of corotating ions averaged over the Io plasma torus is $F_{CR} \simeq 10^{10}$ cm^{-2} s^{-1} (ref. 10). The escaping flux due to atmospheric sputtering is therefore $F_{escape} \approx 9 \times 10^{27}$ O atoms s^{-1} $\simeq$ 200 kg s^{-1}. This is sufficient to supply the neutral oxygen cloud that exists along the orbit of Io[16]. Sulfur atoms will be sputtered from the atmosphere in approximately the same proportion in which they exist in the atmosphere at the exobase.

Voyager I measurements of the plasma torus indicate a large but negative radial gradient in the concentration of corotating ions across the orbit of Io[17]. This is of key importance since the flux of sputtered atoms is proportional to the flux of incoming ions. The observed gradient in ion density (and hence corotating flux) is sufficiently large that if Io's exobase is located at 2.0 Io radii from its surface, then the flux of sputtered atoms due to impacting S^+ and O^+ is approximately a factor of 2 greater on Io's inner hemisphere (facing Jupiter) than on the outer hemisphere. Therein may lie a particularly simple explanation of the Na and K ejection asymmetry[18,19,20]. If Na and K can be supplied to the atmosphere at the required rate, then there should be greatly enhanced atmospheric sputtering of Na, K, O, and S on Io's inner hemisphere. This would lead to ejection asymmetries not only for Na and K (observed) but also for S and O (as yet unobserved).

Many questions remain to be answered in order to understand the details of this two-stage mechanism. Some of these are: How are Na and K species affected by photochemistry and diffusion? What fraction of the atoms sputtered from the surface eventually escape into the torus? What are the characteristics of the asymmetric escape of S and O? These questions provide the thrust of an in-depth study that is in progress.

It is with pleasure that we acknowledge J. Trauger, T. Johnson, A. Dessler and A. Summers for many helpful discussions; and K. Cherrey for helpful numerical calculations. This research has been supported by NASA grants NAGW-202 and NAGW-313.

REFERENCES

1. Kumar, S. J. Geophys. Res., **87**, 1677-1684 (1982).
2. Haff, P.K. et al. J. Geophys. Res., **86**, 6933-6938 (1981).
3. Kumar, S. and Hunten, D.M. in Satellites of Jupiter (ed. D. Morrison) 782-806 (University of Arizona Press, 1982).
4. Haff, P., and Watson, C.C., J. Geophys. Res., **84**, 8436-8442 (1979).
5. Macy, W. and Trafton, L. Astrophys. J., **200**, 510-519 (1975).
6. Brown, R.A. and Yung, Y.L. in Jupiter (ed. T. Gehrels) 1102-1145 (University of Arizona Press, 1976).
7. Trafton, L. Astrophys. J., **247**, 1125-1140 (1981).
8. Pearl, J. et al. Nature, **280**, 755-758 (1979).
9. Kumar, S. Geophys. Res. Lett., **7**, 9-12 (1980).
10. Lanzerotti, L.J. et al. Astrophys. J., **259**, 920-929 (1982).
11. Melcher, C.L. et al., Geophys. Res. Letters, **9**, 1151-1154 (1982).
12. Watson, C.C. and Tombrello, T.A., Submitted to Radiation Effects (1983).
13. Fanale, F.P. et al. in Satellites of Jupiter (ed. D. Morrison) 756-781 (University of Arizona Press, 1982).
14. Lang, K.R. Astrophysical Formulae. (Springer-Verlag, 1978).
15. Summers, M.E. and Yung, Y. Preprint (1983).
16. Shemansky, D. and Smyth, W., Submitted to J. Geophys. Res. (1983)
17. Belcher, J.W. in Physics of the Jovian Magnetosphere (ed. A. Dessler) 68-105 (Cambridge University Press, 1983).
18. Smyth, W.H. and McElroy, M.B. Astrophys. J., **226**, 336-346 (1978).

19. Carlson, R.W. et al. Geophys. Res. Lett., **10**, 469-472 (1975).

20. Matson, D.L. Science, **199**, 531-533 (1978).

21. Wagman, D.D. (Personal Communication, 1979).